Electrochemical silver sensors for photographic processes

Johnston, Brian

Electrochemical Silver Sensors for Photographic Processes

by

Brian Johnston

Department of Chemistry

University of Durham

A thesis submitted for the degree of Doctor of Philosophy

October 1998

Abstract

Electrochemical Silver Sensors for Photographic Processes

A range of novel silver ionophores was synthesised based on the 1,3-dithiole-2-thione-4,5-dithiolate (DMIT) building block. These were incorporated in ion-selective electrodes (ISEs) and applied to the determination of silver ion in photographic process solutions of interest to Kodak.

Two classes of compounds were synthesised incorporating acyclic silver binding sites. The first class of compounds were 1,3 dithiole–2-ones functionalised with (i) a silver binding chain, and (ii) an alkyl chain, the latter allowing a range of compounds to be synthesised of varying lipophilicity. These compounds were applied as silver ionophores in plasticised PVC membranes and incorporated in ion-selective electrodes. The newly synthesised ionophores were compared to silver ionophores in the literature and to those previously used by Kodak. The membrane composition was optimised for silver ion selectivity over a range of metal cations of relevance to photographic process solutions. Samples of photographic emulsions were supplied by Kodak and subsequent analysis demonstrated successful detection of silver ion to micromolar levels with the ISE incorporating the newly synthesised ionophores.

The second class of compounds was based on the tetrathiafulvalene (TTF) building block. A TTF derivative was synthesised incorporating two acyclic silver binding chains and a hydrophobic domain. The reversible redox properties of this compound enabled it to be applied as a transducer suitable for voltammetric analysis of silver ion. Titration of a solution of the new TTF compound with silver ion revealed that it was very sensitive; an equimolar quantity of silver ion resulting in a marked change in voltammetric behaviour. A silver ion binding constant was determined by ultraviolet spectrophotometry.

Declaration

The work described herein was carried out in the Department of Chemistry at the University of Durham, and the Technical University of Budapest between October 1995 and September 1998. All the work is my own, unless otherwise stated and it has not been submitted for a degree at this or any other university.

Statement of Copyright

Acknowledgements

I am grateful for the assistance of many people involved, either directly or indirectly, in the completion of this work. I would particularly like to acknowledge the following:

Doctor Ritu Kataky and Professor Martin Bryce for their supervision, ideas and guidance during the course of this work. I would also like to thank Kodak UK, Harrow for the funding of this work and the opportunity to work in their research facility and my industrial supervisors Dr John McBride and Steve Edwards.

A big "kosonum" to Professor Klara Toth, and everybody in the Technical University of Budapest for the opportunity I had to work there. Thanks also to Eva, Robbie Ye and everybody who contributed to my enjoyable stay.

To everybody in the MRB group for the assistance with the synthetic work including Chez, Adrian, Derek, Alex, Andy, Terry, Richard, Naveed, Changsheng and everyone who contributed along the way and thanks to Nathalie for introducing me to Endnote.

To Rosie and Jose (Bob), my co workers in lab 138 for all the assistance and counselling when things always worked !

To the support staff, especially Terry and Colin, for keeping the computers going and me sane ! To Neil in the mechanical workshop for fixing and making things !

To all residents of 32 Albert St for providing me with a home from home in Durham and a venue for some great parties.

Thanks to my parent for their support, and yes I am going to start earning now !

To my parents

Contents

CHAPTER THREE: Complexation Studies

CHAPTER FOUR: Potentiometry Using Ion Selective Electrodes

CHAPTER FIVE: Determination of Silver in Photographic Emulsion

CHAPTER ONE

General Introduction

1.1 The Chemistry of Photography

The process involved in the formation of a photographic image is summarised in Figure 1.1. When photographic film, which consists of an emulsion (a thin layer of gelatin) and a base of transparent cellulose acetate or polyester, is exposed to light, silver halide crystals suspended in the emulsion undergo chemical changes to form what is known as a latent image on the film. This is the invisible precursor of the image and results in such a minute change in the sensitive material that no transformation is detectable by existing analytical methods[1]. The formation of the image then involves the action of a developer, which is a reducing agent that selectively reduces the exposed crystals to solid silver particles. The image produced in this manner is called a negative because the tonal values of the subject photographed are reversed; that is, areas in the scene that were relatively dark appear light, and areas that were bright appear dark. Once the image is formed it has to be fixed, which is achieved by removing the unexposed silver halide using a solution of either sodium thiosulfate or ammonium thiosulfate.

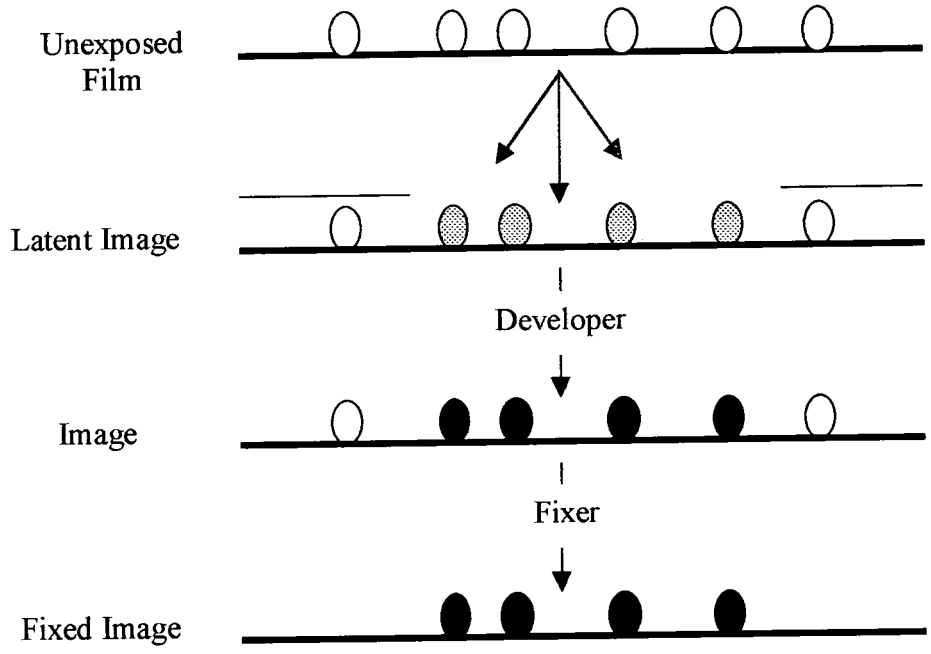

Figure 1.1 Schematic representation of the photographic process.

1.2 Preparation of Photographic Emulsions[2]

A photographic emulsion is defined as a dispersion of photosensitive solid microcrystals in a protective colloid, such as gelatin. This differs from the definition of a colloid in colloidal science where it designates a heterogeneous mixture of two or more phases that do not normally dissolve in each other but form a relatively stable dispersion. The preparation of photographic emulsions is a highly complex process that involves several distinct phases that are carried out in sequence

1. The formation of a dispersion of microcrystals of silver halide in a solution of protective colloid.
2. Physical ripening to achieve the desired grain size
3. The isolation of the dispersion from excess soluble salts
4. A heat treatment phase which is often carried out in the presence of sensitizing agents, which results in the light sensitivity of the emulsion
5. The addition of specific agents which confer desired properties such as sensitizing dyes, anti-foggants and stabilisers.

The primary process in the preparation is the precipitation of the silver halide salt. This is achieved by mixing of the alkali metal halide and the silver salt (typically the nitrate) in a protective colloid such as gelatin. If a solution of alkyl halide and silver salt were mixed in aqueous solution the silver halide would just precipitate from the solution. However, when this reaction is performed in a solution of gelatin, the gelatin effectively suspends the silver in solution. The actual mixing of the halide and silver solutions is done under very controlled conditions of temperature, concentration, sequence of addition and rates of addition to produce the required dispersion. Two precipitation schemes can be used, one is termed the single jet method and the other the double jet method. In the single jet method all of the halide is added to the mixing vessel from the start, whereas the silver nitrate solution is added gradually, however in the double jet method the halide and silver nitrate solutions are added simultaneously to the mixing vessels.

The second process, termed physical ripening, involves keeping the dispersion in the presence of the solvent to permit the growth and recrystallisation of the individual particles

of silver halide to the desired grain size. This ripening stage is intended to establish the grain size and distribution of the sizes. After ripening, the gelatin may be freed from excess soluble salts by either washing or coagulation. Washing of gelatin involves adding additional gelatin then cooling to allow it to solidify. The soluble salts and ripening agents are then washed from the dispersion with chilled water by osmotic diffusion. Alternatively, the gelatin can be cleaned by coagulation, this involves the coagulation of the dispersion which allows the supernatant liquid to be removed, followed by the coagulate being redispersed in pure water or in a gelatin solution.

1.3 Properties of Silver

A good starting point in the design of a silver ligand is to examine the properties and orbital arrangements of the Ag^+ cation itself. Elemental silver shares a group with copper and gold which all share a single s electron outside a completed d shell. However, despite their similar electronic structure and ionisation potentials they exhibit few similarities and there are no simple explanations for many of the differences[3]. A good illustration of this point lies in the comparison of the stability constant sequence for halide complexes of metals. Most metals display a stability sequence in the order F > Cl > Br > I whilst Cu^+ and Ag^+ show the reverse order. Looking at simple silver compounds such as the halides there appears to be appreciable covalent character in the Ag--X, interactions, with AgCN and AgSCN showing predominantly covalent character. Another notable feature of Ag^+ is its striking tendency to exhibit linear, 2-fold co-ordination. An examination of the atomic orbitals reveals a relatively small difference in energies between the filled 4d and the unfilled 5s orbitals, allowing facile hybridisation, as shown in Figure.1.2.

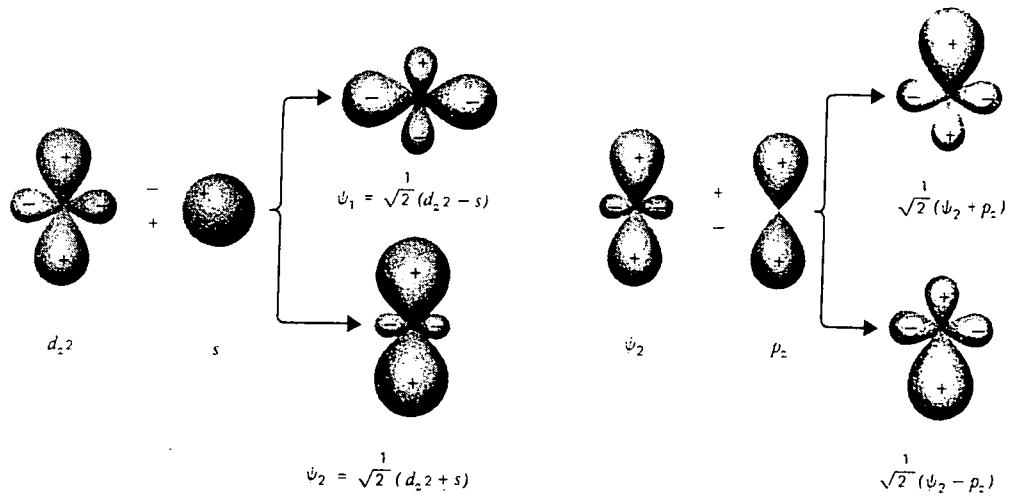

Figure 1.2 Hybrid orbitals of the silver atom[3]

The hybrid orbital Ψ_2 can then further mix with the pz orbital forming hybrid orbitals suitable for forming a pair of linear covalent bonds. Examination of some silver complexes shows a greater stability towards ligands containing sulfur atoms, which is rationalised as resulting from the polarising power of Ag^+ and the polarisability of the "soft" sulfur atom. The ability of Ag^+ to form complexes extends beyond metal ions and studies have shown than virtually all alkenes[4] and aromatic[5] compounds form complexes when shaken with aqueous solutions of silver salts. Recent work on bridged stilbene ligands produced the first crystal structure of a silver complex which displayed simultaneous coordination at hard ether oxygen atoms and a soft π bond[6].

1.4 Silver Complexation by Organic Ligands

In this section some general points on silver complexation by organic ligands are discussed; a more specific discussion on silver ionophores is given in section 4.1.4. The recognition of a particular metal ion by a ligand occurs when the properties of the ligand best match the steric and electronic demands of the metal ion. The most important factors in ligand design include the number and type of donor atom, their relative positions, the number and size of chelate rings and the solvation demands of the metal ion-complex[7]. The original synthetic ligands were macrocyclic as they were based on naturally occurring metal binding molecules such as valinomycin and accordingly the majority of synthetic ligands are also macrocyclic.

Crown ethers are one of the most important classes of macrocyclic ligands. In complexation studies between cyclic polyethers and various cations, it was found that substitution of oxygen by sulfur or nitrogen greatly influences complexation. Studies carried out by Frensdorff using 18-crown-6 and dibenzo-18-crown-6 showed that substitution by nitrogen or sulfur increased the affinity of the macrocycle for Ag^+ whilst decreasing its affinity for K^+[8]. This observation was taken as evidence for the predominance of covalent bonding over electrostatic bonding. Since then a lot of work has been published on macrocyclic thioethers where the donor atoms have been systematically varied by substituting the oxygen donor atoms for sulfur and nitrogen.[9,10]

Owing to the popularity of thia crown ethers in ligand design, a lot of work has been published on their structural and conformational properties[11], in particular the $SCH_2CH_2SCH_2CH_2S$ "bracket" has been examined using crystallography, NMR spectroscopy and molecular dynamics (MD). Early crystallographic work by Dalley[12] on dithia- and trithia-crown ethers showed that the macrocyclic thioethers adopted structures where the sulfur atoms were directed out of the ring, away from the cavity. Similar work on a wider range of crown ethers by Dale[13] illustrates the different conformations adopted by a 12O4 and a 12S4 crown ethers when viewed as a projection on a molecular plane which can be seen in Figure 1.3. The sulfur atoms preference to be out of the ring manifests in the 12-membered ring adopting a conformation with the sulfur atoms placed at the corners,

compared to the equivalent 12O4 structure where the oxygen atoms appear in the sides of the square.

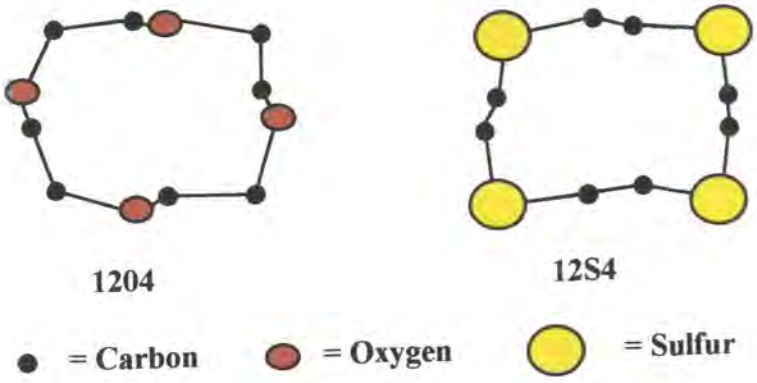

Figure 1.3 Conformation of 12S4 crown compared to the 12O4 crown, heteroatoms are designated by arrows.

This can be explained by considering the 1,4 E-C-C-E interactions (E = O or S) where the O-C-C-O unit favours gauche placements, whilst the S-C-C-S unit favours anti placements. This work was extended by Casabó *et al* to specific thia-crown ethers based on xylyl subunits supplemented by NMR and MD observations[14]. They studied the timescale of torsional changes causing the bracket to flip between various conformations, arguing that the timescale for torsional changes is expected to be shorter than the diffusion controlled ligation process making it pertinent to ion binding. They predicted that complexation was more likely to occur between the terminal S atoms of the $SCH_2CH_2SCH_2CH_2S$ "rope" of these xylyl thia-crown ethers. Whilst these calculations provide a good insight into the most likely binding conformation of a given ligand, they are somewhat restricted by the fact that they are based on gas phase predictions and do not include ligand reorganisation after binding or solvent effects.

The predominance of the anti or transoid conformation of the S-C-C-S in thioether compounds, results in the sulfur atoms occupying exodentate positions which are unfavourable for metal binding in macrocycles. This has resulted in a lot of work towards the design of compounds with preorganised endodentate sulfur atoms by introduction of rigid units into macrocyclic rings[15,16].

1.5 Aim of this work

The silver sensor presently in use at Kodak UK; Harrow, is the silver halide electrode which is unsatisfactory. The aim of this work is to develop a new silver sensor system. This work involves the design of new silver ionophores which should be selective for silver ion over a range of interfering cations. These new ionophores will be incorporated into new silver ion electrodes and tested in solutions of interest to Kodak.

1.6 Bibliography of Chapter 1

1. J. F. Hamilton, in "The Theory of the Photographic Process" (T. H. James Ed.), Macmillan Publishing Co, London, 1977, 105.
2. C. R. Berry, in "The Theory of the Photographic Process" (T. H. James Ed.), Macmillan Publishing Co., London, 1977, 88.
3. F. A. Cotton and G. Wilkinson, "Advanced Inorganic Chemistry", John Wiley & Sons, New York, 1980.
4. F. M. Hartley, *Chem. Rev*, 1973, **128**, 89.
5. R. Gut and J. Rueede, *J. Organomet. Chem.*, 1997, **128**, 89.
6. T. Futterer, A. Merz and J. Lex, *Angew. Chem. Int. Ed. Engl.*, 1997, **36**, 611.
7. L. F. Lindoy, *Pure Appl. Chem.*, 1997, **69**, 2179.
8. H. Frensdorff, *J. Am. Chem. Soc.*, 1971, **93**, 600.
9. H. Sakamato, J. Ishikawa and M. Otomo, *Bull. Chem. Soc. Jpn.*, 1995, **68**, 2831.
10. M. Oue, K. Akama, K. Kimura, M. Taneka and T. Shono, *J. Chem. Soc., Dalton Trans.*, 1989, 891.
11. R. Wolf, J. Hartman, J. Storey, B. Foxman and S. Cooper, *J. Am. Chem. Soc.*, 1987, **109**, 4328.
12. N. Dalley, J. Smith, S. Larson, K. Matheson, J. Christensen and R. Izatt, *J. Chem. Soc., Chem. Comm.*, 1975, 84.
13. J. Dale, *Acta Chem. Scand.*, 1973, **27**, 1115.
14. J. C. Lockhart, M. N. Mousley, M. N. Stuart Hill, N. P. Tomkinson, F. Texidor, M. P. Almajano, L. Escriche, J. Casabó, R. Sillanpää and R. Kivekäs, *J. Chem. Soc., Dalton Trans.*, 1992, 2889.
15. R. S. Glass, G. S. Wilson and W. N. Setzer, *J. Am. Chem. Soc.*, 1980, **102**, 5068.
16. B. de Groot, A. Jenkins and S. J. Loeb, *J. Inorg. Chem.*, 1992, **31**, 203.

CHAPTER TWO

Synthesis of Novel Silver Ionophores

2.1 Introduction

2.1.1 DMIT Building Blocks

The ionophores studied in this work are based on the 1,3-dithiole-2-thione-4,5-dithiolate (DMIT) building block. These molecules form a very important part of heterocyclic chemistry, with major interest resulting from their applications in modern material science and their use as building blocks on tetrathiafulvalene (TTF) chemistry. The rich redox chemistry of 1,3-dithioles and, in particular, the polarizability of the sulfur atoms makes their chemistry very interesting as they can support a number of stable oxidation states as outlined in Figure 2.1

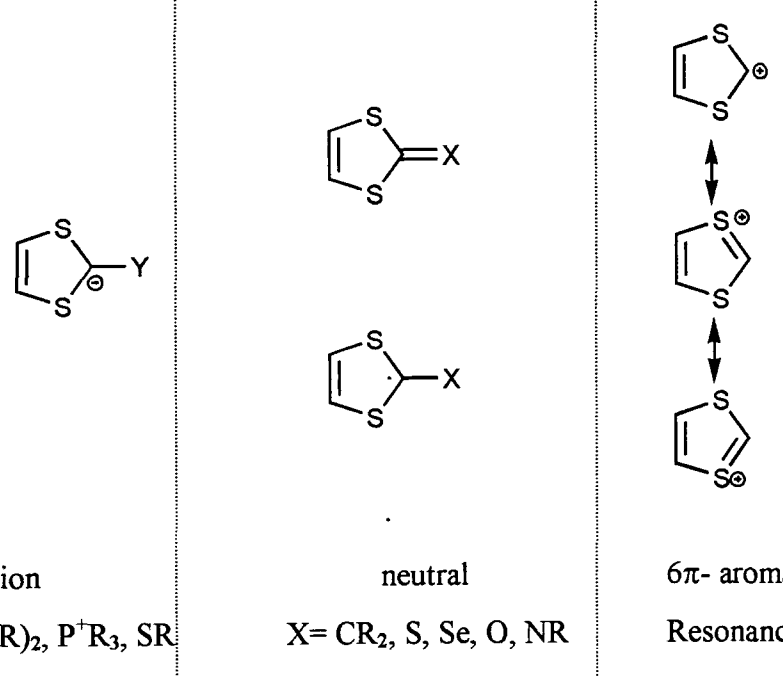

8 π - anion	neutral	6π- aromatic
Y = H, $P(O)(OR)_2$, P^+R_3, SR	X= CR_2, S, Se, O, NR	Resonance hybrids

Figure 2.1 Stable oxidation states of the 1,3-dithiole system. [1]

The original preparation of DMIT was as a side product of a reaction where Fetkenheuer *et al*[2] attempted to prepare the all sulfur analogue of the product from the Kolbe synthesis of oxalic acid.[3] Since then it has been prepared in a variety of ways and the most convenient synthesis is that developed by Hoyer *et al*[4] which involves the reaction of carbon disulphide with elemental sodium, forming the Na_2DMIT salt in solution; further reaction of this species with zinc chloride and tetraethylammonium bromide allows the

DMIT to be trapped as the tetraethylammonium salt of its zinc chelate, as outlined in scheme 2.1

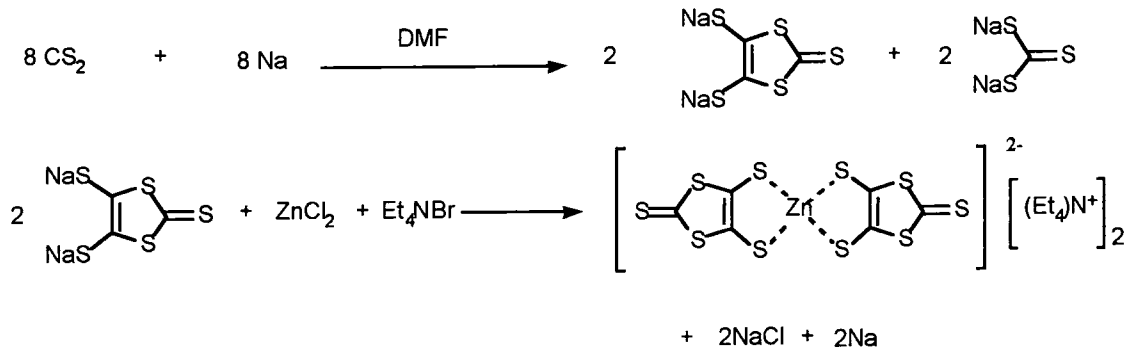

Scheme 2.1 Present synthesis of DMIT

The mechanism of this reaction has been widely investigated by many groups and is still a matter of some debate. Initial investigations involved attempts to trap intermediates using high performance liquid chromatography (HPLC)[5] whilst other groups used electrochemical techniques.[6] The presently accepted mechanism involves the reduction of carbon disulfide forming a radical species which dimerises to form a tetrathiooxalate species which reacts with two further equivalents of carbon disulfide and a final reduction to form the disodium salt of DMIT, scheme 2.2.

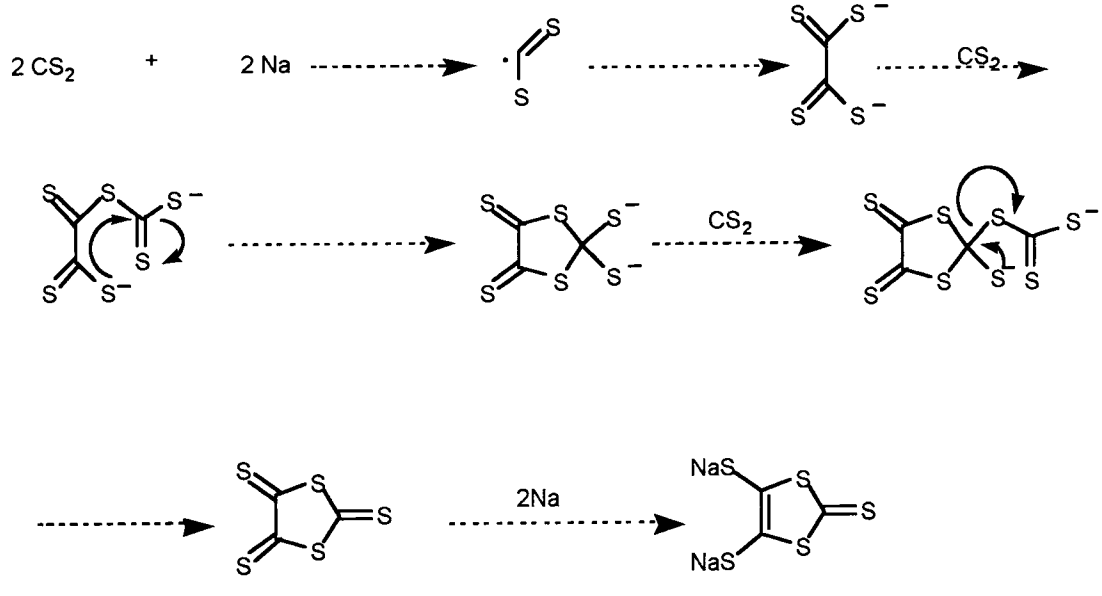

Scheme 2.2 Mechanism of Na_2 DMIT synthesis

2.1.2 TTF Building Blocks

A class of building blocks used in this study are those based on tetrathiafulvalene (TTF). These compounds can be prepared in various ways depending on the functionalisation required. The scope and versatility of the TTF framework is outlined in Figure 2.2

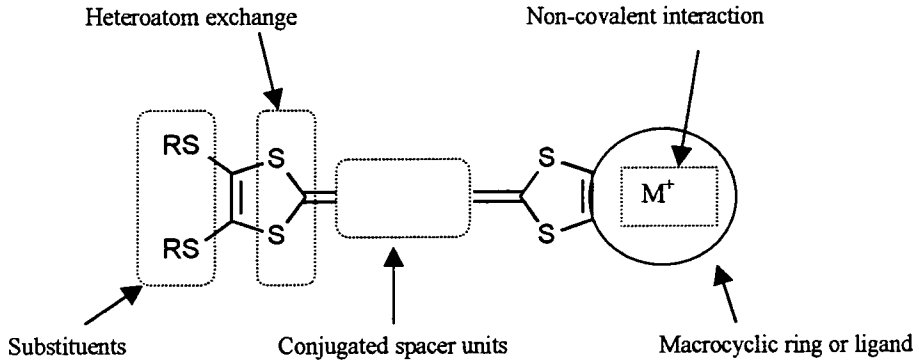

Figure 2.2 Schematic representation of the versatility of TTF building blocks [1]

As a result of the intense study of TTF derivatives for the preparation of electrically conducting and superconducting solids there now exists a diverse range of synthetic methodologies for framework assembly[7]. The key step in the majority of the syntheses of TTFs involve the formation of the central C=C bond, and this is assembled by coupling reactions. These methods involve joining the two halves of the TTF molecule involving the formation of the central C=C bond in the last step and they can be applied to symmetrical and unsymmetrical molecules making this the most widely used method. Within this class of reactions the coupling can be achieved chemically, photochemically or electrochemically depending on the functionalisation required. Other methods rely on the central C=C bond already formed and dithiole rings are assembled onto it, these are termed non-coupling methods. The non-coupling methods are not as widely used where sulfur is substituted for other chalcogens, however, they do account for all the presently known methods for preparing the tetratellurafulvalenes. Of the preparative methods, one stands out as the workhorse in TTF synthesis and this is the coupling reaction discovered by Corey, Corey and Winter[8]. This method involves the coupling of DMIT "half units" using trivalent phosphorus compounds (tri methyl-, ethyl- or phenyl- phosphites) as shown in scheme 2.3.

These couplings can be symmetrical (self coupling) or asymmetrical (cross coupling). The scope of this reaction is very wide and of particular interest is the cross coupling reaction.

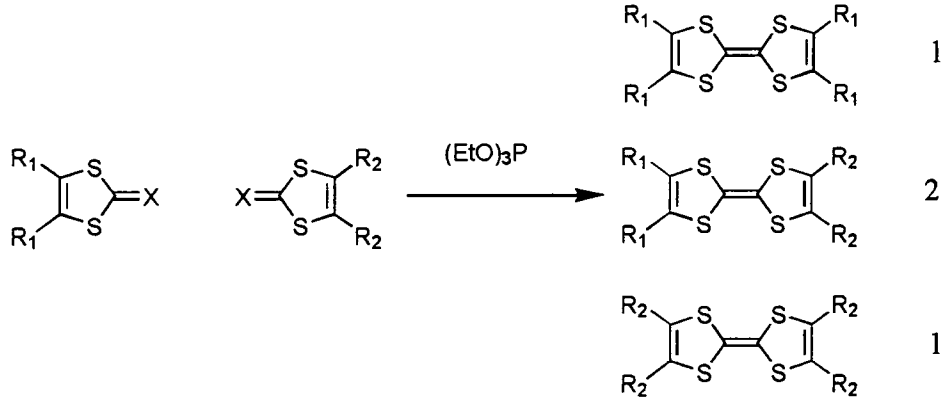

Scheme 2.3 Synthesis of unsymmetrical TTFs, where X = S, O, Se, showing the stoichiometry of the statistical mixture of random coupling.

The proportion of the required cross coupled product can be increased by raising the concentration of one of the half units, inevitably leading to a concomitant high concentration of one self coupled TTF half units. The separation of mixtures can (and often does) pose serious problems, resulting in ease of separation being paramount in choice of coupling strategy. There are no "rules " governing the outcome of cross coupling reactions but rather a few "pointers" which may be followed to achieve the desired product. The ratio of products may be also be altered by activating one of the DMIT units, which can be achieved by a transchalcogenation reaction[9] where the thione is converted to a ketone using mercuric acetate in chloroform-glacial acetic acid solution, as shown in scheme 2.4.

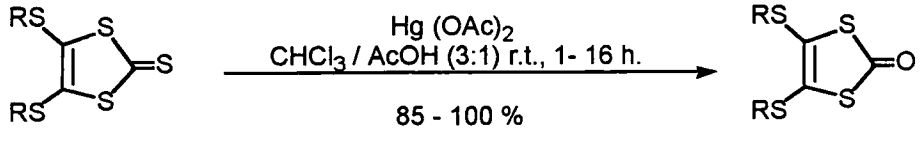

R = alkyl

Scheme 2.4 Conversion of a thione to a ketone

Reacting one of the half units as a ketone can favour the cross coupled product particularly where the ketone has electron withdrawing groups attached. Careful selection of the half units will allow separation of any self coupled products.

The mechanism of this reaction proceeds through a Wittig type mechanism as outlined in scheme 2.5[10].

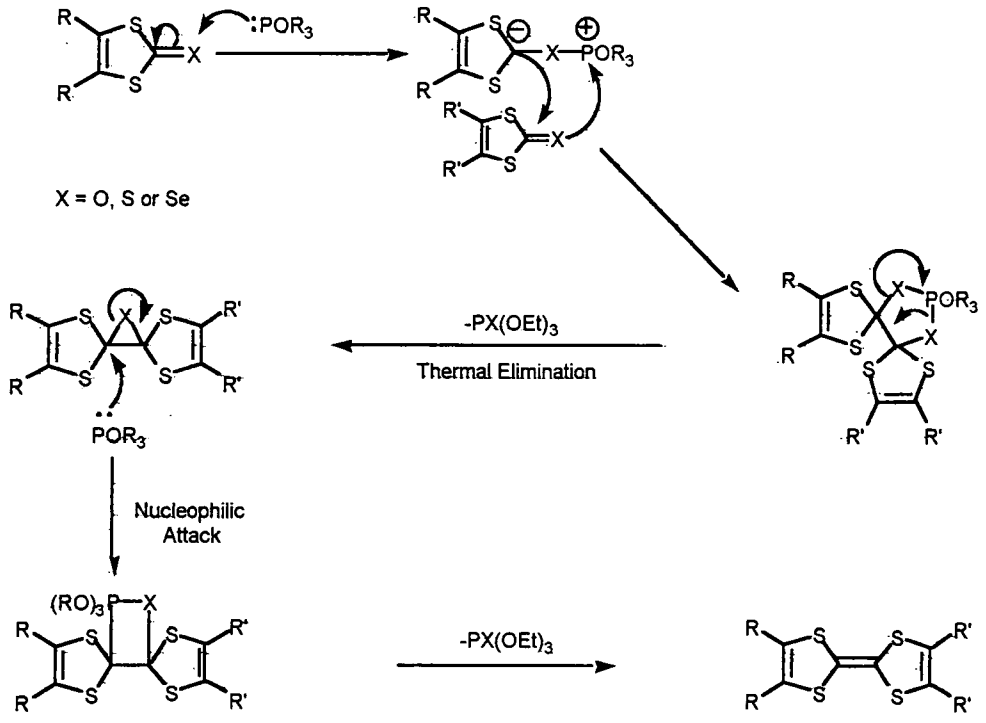

Scheme 2.5 Mechanism of TTF cross coupling reaction.

Initial attack of one molecule of trialkylphosphite ketone on the chalcogen of the C=X group polarises the bond making the carbon nucleophilic allowing it to attack a second equivalent of C=X forming a five membered ring which collapses, eliminating one equivalent of trialkyl phosphate forming an epoxide. This is then attacked by a second equivalent of trialkyl phosphite forming a four membered ring which eliminates a further equivalent of trialkyl phosphate forming the final cross coupled TTF. It is the strength of the P=X bond which drives this reaction.

2.2 Experimental

2.2.1 General Methods

2.2.1.2 Synthetic

Reactions were carried out under an inert atmosphere of argon, the gas first being dried by passing it through a column of phosphorus pentoxide. All reagents were of commercial quality and used as supplied (unless otherwise stated). Solvents were dried and distilled using the following reagents; diethyl ether and tetrahydrofuran (sodium metal); chloroform and dichloromethane (phosphorus pentoxide); methanol (magnesium methoxide). Acetone used was analytical grade and was used without further purification. Column chromatography was carried out using Merck silica gel (70-230 mesh).

2.2.1.2 Characterisation

Melting points were recorded on a Kofler hotstage microscope apparatus and were uncorrected. Infra-red spectra were recorded on a Perkin-Elmer 337 spectrophotometer with samples being prepared as KBr disks or as films on sodium chloride plates. Proton NMR spectra were recorded on Varian Gemini 200 (operating frequency of 199.9077 Hz) and XL 400 (operating frequency of 399.9906 Hz) instruments. Carbon-13 NMR spectra were recorded on Varian Gemini 200 and 400 instruments. Unless otherwise stated chemical shift values are quoted in ppm relative to tetramethylsilane (TMS) as an internal reference (0 ppm) and coupling constants are quoted in Hz. Mass spectra were obtained on a VG 7070E instrument with ionisation modes as indicated; the ionising gas used was ammonia.

2.2.2 Compounds Synthesised

Phenylmethylthia-2-ethanol **2**

To a solution of benzyl mercaptan (10 g, 80.51 mmol) and sodium ethoxide from slow addition of sodium (1.86 g, 80.51 mmol) to dry ethanol (200 ml)) was added chloroethanol (6.48 g, 80.51 mmol), the reaction mixture was raised to reflux temperature and stirred for 12 h. After cooling, the solvent was removed and the residue taken up in chloroform (200 ml), washed with water (100 ml) and dried ($MgSO_4$); evaporation of solvent in vacuo afforded a colourless liquid. The product was distilled using a Kugul Rohr apparatus to afford **2** (12.3 g, 91%) b.p. 150 °C @ 0.1 mbar; δ_H 250 MHz, $CDCl_3$), 7.36 - 7.21 (5H, m), 3.72 (2H, s), 3.67 (2H, t, *J* 6), 2.63 (2H, t, *J* 6) and 2.15 (1H, bs). These data are in good agreement with literature data.[11]

Benzyl 2-iodoethyl sulfide **3**

To a solution of compound **2** (0.5 g, 2.97 mmol) in dry diethyl ether (50 ml) was added phosphorus triiodide (1.83 g, 4.46 mmol). This solution was stirred for 4 h; water (100 ml) was slowly added and the organic layer washed with brine (3 x 50 ml), dried ($MgSO_4$) and concentrated in vacuo to yield a colourless oil **3** (0.83 g, 81%); δ_H (200 MHz, $CDCl_3$) 7.38 - 7.27 (5H, m), 3.75 (2H, s), 3.18 (2H, t, *J* 10) 2.87 (2H, t, *J* 10). These data are in good agreement with literature data. [12]

Bis(tetraethylammonium)bis(1,3-dithiole-2-thione-4,5-dithiolato) zincate **4**

This was prepared according to the literature method and isolated as a red solid, m.p. 202-205 °C (lit., mp[4] 208-210 °C).

4,5-Bis(2'-cyanoethylthio)-1,3-dithiole-2-thione **5**

This was prepared according to the literature method and isolated as a yellow solid, m.p. 82°C (lit., mp[13] 84°C).

General procedure for compounds **6a-d**:

To a solution of **5** (1 g, 3.28 mmol) in chloroform (50 ml) at room temperature was added a solution of caesium hyroxide (0.61 g, 3.28 mmol) in ethanol (5 ml) and stirred for 1.5 h, the appropriate alkyl iodide (3.28 mmol) was then added and the mixture stirred for 12 h. The solvent was removed in vacuo and the product purified by column chromatography (silica gel, eluent chloroform : hexane 1 : 1 v/v) to afford the following compounds.

4(Methylthio)-5-(2'-cyanoethylthio)-1,3-dithiole-2-thione **6a**

From methyl iodide (0.47 g, 3.28 mmol) and isolated as an orange solid , (0.56 g, 63%); mp 90-91° C (lit.,[14] mp 90-91° C); δ_H (200 MHz, $CDCl_3$) 3.08 (2H, t, *J* 6), 2.78 (2H, t, *J* 6) and 1.56 (3H, s), this compared well with the literature data.[15]

4(Ethylthio)-5-(2'-cyanoethylthio)-1,3-dithiole-2-thione **6b**

From ethyl iodide (0.51 g, 3.28 mmol) and isolated as a burgundy solid (0.52 g, 52%); mp 43 - 44 °C; m/z (EI^+) 279 (M^+=, 100 %); δ_H (200 MHz, $CDCl_3$) 3.06 (2H, t, *J* 7 Hz), 2.93 (2H, q, *J* 8), 2.72 (2H, t, *J* 7), 1.34 (3H, t, *J* 8); δ_C ($CDCl_3$) 210.34, 140.78, 132.57, 117.02, 41.96, 31.91, 23.26, 23.04 and 18.72; ν_{max} (NaCl, film)/ cm^{-1} 2249 and 1064; Analysis found % C 34.34, H 3.24, N 4.70 ($C_8H_9S_5N$ requires C 34.38, H 3.25, N 5.0).

4(Isopropylthio)-5-(2'-cyanoethylthio)-1,3-dithiole-2-thione **6c**

From isopropyl iodide (0.56 g, 3.28 mmol) and isolated as a burgundy oil (0.53 g, 37%); m/z (EI^+) 363 (M^+, 100 %); Mass Spectrometry (high resolution) for $C_9H_{11}N_5$ requires 292.9495, Analysis found 292.9485; δ_H (200 MHz, $CDCl_3$) 3.42 (1H, h, *J* 6), 3.09 (2H, t, *J* = 6 Hz), 2.72 (2H, t, *J* 6), and 1.36 (6H, d, *J* 6); δ_C ($CDCl_3$) 210.54, 140.78, 132.57, 117.02, 41.96, 31.91, 23.26, 23.04, and 18.72; ν_{max} (NaCl, film)/ cm^{-1} 2250 and 1065.

4(Butylthio)-5-(2'-cyanoethylthio)-1,3-dithiole-2-thione **6d**

From butyl iodide (0.60g, 3.28 mmol) and isolated as an orange / brown solid (1.01 g, 50%); mp 60-61 °C; m/z (EI^+) 307; Mass Spectrometry (high resolution) for $C_{10}H_{13}N_5$ requires 306.9652, Analysis found 306.9650; δ_H (200 MHz, $CDCl_3$) 3.06 (2H, t, *J* = 6 Hz), 2.92 (2H, t, *J* 8), 2.72 (2H, t, *J* 8), 1.73 - 1.56 (2H, m), 1.54 - 1.32 (2H, m) and 0.91 (3H, t, *J* 7); δ_C ($CDCl_3$) 210.30, 143.17, 128.52, 117.08, 36.33, 31.88, 31.61, 21.65, 18.78 and 13.48; ν_{max} (NaCl, film)/ cm^{-1} 2249 and 1062.

General Procedure for compounds **7a-d**:

To a solution of **6a-d** (as appropriate) (1.79 mmol) in chloroform (50 ml) at room temperature was added a solution of caesium hydroxide (0.30 g, 1.79 mmol) in methanol (5 ml) and stirred for 1.5 h. The ligating chain iodide **3** (2.69 mmol except for **7c** which required 7.16 mmol) was then added and the mixture stirred for a further 12 h. The solvent was removed in vacuo and the product purified by column chromatography (silica gel, eluent chloroform : hexane; 1 : 1 v/v) to give the following compounds.

4-(Methylthio)-5-(phenylmethylthioethylthio)-1,3-dithiole-2-thione **7a**

A burgundy oil (0.47 g, 72 %); m/z (CI^+) 363 (MH^+); Mass Spectrometry (high resolution) for $C_{13}H_{14}S_6$ requires 361.9420, Analysis found 361.9419; δ_H 200 MHz, $CDCl_3$) 7.34 - 7.24 (5H, m), 3.74 (2H, s), 2.95 - 2.85 (2H, m), 2.70 - 2.60 (2H, m) and 2.46 (3H, s) δ_C ($CDCl_3$) 210.59, 141.18, 137.53, 130.30, 128.78, 128.61, 127.28, 36.26, 36.17, 30.78 and 19.05; ν_{max} (NaCl, film)/ cm^{-1} 3081, 3058, 1600 and 1064.

4-(Ethylthio)-5-(phenylmethylthioethylthio)-1,3-dithiole-2-thione **7b**

A burgundy oil (0.34 g, 51%) m/z (CI^+) 377 (MH^+ Mass Spectrometry (high resolution) for $C_{14}H_{16}S_6$ requires 375.9677, Analysis found 375.9672 δ_H (200 MHz, $CDCl_3$) 7.38-7.25 (5H, m), 3.75 (2H, s), 2.98 - 2.83 (4H, m), 2.71 - 2.62 (2H, m) and 1.33 (3H, t, *J* 6);δ_C ($CDCl_3$) 210.89, 138.95, 137.51, 133.52, 128.77, 128.60, 127.28, 36.27, 36.19, 30.85, 30.74 and 14.87; ν_{max} (NaCl, film)/ cm^{-1} 3058, 3025, 1600 and 1065.

4-(Isopropylthio)-5-(phenylmethylthioethylthio)-1,3-dithiole-2-thione **7c**

A burgundy oil (0.29 g, 37%) m/z (CI^+) 391 (MH^+) Mass Spectrometry (high resolution) for $C_{15}H_{18}S_6$ requires 389.9834, Analysis found 389.9830; δ_H (200 MHz, $CDCl_3$) 7.37 - 7.25 (5H, m), 3.75 (2H, s), 3.37 (1H, h *J* 6). 3.00 - 2.91 (2H, m), 2.71 - 2.60 (2H, m) and 1.31 (6H, d, *J* 6); δ_C ($CDCl_3$) 211.11, 137.54, 137.25, 136.65, 128.81, 128.66, 127.35, 41.73, 36.31, 36.25, 30.78 and 23.22; ν_{max} (NaCl, film)/ cm^{-1} 3059, 3025, 1600 and 1066.

4-(Butylthio)-5-(phenylmethylthioethylthio)-1,3-dithiole-2-thione **7d**

A burgundy oil (0.68 g, 95%) m/z (CI^+) 406 (MH^+) Mass Spectrometry (high resolution) for $C_{16}H_{20}S_6$ requires 403.9991, Analysis found 403.9996; δ_H (200 MHz, $CDCl_3$) 7.37 - 7.24 (5H, m), 3.74 (2H, s), 2.87 - 2.81 (4H, m), 2.70-2.61 (2H, m) 1.69 -1.52 (2H, m) and 1.48 - 1.34 (2H, m) and 0.93 (3H, t, *J* 7); δ_C ($CDCl_3$) 210.84, 139.43, 137.49, 132.88, 128.74, 128.56, 127.23, 36.27, 36.23, 36.12, 31.48, 30.70, 21.53 and 13.43; ν_{max} (NaCl, film)/ cm^{-1} 3059, 3025, 1601 and 1064.

General Procedure for compounds **8a** to **8d**:

To solution of **7a-d** (as appropriate) (0.25 mmol) in chloroform / acetic acid (3:1 v/v, 20 ml) was added mercuric acetate (0.625mmol) at room temperature and stirred for 16 h. The precipitate was recovered by filtration using celite and washed with chloroform (3 x 25 ml). The organic extract was refluxed with activated charcoal, washed with sodium bicarbonate (4 x 25 ml), dried ($MgSO_4$) and concentrated in vacuo yielding the following compounds.

4-(Methylthio)-5-(phenylmethylthioethylthio)-1,3-dithiole-2-one **8a**

A clear oil (70 mg, 73 %); m/z (EI^+) 346; δ_H 200 MHz, $CDCl_3$) 7.32 - 7.20 (5H, m), 3.74 (2H, s), 2.95 - 2.85 (2H, m), 2.70 - 2.60 (2H, m) and 2.44 (3H, s); δ_C ($CDCl_3$) 189.53, 137.68, 132.12, 128.83, 128.65, 127.29, 121.86, 36.20, 36.11, 30.81, and 19.22; ν_{max} (NaCl, film) cm^{-1} 2919, 1667 and 1614 , Analysis found % C, 44.76, H 4.07 ($C_{13}H_{14}S_5O$) requires C, 45.06, H, 4.07)

4-(Ethylthio)-5-(phenylmethylthioethylthio)-1,3-dithiole-2-one **8b**

A clear oil (34 mg, 51%) m/z (EI^+) 360 δ_H (200 MHz, $CDCl_3$) 7.25 - 7.19 (5H, m), 3.67 (2H, s), 2.84 - 2.71 (4H, m), 2.61 - 2.55 (2H, m) and 1.24 (3H, t, *J* 6). δ_C ($CDCl_3$) 189.70, 137.68, 129.74, 128.84, 128.67, 127.32, 124.86, 36.24, 36.17, 30.84, 30.82 and 14.89; ν_{max} (NaCl, film)/ cm^{-1} 2963, 2924, 1667 and 1612; Analysis found % C, 46.49; H 4.07 ($C_{14}H_{16}S_5O$ requires C 46.43; H 4.47).

4-(Isopropylthio)-5-(phenylmethylthioethylthio)-1,3-dithiole-2-one **8c**

A clear oil (53 mg, 55 %); m/z (EI^+) 374; δ_H (200 MHz, $CDCl_3$) 7.29 - 7.19(5H, m), 3.67 (2H, s), 3.23 (1H, h *J* = 6 Hz). 2.90 - 2.82 (2H, m), 2.62 - 2.54 (2H, m) and 1.26 (6H, d, *J* 6); δ_C ($CDCl_3$) 189.78, 132.20, 128.84, 128.67, 127.60, 127.33, 41.48, 36.26, 36.21, 30.84, 29.68 and 23.14; ν_{max} (NaCl, film)/ cm^{-1} 2963, 2921, 2851, 1667 and 1608; Analysis found % C, 48.20; H 4.84 ($C_{15}H_{18}S_5O$ requires C 48.09; H 5.07).

4-(Butylthio)-5-(phenylmethylthioethylthio)-1,3-dithiole-2-one **8d**

A clear oil (69 mg, 72 %);m/z (EI^+) 388; δ_H (200 MHz, $CDCl_3$) 7.37-7.24 (5H, m), 3.74 (2H, s), 2.95 - 2.79 (4H, m), 2.70 - 2.61 (2H, m) 1.69 - 1.55 (2H, m), 1.48 - 1.34 (2H, m) and 0.93 (3H, t, *J* 7); δ_C ($CDCl_3$) 189.71, 137.67, 130.20, 128.83, 128.65, 127.30, 124.30, 36.33, 36.20, 36.15, 30.80, 21.60 and 13.51; ν_{max} (NaCl, film)/ cm^{-1} 2957, 2926, 1667 and 1612. Analysis found % C, 49.34; H 5.17 ($C_{16}H_{20}S_5O$ requires C 49.45; H 5.18).

4,5-Bis(butylthio)-1,3-dithiole-2-thione **10**

This was prepared according to the literature method and isolated as a burgundy oil (2.16 g, 50%); δ_H (200 MHz, $CDCl_3$) 2.87 (2H, t, *J* 6) 1.75 - 1.58 (2H, m), 1.56 - 1.36 (2H, m), 0.94 (2H, *J* 7), this compared well with literature data[16].

4,5-Bis(phenylmethylthioethylthio)-1,3-dithiole-2-thione **11**

To a solution of **4** (1.0 g, 3.28mmol) in chloroform (50 ml) was added a solution of caesium hydroxide (1.38 g, 8.21 mmol) in methanol (5 ml) and stirred for 1.5 h. The ligating chain iodide **3** (2.30 g, 8.26 mmol) was added and the mixture stirred at room temperature for 12 h. The solvent was removed in vacuo and the product purified by column chromatography (silica gel, eluent chloroform : hexane, 1 : 1 v/v) to give a burgundy liquid (0.70 g, 43%); m/z (CI^+) 498; (M^+) Mass Spectrometry (high resolution) for $C_{21}H_{22}S_7$ requires 497.9758, Analysis found 497.9767 δ_H (200 MHz, $CDCl_3$) 7.34 - 7.19 (5H, m), 3.74 (2H, s), 2.97 - 2.88 (2H, m) and 2.59 - 2.68 (2H, m); δ_C ($CDCl_3$) 210.43, 137.53, 136.19, 128.74, 128.64, 127.28, 36.21, 36.16 and 30.72; ν_{max} (NaCl, film)/ cm^{-1} 3059, 3024, 1600 and 1064.

4,5-Bis(2'-cyanoethylthio)-1,3-dithiole-2-one **12**

This was prepared according to the literature method and isolated as a white solid m.p. 81° C (lit., mp[9] 83° C).

4,5-bis(2'-cyanoethylthio)-4', 5'-bis(phenylmethylthioethylthio)tetrathiafulvalene **14**
The literature method was used to produce an orange solid m.p. 148-150° C (lit., mp[16] 149-152° C) δ_H (200 MHz, $CDCl_3$) 3.09 (4H, t, *J* 8), 2.83 (4H, t, *J* 8), 2.72 (2H, t, *J* 8), 1.70-1.52 (4H, m), 1.51-1.38 (4H, m) and 0.93 (6H, t, *J* 7). this compared well with literature data[16].

4,5-bis(butylthio)- 4', 5'-bis(butylthio)tetrathiafulvalene **9**

To a solution of **14** (0.250 g, 0.40 mmol) in tetrahydrafuran/methanol (1:1) v/v (100 ml) was added sodium hydride (60% suspension in oil) (0.31 g, 1.36 mmol) at room temperature and stirred for 1 h. To this solution the iodide **3** (0.38 g, 1.36 mmol) was added in tetrahydrafuran (10 ml) and the mixture stirred for 12 h. The solvent was removed in vacuo and the product purified by column chromatography (silica gel, eluent chloroform :

hexane 1 : 1v/v) to give an orange oil (0.18 g, 67%); m/z (CI^+) 744; (M^+) Mass Spectrometry (high resolution) for $C_{32}H_{40}S_{10}$ requires 744.0340, Analysis found 744.0337 δ_H (200 MHz, $CDCl_3$) 7.35 - 7.24 (10H, m), 3.70 (4H, s), 2.78 - 2.92 (8H, m), 2.50 - 2.63 (4H, m) 1.66 - 1.50 (4H, m) and 1.50 - 1.25 (4H, m) and 0.88 (6H, t, *J* 8); δ_C ($CDCl_3$) 137.90, 128.85, 128.59, 128.08, 127.83, 127.12, 112.21, 109.17, 36.05, 36.02, 35.75, 31.69, 30.84, 21.59 and 13.56; ν_{max} (NaCl, film)/ cm^{-1} 3059, 3025 and 1600.

2.3 Results

2.3.1 DMIT Results

The aim of this work is to synthesise silver ligating chains suitable for attachment to the DMIT building block, functionalisation of this molecule will be at the 4,5 sites (Figure. 2.3). Ideally one of the sites will be functionalised with a silver ligating group and the other site with a hydrophobic alkyl chain, which will allow the hydrophobicity of this molecule to be varied, the series selected being methyl, ethyl, isopropyl and butyl. The isopropyl group was chosen as it is a relatively bulky group allowing subsequent complexation analysis to determine if this group will affect the binding of silver.

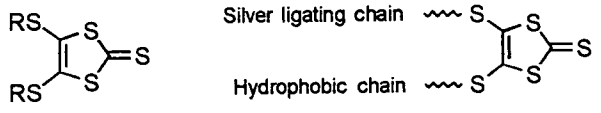

(i) (ii)

Figure 2.3 DMIT unit showing (i) building block and (ii) proposed functionalisations.

The design of a suitable silver ligating chain was based on an examination of the literature. From the earlier discussion (Section 1.6) this fragment should contain sulfur atoms[17] and allow a mode of binding where the Ag^+ can adopt a linear conformation.[18] There is also some evidence to suggest that inclusion of an aromatic group also favours silver binding.[19,20] The SCH_2CH_2S bracket (as discussed in section 1.4) was incorporated into the acyclic ligating chain, this fragment has found widespread use in thiacrown systems.[21,22] The combination of these required fragments led to the proposal of the $PhCH_2SCH_2SH_2$- fragment which may be reacted as an iodide. The most useful method of functionalising the DMIT unit at the 4,5 positions is via a nucleophilic displacement reaction of an alkyl iodide.[23]

Iodide **3** was synthesised as outlined in scheme 2.6. Starting with the readily available precursor benzylmercaptan **1**, 2- chloroethanol was used to extend the chain by a further two carbons, producing compound **2**, which was converted to the iodide **3** using phosphorus triiodide.

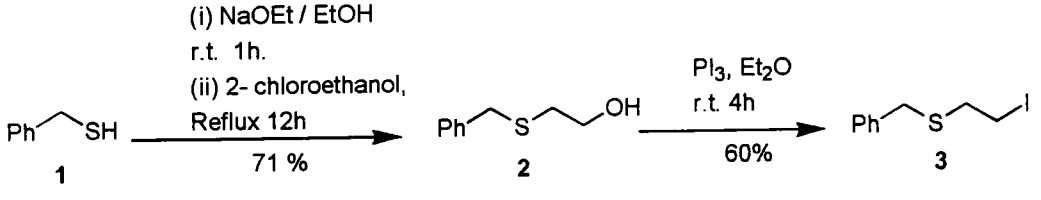

Scheme 2.6 Preparation of ligating chain as an iodide.

Compound **3** was a colourless oil which decomposed after a few days. This did not pose a problem as compound **2** was stable and could be synthesised on a multi-gram scale allowing compound **3** to be synthesised rapidly as required. Both compounds **2**[24] and **3**[11] have been made previously via a different route.

Zincate salt **4**[4] was reacted with 3-bromopropionitrile in refluxing acetonitrile to yield 4,5-bis(2-cyanoethylthio)-1,3-dithiole-2-thione **5** in good yield[13] as outlined in scheme 2.7. Deprotection of one of the cyanoethyl chains of **5** using 1 equivalent of CsOH in MeOH followed by reaction with one equivalent of the appropriate alkyl iodide produced the mono alkylated products **6a-d**. The yields of these reactions were 40-53 %, except for **6c** which was less than 5 % from initial attempts,. This low yield was presumably due to a competing reaction of the isopropyl cation where it lost a proton and formed propene. The yield in this reaction was increased to 40 % by reaction with four equivalents of the isopropyl iodide. Of these intermediates **6a,b,d** were solids whilst **6c** was an oil. In the next step, the alkyl substituted intermediates **6a-d** were reacted with one equivalent of caesium hydroxide to remove the second cyanoethyl protecting group and the derived thiolate anion was reacted with freshly-made ligating chain **3** to produce the thione compounds **7a-d**. These products were all viscous wine /brown oils after purification by column chromatography. A series of corresponding ketones **8a-d** was synthesised by reaction with mercuric acetate yielding colourless oils.

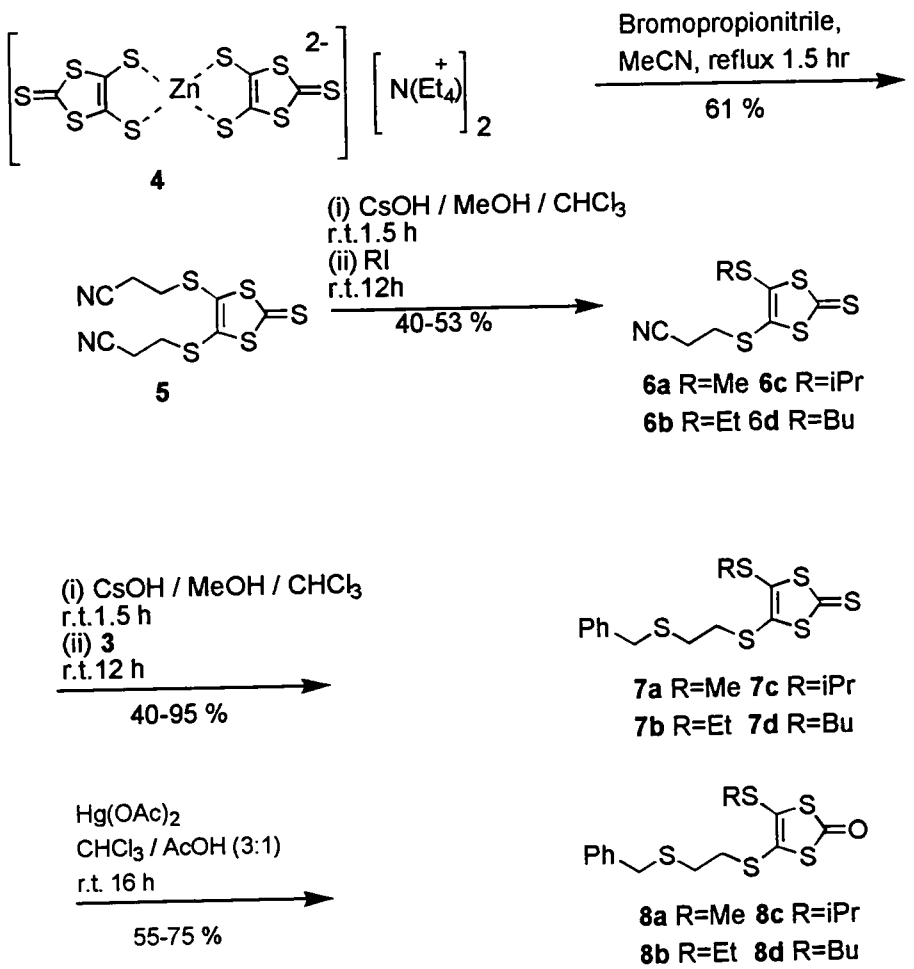

Scheme 2.7 Preparation of compounds **7a-d** and **8a-d** based on DMIT building block.

2.3.2 Compounds based on TTF building block.

Recent work on the application of thiacrown TTFs in metal sensing systems prompted this work.[25] We were interested in developing a TTF sensory system using an acyclic metal binding site. The same functionalisation as that used for the DMIT unit was envisaged, i.e. a hydrophobic domain and a ligating domain, resulting in molecule **9** being proposed. This molecule offers great potential for silver binding owing to the availability of two flexible ligating chains which between them contain four sulfur atoms.

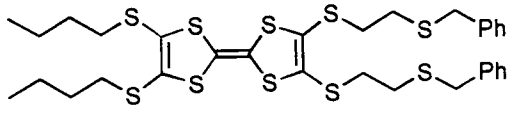

9

Hydrophobic domain Ligating domain

Figure 2.4 Proposed TTF ionophore.

Several synthetic approaches were attempted in pursuit of molecule **9.** In the first approach as outlined in scheme 2.8, the bis butyl functionalised thione **10** was prepared directly from the zincate salt **4** by reaction with four equivalents of butyl iodide, whilst the ligating half unit **11** was prepared from **5** upon reaction with ligating chain **3**. Compounds **10** and **11** were directly coupled in refluxing trimethylphosphite, and the reaction was monitored by TLC. This reaction produced several products which were very difficult to separate. The various fractions obtained by column chromatography were analysed by mass spectrometry which revealed qualitatively that some of the desired product **9** had been produced along with self-coupled products. However, the mixture of products defied separation so a new approach was required.

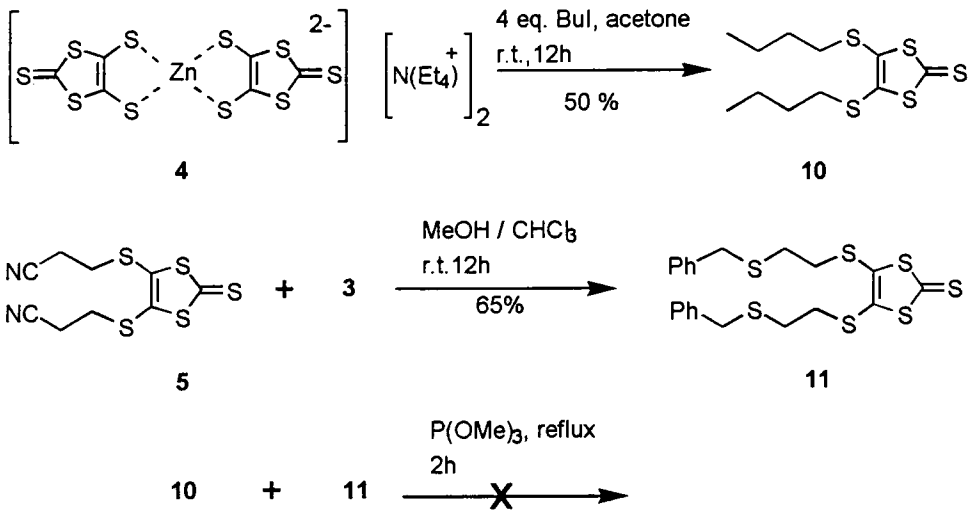

Scheme 2.8 Initial attempts at cross couplings reacting both half units as thiones.

In an attempt to overcome the separation problems encountered in scheme 2.8 another route was tried, whereby one of the half units remained protected by cyanoethyl chains, thus making it more polar allowing easier separation as shown in scheme 2.9. In this reaction the bis butyl thione **10** was coupled to the bis protected thione **5**. This allowed easier separation than that for scheme 2.8, but the product formed could not be isolated in reasonable purity.

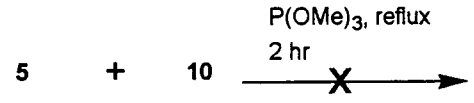

Scheme 2.9 Attempt at cross coupling to produce a bis cyanoethyl protected TTF

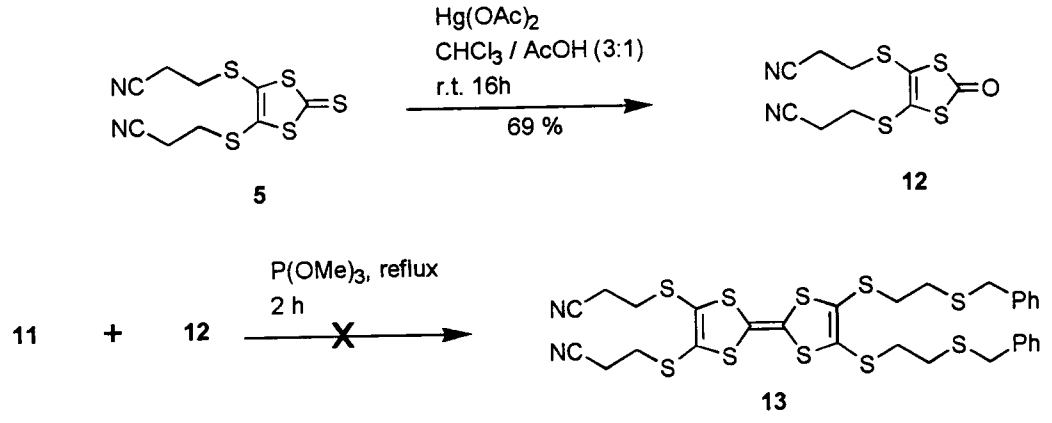

Scheme 2.10 Unsuccessful cross-coupling reactions using one thione and one ketone half unit.

A cross coupling between a thione and ketone was attempted as this may lead to favouring of the cross coupled product as discussed in section 2.1.2. The ketone of the bis cyano protected dithiolato **12** was prepared in good yield from its corresponding thione **5** by reaction with mercuric acetate,[9] as shown in scheme 2.4. The bis ligating functionalised thione **11** was reacted with the bis protected ketone **12** as shown in scheme 2.10. Upon workup of the reaction no TTF products could be identified in the reaction mixture (these are normally identified owing to the ease with which these products stain on silica with iodine) indicating that no coupling had occurred.

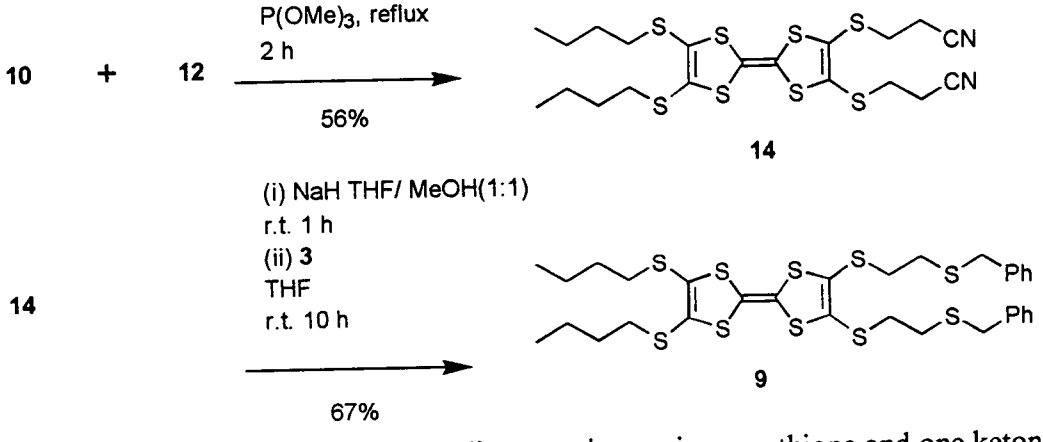

Scheme 2.11 Successful cross-coupling reactions using one thione and one ketone half unit.

In scheme 2.11 compound **10** was coupled to the **12** and this reaction proceeded cleanly allowing isolation of **14** as a bright orange solid after column chromatography. The final step in this synthesis, which involved the deprotection to form the dithiolate of **14**, followed by addition of 2 equivalents of **3** was carried out in tetrahydrofuran / methanol (1:1) v/v and produced an orange oil **9** in 67 % yield.

2.4 Conclusions

In this work two new sets of compounds have been synthesised. The DMIT compounds **8a-d** were produced in four steps from the zincate starting material in 5 to 25% overall yield. These compounds are suitable for incorporation into ion-selective electrodes and provide a good range of hydrophobicity which allows versatility in electrode design, this work is described in chapter 4. A TTF compound **9** was also synthesised by a convergent synthesis in 40% overall yield. The redox properties of this compound are potentially very interesting as no known work has been published on the use of non macrocyclic TTFs in sensor systems. This compound is examined in chapter 3 for its redox properties, affinity for silver ion and ultimately its potential as a redox active silver sensor.

2.5 Bibliography for Chapter 2

1. T. K. Hansen and J. B. Becher, *Adv. Mater.*, 1993, **5**, 288.
2. B. Fetkenheuer, H. Fetkenheuer and H. Lecus, *Chem. Ber.*, 1927, **60**, 2528.
3. E. Dreschel and H. Kolbe, *Ann. Chem. Pharm.*, 1868, **146**, 140.
4. G. Steimecke, R. Kirmse and E. Z. Hoyer, *Chem. Ber.*, 1975, **15**, 28.
5. J. Lodmell, W. Anderson, M. Hurley and J. Chambers, *Anal. Chim. Acta*, 1981, **129**, 49.
6. S. Wawzonek and S. Heilman, *J. Org. Chem.*, 1974, **39**, 511.
7. A. Krief, *Tetrahedron*, 1986, **42**, 1209.
8. E. Corey, F. Corey and R. Winter, *J. Am. Chem. Soc.*, 1965, **87**, 934.
9. K. Hartke, T. Kissel, J. Quante and R. Matusch, *Chem. Ber.*, 1980, **113**, 1898.
10. Y. Yoshida, T. Kawase and S. Yoneda, *Tetrahedron Lett.*, 1975, 331.
11. E. Eliel, L. Pilato and V. Badding, *J. Am. Chem. Soc.*, 1962, **84**, 2377.
12. U. Scöllkopf and R. Lonsky, *Synthesis*, 1983, 675.
13. N. Svenstrup, K. M. Rasmussen, T. K. Hansen and J. Becher, *Synthesis*, 1994, 809.
14. K. B. Simonsen, N. Svenstrup, J. Lau, O. Simonsen, P. Mork, G. J. Kristensen and J. Becher, *Synthesis*, 1996, **3**, 407.
15. N. Svenstrup and J. Becher, *Synthesis*, 1995, 216.
16. N. Le Navour, N. Robertson, E. Wallace, J. D. Kilburn, A. E. Underhill, P. N. Bartlett and M. Webster, *J. Chem. Soc., Dalton Trans.*, 1996, 823.
17. H. Frensdorff, *J. Am. Chem. Soc.*, 1971, **93**, 600.
18. F. A. Cotton and G. Wilkinson, "Advanced Inorganic Chemistry", John Wiley & Sons, New York, 1980 (Fourth Edition).
19. R. Gut and J. Rueede, *J. Organomet. Chem.*, 1997, **128**, 89.
20. W. Wróblewski and Z. Brzózka, *Sens. Actuators, B*, 1995, **24**, 183.
21. J. Casabó, L. Mestres, L. Escriche, F. Texidor and C. Pérez-Jiménez, *J. Chem. Soc., Dalton Trans.*, 1991, 1969.
22. M. Lai and J. Shih, *Analyst*, 1986, **111**, 165.
23. M. R. Bryce, *Chem. Soc. Rev.*, 1991, **20**, 355.
24. Z. Brzozka, P. Cobben, D. Reindoudt, J. Edema, J. Buter and R. Kellog, *Anal. Chim. Acta*, 1993, **273**, 139.
25. T. K. Hansen, T. Jørgensen, P. C. Stein and J. Becher, *J. Org. Chem.*, 1992, **57**, 6403.

CHAPTER THREE

Complexation Studies

3.1 Introduction

3.1.1 Metal Complexation by Redox Active Macromolecules

Redox active macrocyclic ligands have found applications in the field of metal complexation, in systems where the complexation of a guest metal ion results in a change in the electronic properties of the host macrocycle[1]. To understand these systems, the principle of chemical transduction has to be introduced[2]. A schematic diagram of a sensor molecule is shown in Figure 3.1

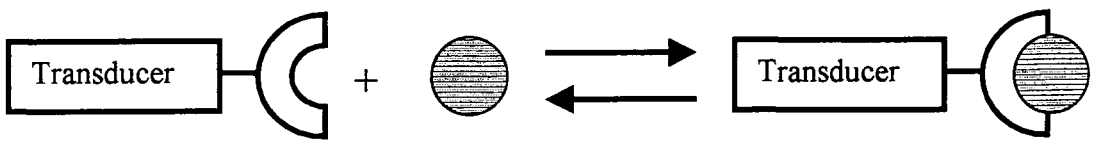

Figure 3.1 Schematic representation of a sensor molecule showing reversible binding of a guest molecule.

In principle a transducer can be any chemical moiety that undergoes an observable change in a physical property upon complexation of a guest molecule. The molecule has to possess (i) a binding site, (ii) a physical property that can be easily measured (UV absorption, redox activity, NMR chemical shift etc) and (iii) a good link (usually a conjugated system) between the binding site and the redox centre. This system allows the presence of a guest molecule to be detected in the sensor molecule, or conversely the binding of a guest molecule to be controlled by a physical property.

One of the first application of macrocycle cation electrochemical recognition was by Sagi, who reported on changes in the electrochemistry of a ferrocene complex **15** upon addition of a metal ion.[3] Two distinct voltammetric waves corresponding to complexed and uncomplexed were observed for Na^+ and Li^+ as guest species..

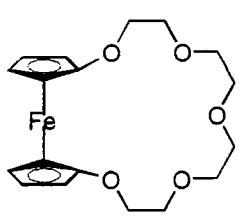

15

Other authors report redox systems where a single wave shifts in position relative to the original redox couple upon metal complexation.[4,5] These systems were studied using digital simulation by Kaifer *at al.* who concluded that two wave behaviour is observed when the binding constant is very large (typically > 10^4) and that weaker binding results in the shift of a single wave.[6] This is likely to be a kinetic effect as a single peak would be observed if the timescale of the complexation reaction was very fast whilst two peaks would be observed for slower complexations. The magnitude of the maximum shift is a complex function of factors such as the polarisablity of the redox system and the distance to, and orientation of, the ligand centre.[2]

3.1.2 Metal complexation by Tetrathiafulvalene Derivatives

It was only a matter of time before the cross fertilisation of the fields of tetrathiafulvalene (TTF) chemistry and supramolecular/macrocyclic chemistry produced TTF derivatives suitable for metal complexation. As a transducer, TTF is particularly appealing owing to its well established redox chemistry[7] which is outlined in scheme 3.1

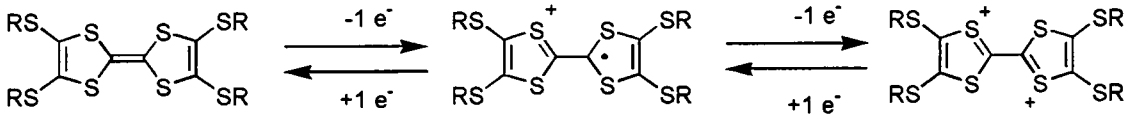

Neutral		Cation Radical		Dication	
7e	7e	6e	7e	6e	6e
non aromatic		aromatic	non aromatic	aromatic	aromatic

Scheme 3.1 Schematic representation of the oxidation states of a TTF molecule.

The first reported use of a TTF compound as an electrochemical transducer was by Hansen *et al.* [8] A macrocyclic TTF-crown compound **16** was synthesised and investigated by cyclic voltammetry (CV). They found an anodic (more positive) shift in the first oxidation wave E_1^{ox} of the TTF scan, but no change in the second oxidation wave E_2^{ox} upon addition of 250 equivalents of Na^+ as shown in Figure 3.2. The bound cation destabilises the radical cationic TTF by coulombic repulsion making the TTF more difficult to oxidise. The fact that the second oxidation peak does not move suggests that the metal ion is ejected before the potential at E_2^{ox} is reached.

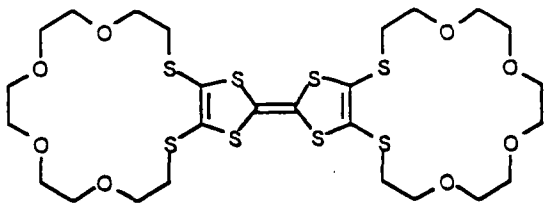

16

The exact shift in potential upon complexation was difficult to determine, as the E_1^{ox} peak moved and merged almost into the E_2^{ox} peak but was estimated to be 80-90 mV. On the reductive sweep of the CV it can be seen that the reduction peak E_1^{red} is unchanged upon metal complexation whilst E_2^{red} undergoes a similar shift to that observed for E_1^{ox}. This was interpreted as evidence for fast complexation of the metal ion to the TTF cation.

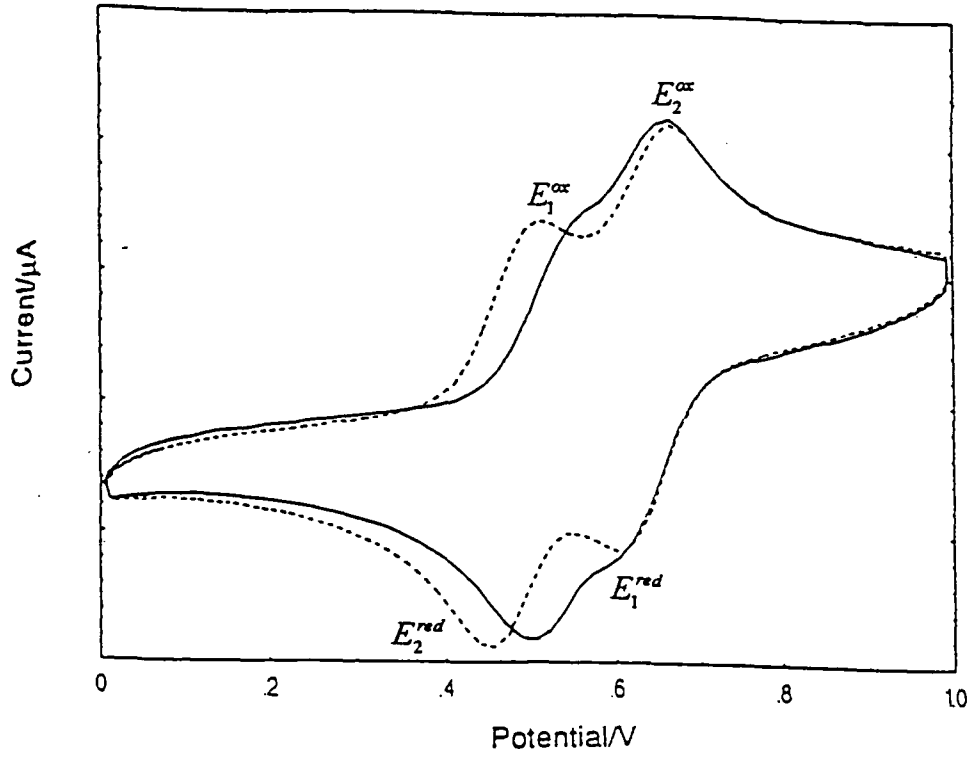

Figure 3.2 Cyclic voltammogram of **16** recorded versus a SCE electrode in MeCN at a scan rate of 100 mV s^{-1} with Bu_4NClO_4 as electrolyte (_____) and with 250 equivalents of $NaPF_6$ added (--------). [8]

In this work the complexation of Na^+ by **16** was also followed ^1H NMR. It was shown that shifts were observed for the $-SCH_2CH_2O-$ protons even at low molar ratios (7 and 23 equivalents) of added Na^+. This is interesting as the changes in the CV were observed at the much higher molar ratio of 250 equivalents.

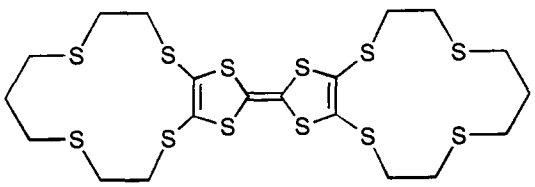

17

A TTF compound that showed a response towards silver ion was synthesised by Jørgensen *et al.*[9] This is a symmetrical TTF incorporating two S4 crown moieties **17**. The CV of this compound shows that it has two reversible oxidations, and that it undergoes a pronounced change upon addition of excess $AgClO_4$, the shifts in potential of E_1^{ox} and E_2^{ox} are 0.20 and 0.06 V respectively as shown in Figure 3.3.

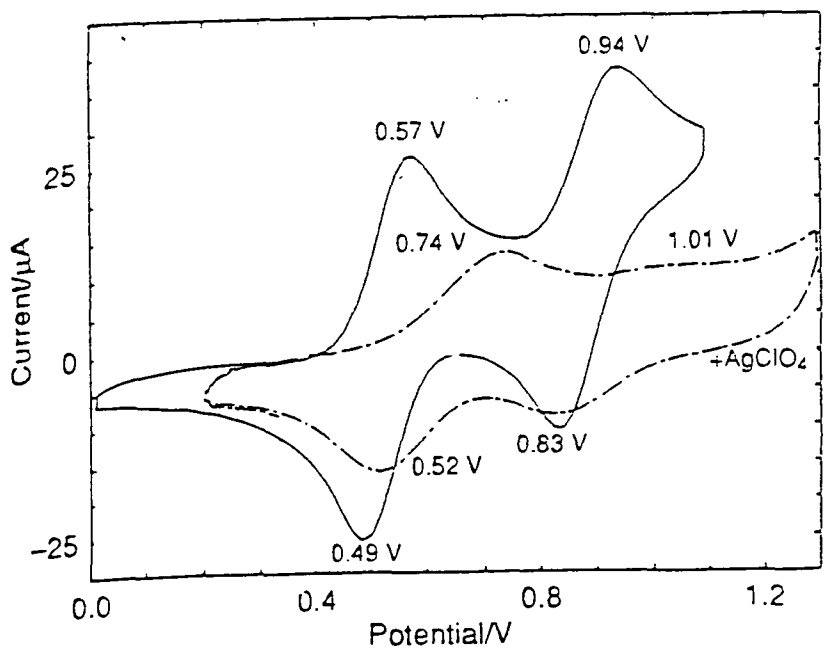

Figure 3.3 Cyclic voltammogram of **17** versus a SCE electrode recorded in MeCN at a scan rate of 100 mV s^{-1} with Bu_4NClO_4 as electrolyte (_____) and with excess $AgPF_6$ added (----------).

It is significant that there little change in the reduction peaks, which suggests that expulsion of the silver ion occurred allowing reduction of the now uncomplexed TTF. As no recomplexation occurred on the anodic sweep, it was assumed that the rate of silver complexation was slow.

Most recently Bryce *et al.* have synthesised a new range of unsymmetrical annealed TTF-S_2O_4 crowns and studied their metal binding by UV/Visible spectroscopic studies and solution electrochemical studies.[10] This paper provided the first reported spectroscopic studies of metal binding to crown-TTF systems, which allowed the authors to study the changes in the electronic spectra of several of the compounds upon complexation with Na^+, Ba^{+2} and Ag^+. These studies showed that the mono crown-TTFs formed 1:1 complexes with Na^+ whilst the bis crown-TTF formed both 1:1 and 1:2 complexes with Na^+. Electrochemical studies were also carried out with these compounds, and their result for bis crown-TTF **16** was very close to that reported by Hansen *et al.* [8], the first oxidation peak moved by 70 mV (c.f. 80 mV[8]) upon addition of 250 equivalents of Na^+. Similar experiments using the new monocrown-TTFs **18** and **19**, gave potential shift values for Na^+ binding of 25-35 mV, which, interestingly, is half that of the bis-crown.

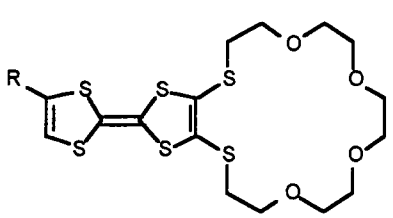

18 R= H

19 R= CO_2H

These studies were extended to silver and barium complexation where the greatest shift in oxidation potential was observed for silver of 70-75 mV, conforming with the spectroscopic data. These results are consistent with Ag^+ primarily binding at sulphur sites inducing a large perturbation in the electronic structure of the TTF moiety. The electrochemical data allowed an estimation of a stability constant for a mono crown-TTF with silver to be log K = 2.26 which was similar to the value obtained from the spectroscopic data.

3.2 Experimental

3.2.1 General Methods

3.2.1.1 Cyclic Voltammetry

Cyclic stationary electrode voltammetry to give it its full title, is the most versatile electroanalytical technique available for the mechanistic study of redox systems.[11] It allows the determination of thermodynamic properties such as redox potentials in addition to kinetic parameters such as rate of electron transfer in both homogeneous and heterogeneous systems.[12] It has found extensive use in the fields of organic, inorganic, electrochemical and analytical chemistry.

The technique involves cycling of the applied potential of an electrode and measuring the resultant current. A typical electrochemical cell consists of three electrodes, namely a working(W), counter(C) and reference electrode(R) as shown in Figure 3.4. The counter electrode serves to prevent current from flowing through the reference electrode.

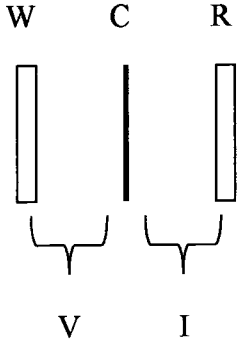

Figure 3.4 Schematic diagram of the three electrodes system used in cyclic voltammetry where W, C, and R represent the working, counter and reference electrodes, and V and I represent the applied potential and resultant current respectively.

The applied potential input has a triangular form, which sweeps the potential of the electrode between two switching potential limits at a linear scan rate, which can typically vary from 0.001 to 200 mV sec^{-1}. Although the potential scan is frequently terminated at the end of the first cycle it can be continued for any number of cycles, hence the name cyclic voltammetry.

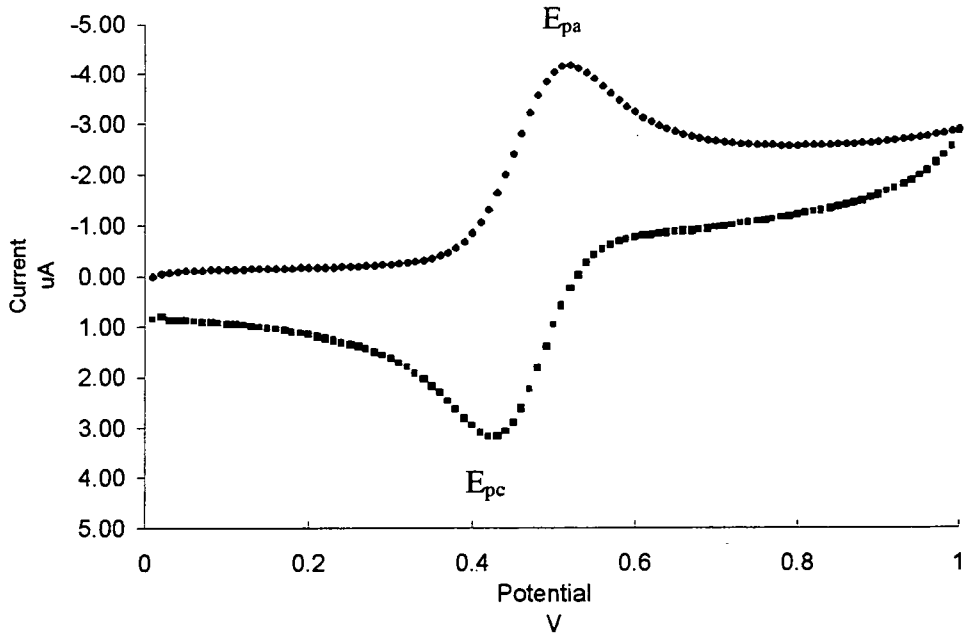

Figure 3.5 Typical cyclic voltammogram of a ferrocene solution.

The output of CV, termed a voltammogram, is a plot of the current flowing in the electrochemical cell versus the potential, and a typical example for a ferrocene solution is shown in Figure 3.5. This plot shows the unsymmetrical but equal heights of the anodic and cathodic peaks. This asymmetry of the plot is due to diffusional mass transport of the oxidisable and reducible species in solution. If the heterogeneous electron transfer is rapid, and both the oxidised and reduced species are stable, then the redox process is said to be reversible. Under these conditions, the difference between the two peak potentials E_{pc} and E_{pa} is 57/n mV (where n is the number of electrons transferred per molecule) for a reversible redox process. For non-reversible systems this difference is larger, which may be as a result of slow electron transfer. This can investigated by varying the scan rate. Some systems appear reversible at one scan rate but irreversible at another. When ideal reversible behaviour is observed, the diffusion current should vary as a function of the square-root of the scan rate [according to the Randles-Sevick equation (3.1)] for the forward sweep of the first cycle.[13]

$$i_p = (2.69 \times 10^5) n^{3/2} A D^{1/2} C \nu^{1/2} \qquad (3.1)$$

where i_p is peak current (Amperes), n is the number of electrons transferred in the electrochemical process, A is the electrode area (cm^2), D is diffusion coefficient (cm^2s^{-1}), C is concentration (mol dm^{-3}) and ν is the scan rate ($V\ s^{-1}$).

3.2.1.2 Osteryoung Square Wave Voltammetry[11]

Osteryoung Square Wave Voltammetry (SQV) is another voltammetric technique. It has several advantages over CV. The current response peak is symmetrical and there is effective discrimination against background charging currents. The applied potential wave form is very different to that of CV and consists of a square wave superimposed on a staircase wave form as shown in Figure 3.6.

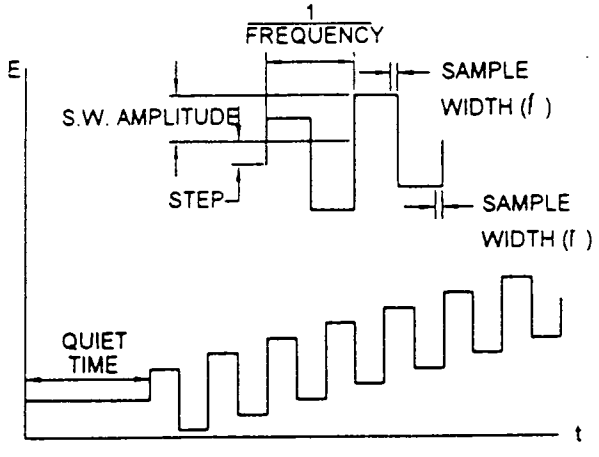

Figure 3.6 Potential waveform for SQW

The current is sampled at the end of each pulse for the forward and reverse directions. The default output is normally given as the difference between the forward and reverse currents. However, these may be examined individually. In reversible redox systems, the reverse current is of the same order as the forward current. Therefore, the difference between them is significant, which is why this method is so sensitive. The other advantage of SQV is speed, allowing scan rates of up to 8 $V\ s^{-1}$. It should be noted that this technique can not be described by a scan rate. However, an effective scan rate is given by the product of the sample width frequency and the potential. The scan rate is significantly faster than other voltammetric techniques, and the sensitivity also increases with increasing scan rate, even for irreversible processes.

3.2.2 Experimental Procedures

3.2.2.1 Voltammetric Analysis

Cyclic voltammetry was carried out using a Bioanalytical Systems CV-50W instrument. The reference was a non aqueous (acetonitrile) silver /silver ion electrode; counter was a platinum wire and the working electrode was a glass carbon electrode. The solvent used for all analysis was acetonitrile (Aldrich; HPLC grade) and the supporting electrolyte used was 0.1 mol dm^{-3} tetrabutylammonium perchlorate (Fluka; puriss grade). The silver salt used for complexation studies was silver nitrate (Aldrich; puriss grade). All silver solutions were stored in the dark. Titrations were carried out using 10 ml of a 5 $x10^{-4}$ mol dm^{-3} ligand solution in a cell to which the silver solution (0.04 mol dm^{-3}) was titrated using a micropipette (50 - 100 μL). This volume of metal solution allowed a range of metal/ ligand ratio from 1 : 1 to 10 : 1 to be covered. Square wave voltammetry was also performed using a Bioanalytical Systems CV-50W at potential step 4 mV, Pulse amplitude 25 mV and frequency of 15 Hz.

3.2.2.2 Spectroscopic Studies

Complexation studies were carried out using silver nitrate (Aldrich; puriss grade) with acetonitrile (Aldrich; HPLC grade) as solvent. Spectra were recorded on a BioPharmacia single beam instrument with an eight sample changer and quartz cells with a path length of 10 mm. The titration experiments were performed using 2 ml of 5 x 10^{-5} mol dm^{-3} ligand and 10^{-1} and 10^{-2} mol dm^{-3} $AgNO_3$ solutions. The data were nonlinearly fitted using the Origin v 4.0 program.

3.2.2.3 ^{1}H NMR Titrations

Spectra were recorded on a Varian Gemini 200 instrument. Samples were prepared using $CDCl_3/CD_3OD$, 2:1 by volume. The volume of ligand solution was 0.7 ml (0.01 mol dm^{-3}) to which additions of $AgCF_3SO_3$ (0.1 mol dm^{-3}) were added using a micropipette. All measurements were carried out at room temperature.

3.3 Results

Complexation studies were carried out to determine the affinity of the newly synthesised molecules (reported in chapter 2) for silver ion. Initial investigations were carried out using voltammetric methods such as cyclic voltammetry (CV) and square wave voltammetry (SWV) and these are reported in section 3.3.1. Spectroscopic studies are described in section 3.3.2 to quantify the strength of silver binding and NMR titrations are discussed in section 3.3.3 to investigate the mode of binding by conformational analysis.

3.3.1 Electrochemical Analysis

Initial investigations involved running a CV of **8d** to examine its redox properties. Reversible redox behaviour was not expected, as the only reports of redox activity with DMIT type molecules is where they are prepared as transition metal dithiolene complexes where the metal ion provides the redox centre.[14] The CV of **8d** shows a clear oxidation peak at 0.98 V versus Ag^{+}/Ag^{0} but no discernible reduction peak as shown in Figure 3.7.

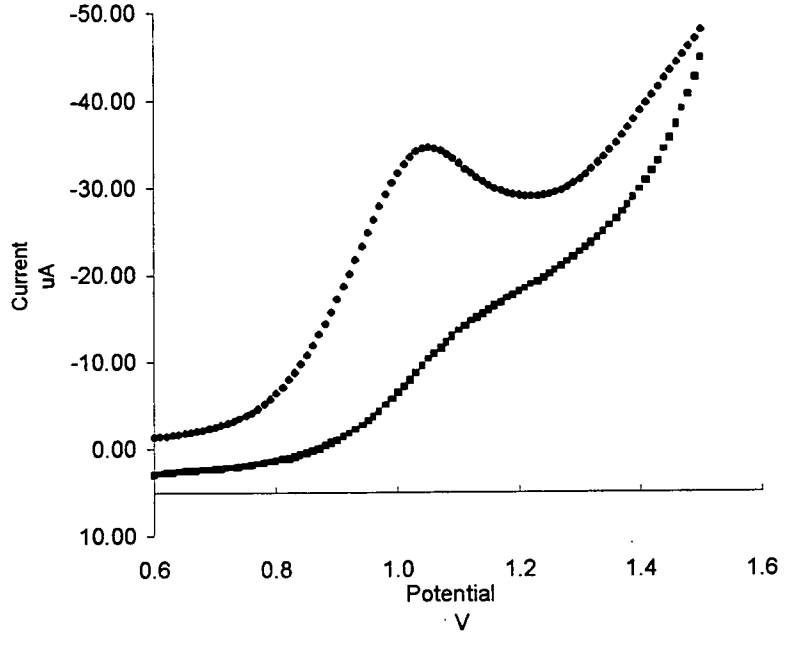

Figure 3.7 Cyclic voltammogram of **8d** (5×10^{-4} mol dm^{-3} in MeCN) versus Ag^{+}/Ag^{0} recorded at a scan rate of 100 mV s^{-1}

The separation between the oxidation wave and the reduction wave can sometimes be a function of the scan rate which can result in a redox system being reversible at one scan rate but irreversible at higher scan rates as described in Section 3.2. The scan rate was varied from 50 to 300 mV sec^{-1} to determine what effect, if any, this would have on the voltammogram. No emergence of a reduction peak was observed but a slight shift in the position of the oxidation peak was observed from 1.08 V at 300 mV sec^{-1} to 0.95 at 75 mV sec^{-1}.

Unlike the DMIT molecule **8d** tested above, the TTF molecule **9** showed typical reversible redox behaviour at with two 1 electron waves at 0.29 and 0.50 V versus Ag^{+}/Ag^{0}. [7] For ideal redox behaviour the diffusion current varies as a function of the square-root of the scan rate according to the Randles-Sevick equation (3.1) as described in Section 3.2. For compound **9**, a plot of the square root of the scan rate (varied in the range 25 to 500 mV s^{-1}) versus the diffusion current is shown in Figure 3.8. This plot is linear in the range of scan rates tested, which demonstrates that **9** displays ideal redox behaviour. This result is also significant as it demonstrates that CV analysis of **9** can be performed over a wide range of scan rates. A scan rate of 200 mV s^{-1} was chosen for subsequent analysis as this rate allowed quick analysis.

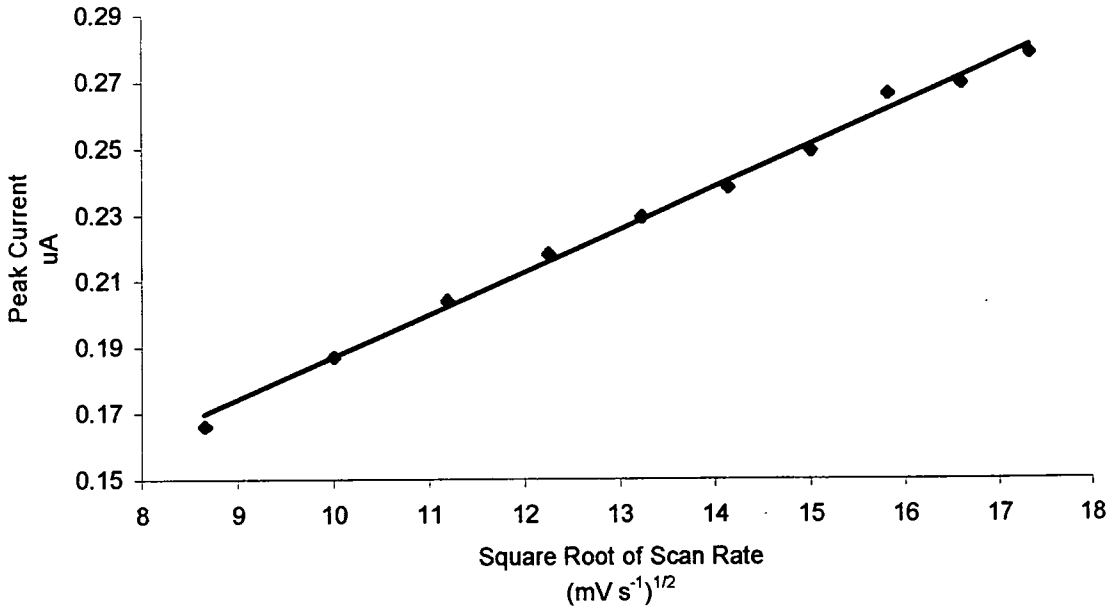

Figure 3.8 Plot of the diffusion current of the first oxidation potential of **9** versus the square-root of the scan rate.

Addition of excess (3 equivalents) $AgNO_3$ to a solution of **9** in acetonitrile produced an anodic shift of 40 mV in the first oxidation wave only with no shift in the second oxidation wave as shown in Figure 3.9. This anodic shift is as a result of the coulombic effect of the complexed silver ion which makes oxidation of the TTF to the TTF radical cation more difficult. Analogous behaviour has been previously observed by Hansen *et al* with a TTF–crown compound **16.** upon complexation with $NaClO_4$ (see section 3.1.2).[2] However, it is significant that the complexation of **9** with silver ion is significantly more sensitive requiring less than two equivalents of silver to produce a 40 mV shift compared to the large excess (250 equivalents) of $NaClO_4$ required to produce a 70 mV shift in Hansen's work.

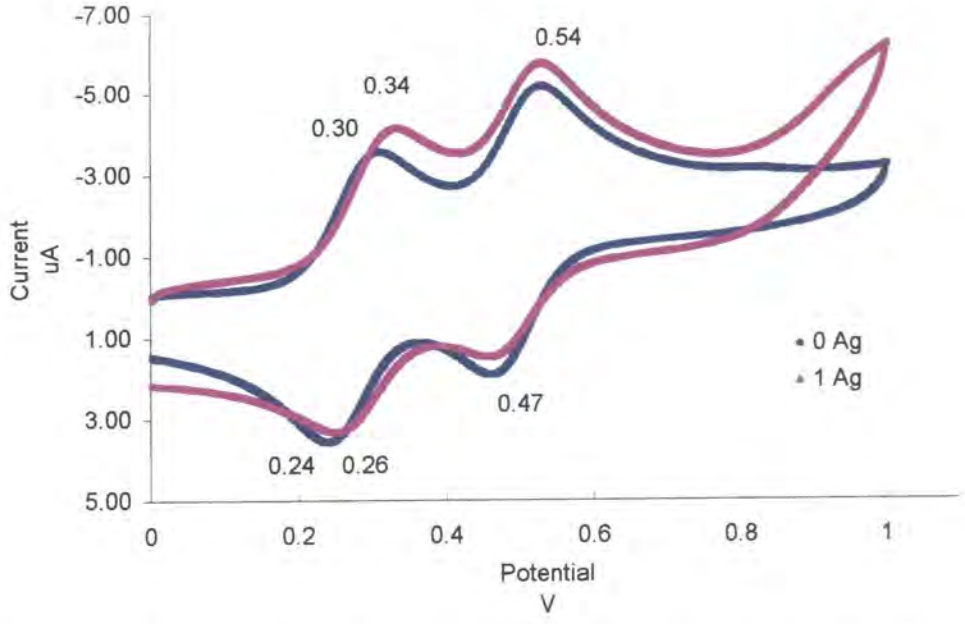

Figure 3.9 Cyclic voltammogram of **9** (——) in acetonitrile (5 x1 0^{-4} mol dm^{-3}) showing the shift in the first oxidation wave upon addition of $AgNO_3$ (——).

This contrasts with the behaviour of **17** also published by Hansen et al where the complexation of silver resulted in a shift in both oxidation waves (section 3.1) which indicated that the cation was ejected after the second oxidation.[9] However, on the reduction cycle, the potential of the peaks was no different to that of the uncomplexed **17** which was synonymous with a slow rate of complexation. The complexation of silver ion by **9** also results in a shift in the reduction peak which suggests that the complexation of silver is fast.

The shift in the first oxidation wave of **9** after addition of $AgNO_3$ was further investigated by square wave voltammetry (SWV) which is a more sensitive technique than CV (section 3.2). The sharper peaks of SQV allow easier monitoring of shifts in potential as shown in Figure 3.10 where the voltammograms of **9** with 0, 1 and 3 equivalents of added $AgNO_3$ are shown.

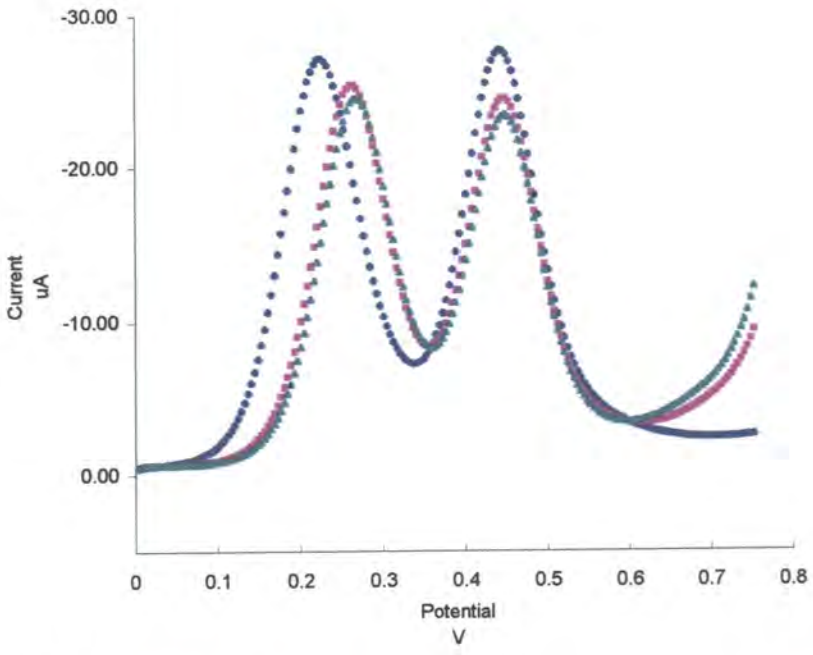

Figure 3.10 Square wave voltammograms of **9** (—) in acetonitrile (5 x 10^{-4} mol dm^{-3}) with the addition of 1 (—)and 3 (—)equivalents of $AgNO_3$.

Titration of **9** with $AgNO_3$ (0 – 3 equivalents) and the monitoring of the observed shift in the first peak of the voltammogram is shown in Figure 3.11. This curve shows that **9** forms a 1:1 complex with silver ion and displays a maximum shift of 40 mV after less than 1.5 equivalents of silver ion have been added. This is remarkably more sensitive than **16** reported above for which 250 equivalents of metal ion were required to observe similar shifts in the first oxidation potential

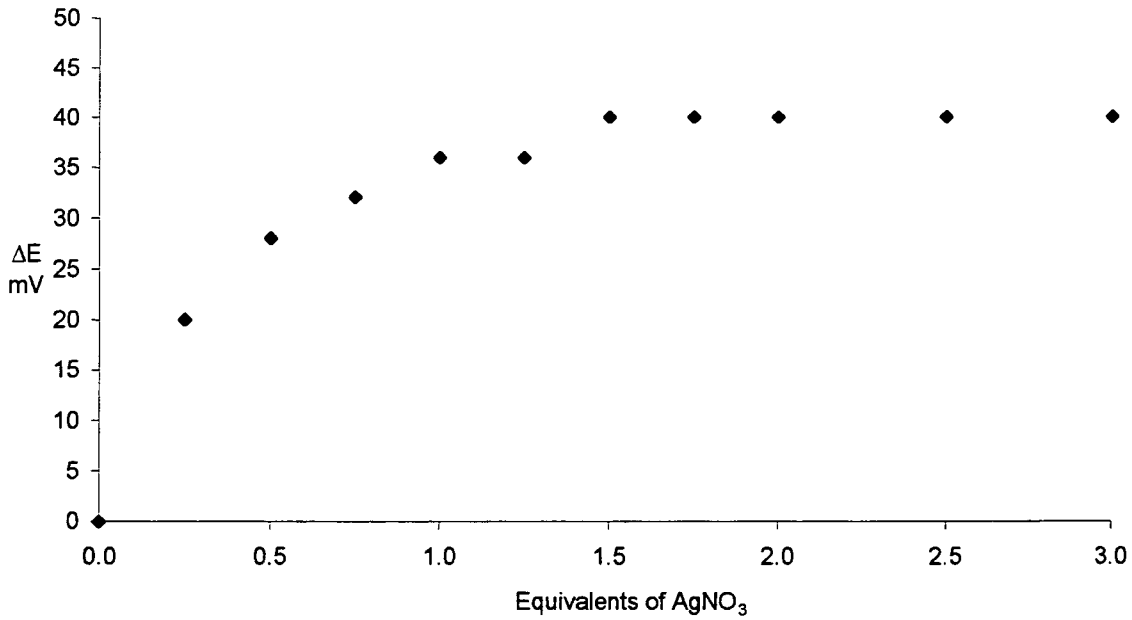

Figure 3.11 Plot of the shift in potential of the first peak in the square wave voltammogram of **9** with added equivalents of $AgNO_3$.

In order to dismiss the possibility that the silver was binding to the TTF framework as opposed to the proposed binding site, the above titration experiment was repeated under exactly the same conditions with a sample of tetrathiomethyl TTF.[15]

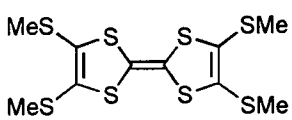

20

Titration of **20** with three equivalents of silver ion produced no change in the CV scan, demonstrating that this molecule does not bind silver. This is a very significant result as it demonstrates that the TTF building block will not interfere with the binding of silver ion in particular the exocyclic sulfur atoms. This suggests that the silver ion is binding between the two ligating chains, two binding conformations are possible as shown in Figure 3.12.

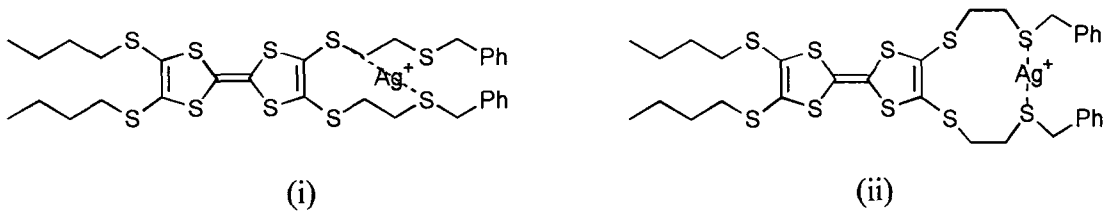

(i) (ii)

Figure 3.12 Two proposed binding conformations of **9** with silver ion based on evidence from binding tests on tetrathiomethyl TTF (**20**).

The binding of silver to this compound needs further work to elucidate its conformation. This could be achieved by synthesis and subsequent electrochemical analysis of a structurally similar molecule such as **21** which has one ligating chain. If **21** could be shown to bind silver ion, then this would make conformation (i) in Figure 3.12 more likely as the mode of silver binding.

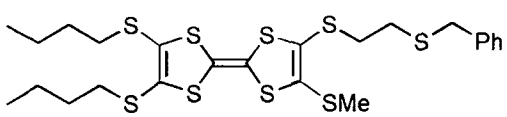

21

3.3.2 Spectroscopic Studies

In recent work on spectroscopic complexation studies on TTF-crowns by Bryce *et al*, a stability constant of log K = 2.26 was found for the formation of a 1:1 complex **16** and Na^+ was reported as shown in section 3.1.2.[10] This technique was applied to compound **9** to investigate if the binding of silver could be followed by UV spectroscopy. To be suitable for UV titration studies, a compound must be a good chromophore and possess a metal binding site which is conjugated with the chromophore. The results from the voltammetric titrations in Section 3.1 showed that **9** does bind silver ion and a similar titration experiment was analysed by UV to investigate if the silver binding could be observed. A spectrophotometric titration for **9** is shown in Figure 3.13. These spectra are corrected for dilution, by multiplying the absorbance values by the quotient of the original volume and the new volume (after addition of silver ion).

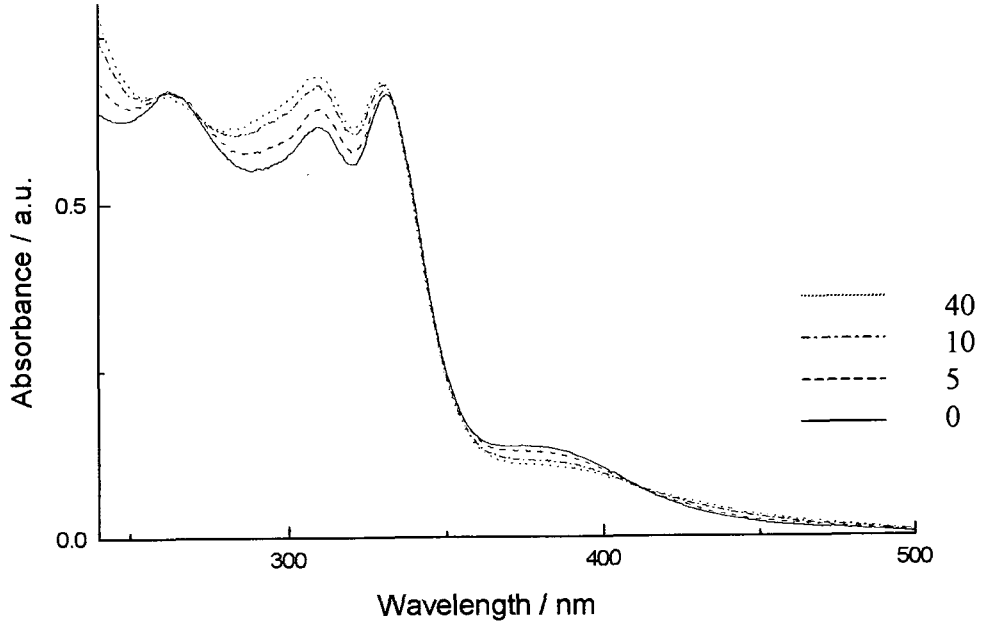

Figure 3.13 Absorption spectrum of **9** (5 x 10^{-5} mol dm^{-3}) showing absorbances at concentrations of 0, 5, 10 and 40 equivalents of $AgNO_3$.

Three clear isosbestic points are observed at the following wavelengths 412, 348 and 270 nm. The changes in absorbance were related to the metal complexation as follows. The strength of complex formation is given by K in equation 3.2

$$L + M^{+} \Leftrightarrow ML$$

$$K = \frac{[ML^{+}]}{[M^{+}][L]} \qquad 3.2$$

The dependence of the absorbance A, of a ligand at a fixed wavelength on metal concentration $[M^{+}]$ is given by equation 3.2

$$K[M^{+}] = \frac{(A_o - A)}{(A - A_i)} \qquad 3.3$$

Where A_o and A_i represent the absorbances at zero and infinite salt concentrations respectively. This equation can then be non-linearly fitted to experimentally determined absorbance versus silver ion concentration to give a value for the stability constant K. The equation 3.3 has to be first rearranged to the format of a non linear equation.

$$[M^{+}] = \frac{1}{K}\frac{(A_o - A)}{(A - A_i)} \qquad 3.4$$

This equation can now be written in the form

$$y = P_1 \frac{(A_o - x)}{(x - P_2)} \qquad 3.5$$

Where y is the concentration of metal ion, x is the absorbance value, P_1 is the inverse of the stability constant and P_2 is A_i. Therefore, a plot of concentration versus absorbance can be fitted by a non-linear function by optimisation of the parameters P_1 and P_2. An example of such a fit is shown in Figure 3.14 for a set of absorbance versus concentration readings at 290 nm. The non-linear curve drawn through the data points in Figure 3.14 is a very good fit to the experimental data. These data fit well to the non-linear function for 1:1 binding which is evidence that a 1:1 complex is formed. The value of the stability constant calculated form P_1 is log K = 3.22 ± 0.01 at 290 nm. Four other wavelengths were chosen

in regions where there was a large change in absorption and values for log K calculated, these are shown in Table 3.1

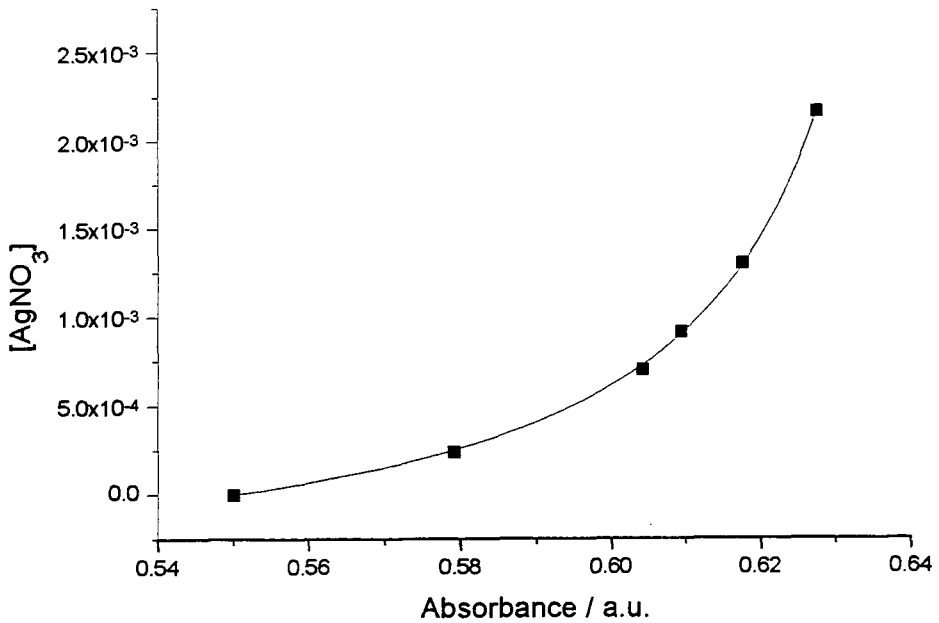

Figure 3.14 A non-linear fit for the complexation of silver ion by **9** using absorbances at 290 nm

Wavelengths nm	436	380	320	290	245
logK	3.07±0.02	3.04±0.04	3.40±0.06	2.69±0.09	2.75+0.09

Table 3.1 Calculated values of log K at different wavelengths. Values represent averages of three determinations

The average value for log K is 2.99 which represents medium strength binding. This is an ideal value for an ionophore for sensor applications, as binding constants that are too high lead to irreversible binding.

3.3.3 ^{1}H NMR Titrations of 6d

To investigate the mode of binding of **6d** and silver ion in solution a titration was followed by ^{1}H NMR. Owing to the number of sulfur atoms in the heterocyclic ring, it was important to know if silver would bind to the heterocyclic backbone of **8d**. Compound **22**[16] was chosen as it represents a structural analogue of **6d** which does not contain a ligating chain. The chemical shifts of the protons on the four butyl carbons were monitored as the molar ratio of silver was increased up to seven equivalents. The resulting changes in chemical shift and the numbering of the protons are shown in Figure 3.15.

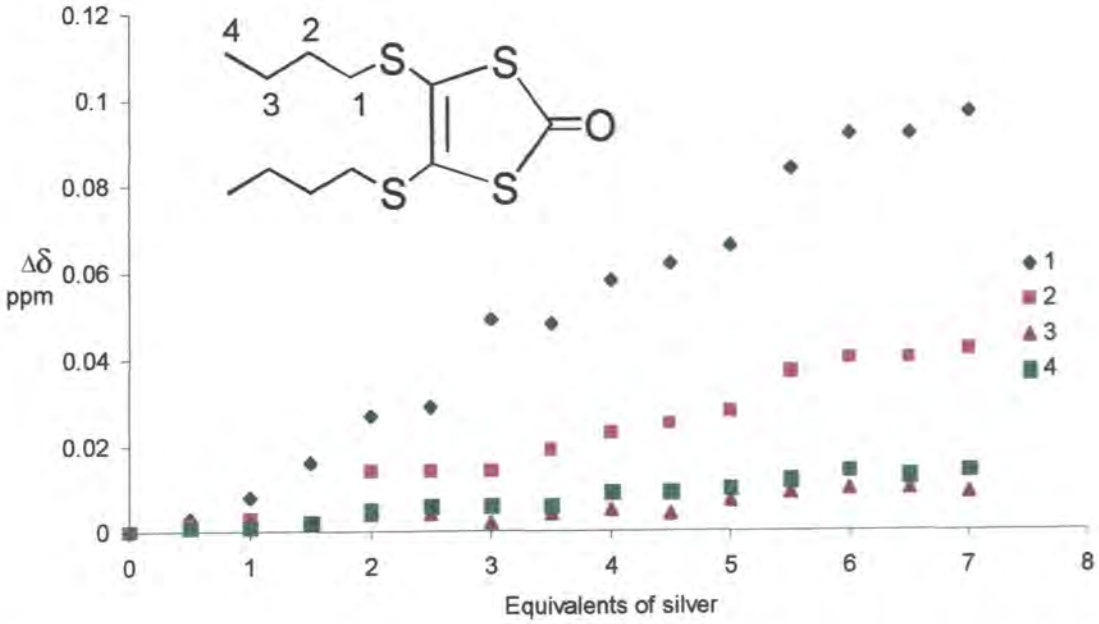

Figure 3.15 ^{1}H NMR titration of **22** (0.01 mol dm^{-3} in $CDCl_3/CD_3OD$, 2:1) with $AgCF_3SO_3$ (0.1 mol dm^{-3}).

It can be seen that a small shift of less than 0.1 ppm in the chemical shift of proton 1 is observed after the addition of 7 equivalents of silver ion. This small shift represents a very small perturbation of the chemical shift of proton 1 which is indicative of weak binding. It is also significant that there is no readily apparent stoichiometry for this binding as the shift increases linearly with the added silver, this is also indicative of weak binding.[17] Therefore, it can be assumed that no significant binding occurs at the building block of the molecule used to synthesise **8d**.

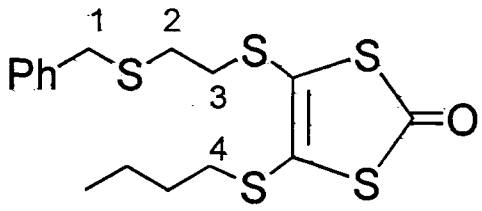

8d

The splitting patterns of peaks 2,3 and 4 of **8d** are very complicated as one would intuitively expect to observe 3 triplets. The splitting of these protons is quite complex and it changes quite dramatically as silver is added to solution as can be seen in Figure 3.16. In a titration up to six equivalents of silver three types of splitting pattern are observed. The splitting pattern in (a) at 0 equivalents of silver shows one central triplet and two very complicated signals which are symmetrical. This suggests that the central triplet can be assigned to the protons on carbon 4 and the other two signals represent those on carbons 2 and 3. This splitting pattern indicates that the protons on carbons 2 and 3 are inequivalent.

As silver is added to **8d** all three signals move upfield and the signals are better resolved. At two equivalents of silver ion in (b), three triplets can be identified which indicates the protons on carbons 2 and 3 are now equivalent. Therefore, the binding of two equivalents of silver ion confers a symmetrical conformation on the ligating chain. All three signals continue to move upfield with further addition of silver ion up to four equivalents as shown in plot (c), the splitting patterns on the protons on carbons 2 and 3 change slightly. However, the splitting patterns of the protons on carbons 2 and 3 changes dramatically after 4 equivalents as the signals are completely inequivalent as shown in plot (d) for 6 equivalents. This suggests that the binding of silver has locked these protons into a conformation where the two protons are in very different environments such as axial and equatorial positions relative to a silver ion.

This suggests that there are large conformational changes in this site. This appears to be a complex pattern of shifts making it difficult to fully interpret the results. The purpose of this experiment was to show that the addition of the ligating chain in the synthesis of **8d** improved the binding of silver; this has been shown, but a lot more work is required to fully understand the system.

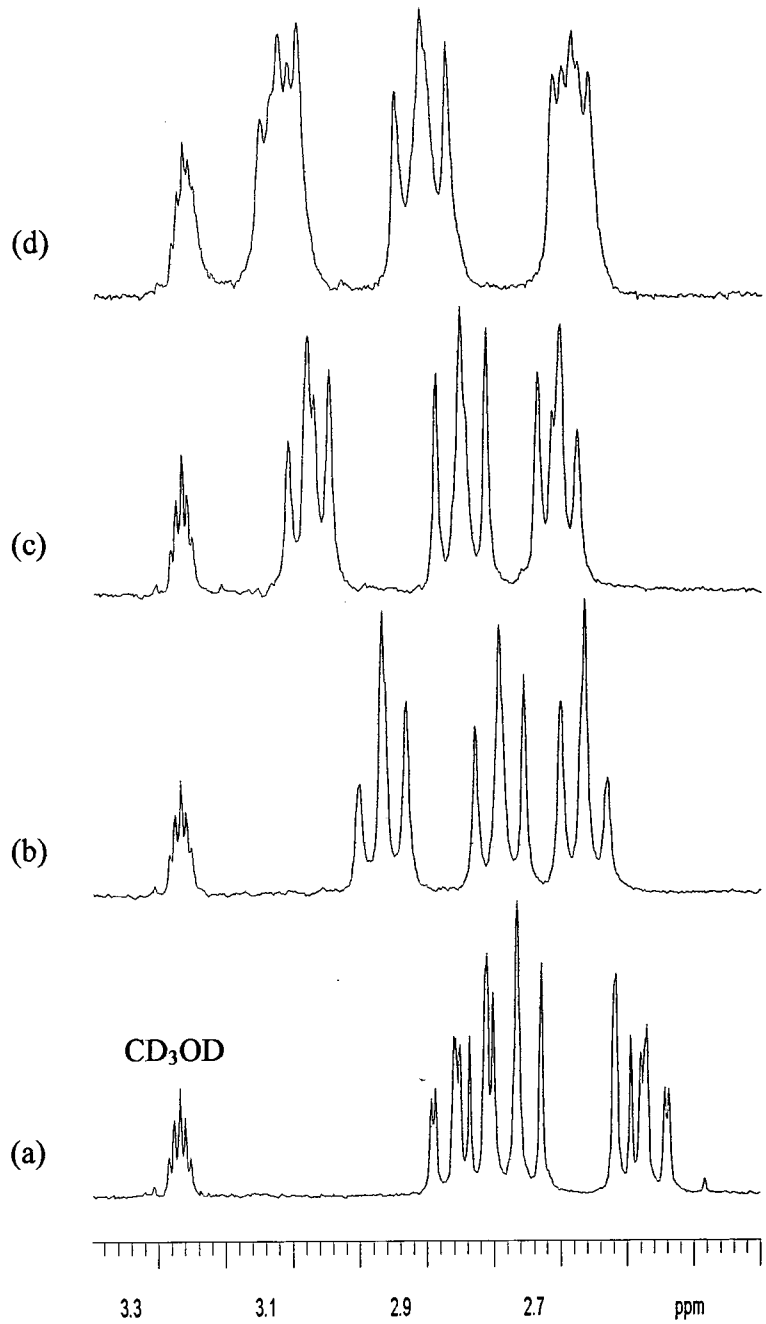

Figure 3.16 ^{1}H NMR splitting patterns of protons on carbons 2, 3 and 4 of **6d** in the presence of $AgNO_3$; (a) 0 equivalents (b) 2 equivalents (c) 4 equivalents and (d) 6 equivalents.

3.4 Conclusions

In this chapter the silver binding ability of compounds **8a-d** and **9** were investigated. The TTF compound **9** displayed reversible redox behaviour and proved ideal as a transducer for voltammetric analysis. UV spectrophotometry was then used to determine a binding constant for **9** with Ag^+ of log K = 2.99 in acetonitrile for a binding stoichiometry of 1:1. The binding of Ag^+ by **8d** was investigated by NMR spectroscopy and it was shown that perturbation of proton signals was observed upon addition of silver at the intended binding site. However, the splitting patterns of the protons investigated was very complicated which made a more rigorous interpretation of the results difficult. This system needs to be further investigated using other techniques such ^{13}C NMR or 2 dimensional NMR.

3.5 Bibliography for Chapter 3

1. G. W. Gokel, *Chem. Rev.*, 1992, **21**, 39.
2. T. K. Hansen, T. Jørgensen, P. C. Stein and J. Becher, *J. Org. Chem.*, 1992, **57**, 6403.
3. T. Saji, *Chem. Lett.*, 1986, 275.
4. R. E. Wolf and S. R. Cooper, *J. Am. Chem. Soc.*, 1984, **106**, 4646.
5. K. Maruyma, H. Sohmiya and H. Tsokube, *Tetrahedron Lett.*, 1985, **26**, 3583.
6. S. R. Miller, A. Gustowski, Z. Chen, G. W. Gokel, L. Echegoyen and A. E. Kaifer, *Anal. Chem.*, 1988, **60**, 2021.
7. G. Schukat, A. M. Richter and E. Fanghänel, *Sulfur Rep.*, 1987, **7**, 155.
8. T. K. Hansen, T. Jørgensen and J. Becher, *J. Chem. Soc., Chem. Comm.*, 1992, 1550.
9. T. Jørgensen, B. Girmay, T. K. Hansen, J. Becher, A. E. Underhill, M. B. Hursthouse, M. E. Harman and J. D. Kilburn, *J. Chem. Soc., Perkin Trans. I*, 1992, 2907.
10. R. Dieing, V. Morrisson, A. J. Moore, L. M. Goldenberg, M. R. Bryce, J. M. Raoul, M. C. Petty, J. Garín, M. Savirón, I. K. Lednev, R. E. Hester and J. N. Moore, *J. Chem. Soc., Perkin Trans. II*, 1996, 1587.
11. P. T. Kissinger and W. P. Heineman, "Laboratory Techniques in Electroanalytical Chemistry", Dekker, New York, 1984.
12. J. Heinze, *Angew. Chem. Int. Ed. Engl.*, 1984, **23**, 831.
13. D. A. Skoog and J. J. Leary, "Principles of Instrumental Analysis", Saunders College Publishing, New York, 1992.
14. M. L. Green, W. B. Heuer and G. C. Saunders, *J. Chem. Soc., Dalton Trans.*, 1990, 3789.
15. T. Akutagawa and G. Saito, *Bull. Chem. Soc. Jpn.*, 1985, **68**, 1753.
16. C. Gemmel, J. D. Kilburn, H. Ueck and A. Underhill, *Tetrahedron Lett.*, 1992, **33**, 3923.
17. R. Kataky, P. E. Nicholson and D. Parker, *J. Chem. Soc., Perkin Trans. II*, 1990, 321.

CHAPTER FOUR

Potentiometry Using Ion Selective Electrodes

4.1 Introduction

4.1.1 General Principles of Ion-Selective Electrodes

4.1.1.1 The Electrochemical Cell

Ion-selective electrodes (ISE) are devices that permit the activity of a given ion in an aqueous solution to be determined potentiometrically despite the interference of other ions. The ion selective electrode forms part of an electrochemical cell as shown in Figure 4.1.

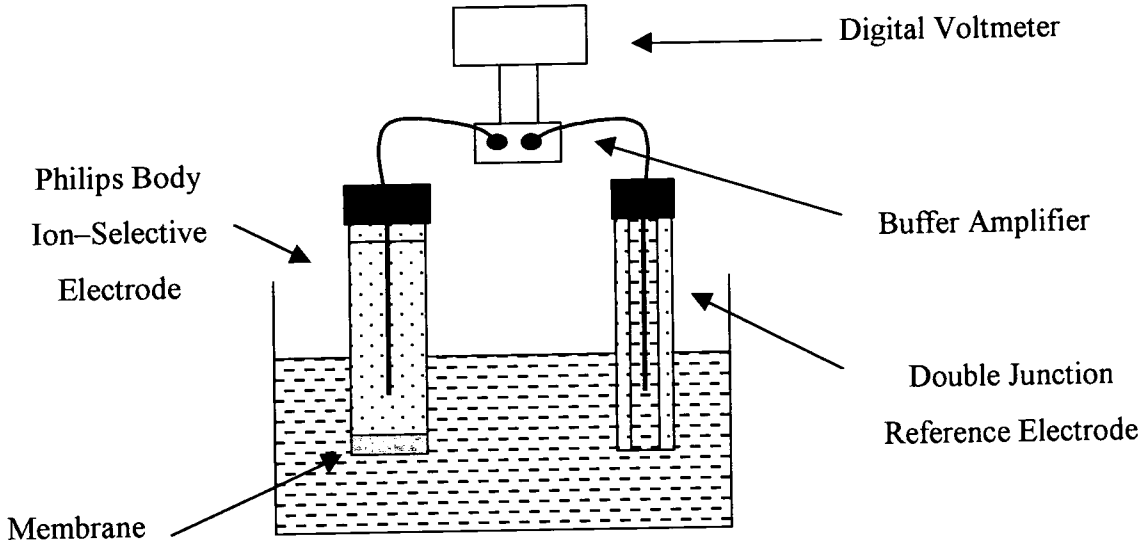

Figure 4.1 Scheme of an electrochemical cell incorporating an ISE.

A typical electrochemical cell assembly consists of an

1. ion selective electrode with a membrane, an internal filling solution and internal reference electrode as one galvanic half cell
2. an external reference electrode with reference electrolyte

A cell potential is established across the membrane when the ion selective electrode and the reference electrode are both in contact with the sample solution. It is important to note that this is a measurement at zero current, i.e. under equilibrium conditions. In practice a buffer amplifier is required between the circuit and the digital voltmeter owing to the very high impedance of the ion selective electrode. The measured potential E_{cell}, is the sum of

different potentials generated at all solid/solid, solid/liquid and liquid/liquid interfaces as shown in equation 4.1

$$E_{cell} = E_I + E_M + E_{LJ} + E_{ER} \quad (4.1)$$

Where

E_I is the contribution from the internal reference solution

E_M is the membrane potential difference

E_{LJ} is the liquid junction potential which develops because of the difference in composition between the sample and bridge solution

E_{ER} is the potential of the external reference electrode

If the sample solution is the only solution to be changed between measurements then the potentials E_{IR} and E_{ER} are constant. The junction potential E_{LJ} will vary between sample solutions, but this variance can be minimised by use of a concentrated solution of an equitransferance salt such as potassium chloride. This allows the constant terms to be summed as E^0 which effectively reduces equation 4.1 to equation 4.2, where the cell potential depends only on the membrane potential which, in turn, depends on the sample ion activity.

$$E_{cell} = E_0 + E_M \quad (4.2)$$

4.1.1.2 Activity, Concentration and Activity Coefficient.

A unique feature of ISEs is that the obtained signal depends on the sample ion activity. The assumption that a thermodynamic equilibrium exists at the membrane sample interface, results in the membrane potential being directly dependent on the sample ion activity. This appears to contradict the thermodynamic assumption that single ion activities can not be determined. However, the potential of the reference half cell is assumed to be sample independent which is not the case owing to the liquid junction potential of the reference electrodes which is sample dependent.

As ion selective electrodes respond to sample ion activity rather than concentration, it is important to look at the activity co-efficient which relates to these two parameters. The term activity is used to determine the active or effective concentration of the ion in

solution[1]. The relationship between the activity and the concentration of an ion is given in equation 4.3

$$a_i = \gamma_i \; c_i \qquad (4.3)$$

where a_i, γi and c_i are the activity, concentration and activity co-efficient of species i respectively. The activity of an ion is equal to its concentration at infinite dilution of the ion, as there are no ion-ion interactions. However, at high concentrations of ion i, it experiences interactions with other ions and solvent, so its effective concentration seems diminished. The term activity coefficient γ_i was introduced to relate the concentration of ion C_i to its effective concentration or activity a_i. However, as the activity co-efficient of individual ions cannot be defined uniquely or measured, only the mean activity co-efficient for a cation/anion pair is measurable and it is defined for a single charged ions by equation 4.4.

$$\gamma_{\pm}^2 = \gamma_+ \gamma_- \qquad (4.4)$$

Although ionic activity coefficients cannot be measured individually, they can be calculated by theoretical means using the Debye Hückel equation. At a given temperature the activity coefficient of ions in aqueous solutions of low concentrations vary chiefly with the distances between the ions and with the number of charges borne by the ions; these factors are combined in the term ionic strength defined in equation 4.5.

$$I = 1/2 \sum c_i z_i^2 \qquad (4.5)$$

In this equation c_i and z_i are the concentrations and valency of the ions in solution and the summation is made for all the ionic species present. Ionic strength is then used to calculate the activity of the ion using the Debye Hückel equation[2], equation 4.6.

$$-\log \gamma_i = \frac{A \; | z_+ z_- | \; I^{1/2}}{1 + \beta \mathring{a} \; I^{1/2}} \qquad (4.6)$$

In this equation z_i is the valence of ion i, a is the ion size parameter or mean distance of closest approach and A and β are constants. This equation is valid for ionic

strengths or concentrations up to 10^{-1} mol dm^{-3}, the values of A and β vary with temperature and dielectric constant of the solvent. For an aqueous solvent at 40 °C these values are A = 0.5262, β = 0.3323 and å the ion size parameter is estimated at 2.5 for Ag^+ which is of the same order of magnitude as the ionic diameter[1].

4.1.1.3 The Nernst Equation

If the membrane is behaving ideally so that it responds to only the primary ion the potential difference across the membrane E_M is described by the Nernst equation,

$$E_M = E° \pm \frac{RT}{z_i F} \ln a_i \qquad (4.7)$$

Where E_M is the membrane potential, E° the reference potential, R is the gas constant, T is the temperature in Kelvin, z_i is the charge on the ion i, F is the Faraday constant and a_i is the activity of ion i in the sample solution. The sign of the equation is positive when i is a cation, and negative when i is an anion. However, in practice this ideal behaviour is not observed as the membrane is normally sensitive to other interfering ions as well as the ion of interest. The membrane potential will now have the contributions for the primary ion i, as well as interfering ions j, which is a cation of the same charge. This interference was first observed with pH electrodes where small hard cations such as sodium interfered. The Nickolskii-Eisenmann equation[3], equation 4.8 has been developed to calculate the interference from the interfering ion j. It is important to note that this equation can only strictly be used in cases where the electrode responds in a Nernstian fashion to the interfering ion j.

$$E_M = E° \pm \frac{RT}{z_i F} \ln\left\{a_i + K_{ij} a_j^{z_i/z_j}\right\} \qquad (4.8)$$

where a_j and z_j are the activity and the charge respectively of the interferent ion j and K_{ij} is the selectivity coefficient.

4.1.1.4 Classification of Ion Selective Membrane Electrodes.

Ion selective membrane electrodes may be classified according to the composition of the membrane, as this is responsible for the selectivity behaviour of the electrode[4].

- Glass membrane electrodes, e.g. pH
- Solid-state membrane electrodes based on crystalline materials, e.g. sulfide, fluoride
- Liquid membrane electrodes, composed of an ion exchanger dissolved in a suitable lipophilic solvent, e.g. Ca^{2+}, NO_3^-
- Neutral carrier membrane electrodes composed of an organic solution of an ion-specific complexing agent, e.g. K^+, Mg^{2+}, Ca^{2+}
- Other electrodes such as gas and enzyme sensitive electrodes

4.1.1.5 The pH Electrode

The pH electrode is an example of a solid electrode and is significant as it was the first ion selective electrode to be studied[5]. The glass electrode operates on an ion exchange process; a cross section of a membrane of a functioning glass electrode comprises several discrete regions[6]. The dry glass layer constituting the bulk of the membrane's thickness is sandwiched between two thinner hydrated layers which are essential for the proper functioning of the glass. The potential given by the glass electrode depends only on the phase boundary potential at the external analytical solution interface which, in turn, is related to the ionic activity by the Nernst equation. It is important to note that the glass membrane itself is impermeable to hydrogen ions; it is in fact sodium ions which behave as the charge carriers on the glass. No single sodium ion moves through the entire thickness of the glass layer; it is the charge that is transported by an interstitial mechanism, where each charge carrier merely needs to move a few atom diameters before transferring its energy to another carrier.

4.1.2 Calibration and Selectivity of ISEs

4.1.2.1 Selectivity

According to the 1976 International Union of Pure and Applied Chemistry[7] (IUPAC), two different methodologies were recommended for the determination of the Nickolskii coefficient in equation 4.8, namely, the separate solution method (SSM) and the fixed interference method (FIM). In the SSM method the potentials of the electrode are measured in separate solutions of primary and interfering ion, the Nickolskii coefficient is then determined from the two observed potentials. In the FIM method, a calibration curve is determined for the primary ion in a constant background of the interfering ion. The linear portion of the curve (corresponding to the primary ion response) is extrapolated until it intersects with the lower limit of the electrode response which corresponds to the interfering ion response, the Nickolskii coefficient is calculated from these two segments. However, these methods rely on the assumption that the interfering ion completely replaces the primary ion at the boundary layer of the membrane, and that the electrode responds to the interfering ion with a Nernstian slope. In practice a Nernstian response is often only observed for the primary ion with the interfering ions displaying non-Nernstian behaviour.

The problem with the requirement for Nernstian behaviour for the interfering ions was very well expressed in a more recent IUPAC recommendation by Umezana.[8] "When a new electrode is constructed, log a vs. E relations are measured first. One is pleased in the case if only a primary ion shows a Nernstian behaviour and the others do not. However as far as the validity of the N-E equation is concerned, this involves a fatal paradox, because the N-E equation assumes a Nernstian behaviour for the interfering ion as well."

In this work, the responses of many typical ISE (including fluoride, bromide, nitrate, calcium and potassium) were tested for Nernstian response toward the interfering ions. Of these electrodes it was only the valinomycin based K^+ ISE which displayed Nernstian behaviour, for both primary and some interfering ions. As very few electrodes display Nernstian behaviour to all ions, most reports have violated the Nickolskii-Eisenmann equation which explains the variance in reported K^{Pot} values.

A new procedure has recently been developed to determine unbiased selectivity coefficients of neutral carrier based cation selective electrode[9]. This method involves use of membranes that have never been in contact with the primary ion. The preparation of these electrodes involves the use of a tetraphenylborate derivative salt of a discriminated ion and conditioning in a chloride solution of this cation. This method allows true selectivity coefficient determination, but is restricted by the strict sequence of exposure to different electrolyte and salt solutions. Once the electrode has been exposed to the primary ion, it no longer responds in a Nernstian fashion to interfering ions. These are severe restrictions which makes this technique impractical outside of research laboratories.

Problems are also encountered with the Nickolskii-Eisenmann equation in situations where the primary and interfering ion are of different charge. This problem manifests in the power term $a_i^{zi/zj}$ of equation 4.8, where different values are obtained depending on the assignment of primary and interfering ions. Numerical calculations illustrated that selectivity coefficients calculated were either unrealistically large or small depending on the choice of primary ion.[8] In these situations the Nickolskii-Eisenmann equation is deemed unsuitable. These inadequacies arise because the equation was established originally for the glass electrode to deal with interference from the alkali metal ions.

IUPAC[8] recommends use of the matched potential method first presented by Gadzekpo and Christian.[10] This method is unique in being completely independent of the Nickolskii-Eisenmann equation. The selectivity coefficients are determined by the ratios of primary and interfering ion activities which give the same potential change in a reference solution. The selectivity coefficient is determined by measuring the change in potential when the primary ion activity is varied, followed by addition of the interfering ion to an identical reference solution to effect the same change in potential. This method gives realistic K_{ij} values as the change in potential must be produced in a constant initial background of the primary ion. This method has several advantages owing to its empirical nature which makes it independent of the charges of the primary and interfering ions and to whether or not the ions show Nernstian behaviour. It has been shown that the selectivity values obtained with this method, in cases where the primary and interfering ions have the same charge, are in very good agreement with those results obtained based on methods using the Nickolskii-Eisenmann equation.

Some authors[11] are critical of the empirical nature of this technique as it does not rely on any theoretical assumptions, giving it no predicting power for varying analytical situations making it difficult to correlate it to the K_{ij} values with physical phenomena such as ion exchange. However, the matched potential method is recommended by IUPAC for ions of unequal charge and for electrodes that do not display Nernstian behaviour for all ions which includes most electrodes (vide infra).

4.1.2.2 Detection Limit

The classic lower detection limit of an electrode as defined by IUPAC [12] as the activity of the primary ion i at the point of intersection of the extrapolated linear midrange and final low concentration level segments of the calibration plot as shown in figure 4.2.

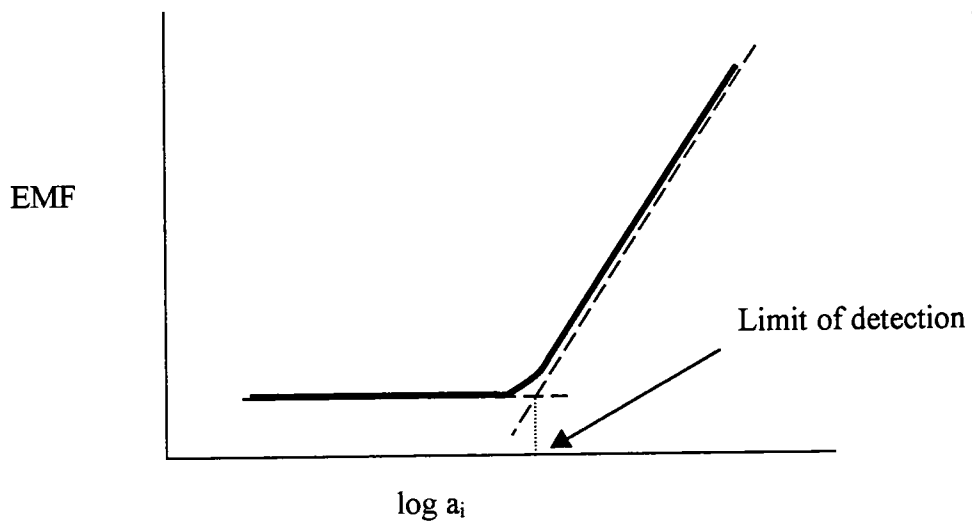

Figure 4.2 Calibration plot of an ISE

The reasons for loss in Nernstian response could be due to a perturbation of the interfacial sample activity or interference by competing sample ions. In a recent publication by Pretsch *et al*, large improvements in the lower detection limit were reported.[13] This group propose a model where the limit of detection occurs at the concentration where the primary ion leaches out of the membrane from the inner fill solution, making the electrode insensitive to sample activity beyond this concentration. Detection limits in the order of 10^{-12} mol dm^{-3} were reported for a Pb^{2+} selective electrode by buffering the inner fill solution to a Pb^{2+} concentration of 10^{-12} mol dm^{-3}. This prevented the primary ions from leaching out of the membrane.

This transport model was reported shortly afterwards by Mathison and Bakker who investigated the mechanism by varying the inner fill solution[14]. The model requires an anion to co-extract with primary ion and the authors postulated that the anion from the inner fill solution would co-extract. Their results did show a dependence of the detection limit on the concentration and nature of the inner fill solution but the concentration range tested showed how the limit could be worsened as opposed to being improved by using very high concentrations of inner fill solution. They admit that 'other effects remain to be studied' before experiments can be designed to lower detection limits to trace levels. In work by Bakker a silver ion selective electrode was reported to be responding to anions by the same mechanism.[15] In this case the source of the anions required to maintain electroneutrality for the leaching silver ions, was 'most likely' to be negative impurities from within the membrane.

The model of the detection limit being governed by the release of primary ions from the membrane (a process which is controlled by the inner reference solution) is appealing owing to its intuitive nature, but it unfortunately raises two serious questions.

(i) If the primary ion is leaching, then a satisfactory source of anions has to be proven.

(ii) The entire process requires transport of primary ion through the membrane, yet most authors, including those who present this present theory, believe that the role of the bulk membrane is negligible and that surface processes govern electrode response (section 4.1.3).

The authors declare in a recent review that the release of small amounts of ions "has indeed been observed" and they cite two papers in support of this claim.[11] The first paper by Bühlmann reports work on transport studies where K^+ was leached into the solution, however this leaching was proven to originate from the membrane and NOT from the inner fill solution.[16] Their results showed that K^+ was leached from the membrane regardless of whether the inner fill solution contained Na^+ or K^+, and that the relatively short exposure times made transmembrane transport improbable. Furthermore these membranes were in contact with tetramethylammonium chloride solutions which meant that the leaching process was actually an exchange process which obeyed electroneutrality. In fact, Pungor[17] showed in earlier work that no leaching to a distilled water receiving solution was observed

across a membrane under a concentration gradient in zero current conditions when the counter ion is not lipophilic.

The second paper cited concerns work on a membrane electrode which showed a response towards silver and halide anions.[18] This electrode was very different to a standard membrane ISE as the ionophore was complexed with silver ion and then used to cast the PVC membrane. The inner fill solution used was KCl. The response of this electrode was then described by the original authors as having a mechanism similar to that of a pressed-pellet electrode. However, Bakker *et al* rationalised the anion response in terms of an ion exchange process at the electrode surface. It is, therefore, unreasonable to suggest that this work presents evidence for primary ion leaching from the membrane.

4.1.3 Mechanism of Membrane Response

The membrane potential can be divided into three separate potential contributions: the inner electrolyte interface, outer sample interface and the diffusion potential within the membrane. The potential at the inner electrolyte can be assumed to be constant as it is independent of the sample. However, the relevance of the diffusion potential is the source of much debate, centring on whether there is a transport mechanism within the membrane. Early models of electrode response relied on a transport mechanism within the membrane however, many authors now believe that the response is governed at the phase boundary.

4.1.3.1 Transport Mechanism

Morf and Simon are among the most cited supporters of the transport mechanism from work published in 1986[4]. This work demonstrates that the diffusion potential is produced by the diffusion of ions within the membrane, which is treated as a non porous ideal phase. Electro-dialysis experiments were conducted using labelled valinomycin in contact with labelled KCl solutions. A carrier-concentration gradient was found which results from the translocation of cationic complexes.

Buck and co-workers evolved a technique to investigate diffusion of neutral molecules (valinomycin was used) within the membrane based on current–voltage curves[19]. A steady state carrier mechanism was proposed, as current is carried through the membrane

by K^+ valinomycin (K^+val) at the same time the free valinomycin back diffused with a flux that exactly balances the current carried by K^+val. At higher potentials the current reached a limiting value when the valinomycin concentration became zero at one interface .

Impedance spectroscopy was used by Pungor and Buck to examine the bulk properties of membranes containing valinomycin compared to those of blank membranes.[20] Their model of electrode behaviour depended on bulk membrane processes, complexation and transport. The cation selectivity of the dummy membranes was attributed to them behaving as low capacity ion exchangers. Results from this work agreed with earlier work on the current-voltage curves which show that the addition of valinomycin reduced the membrane resistance by two orders of magnitude.

4.1.3.2 Phase Boundary Mechanism

Pungor in more recent work in 1992[21] and 1996[17] is one of the strongest opponents of the transport mechanism despite the fact that he has published work earlier in support of it.[20] To demonstrate that the electrode response is a surface and not a bulk effect, the following experiments were performed: (i) response times, (ii) transport and (iii) penetration. In the kinetic studies (i) he showed that response was less that 20 ms, and of the same order as diffusion of ions through the boundary layer, this was interpreted as evidence that the response time is governed by a phase boundary and not a bulk reaction. In transport experiments (ii) across a valinomycin based electrode under zero current conditions he showed that no K^+ was detected in a receiving aqueous layer, meaning that the membrane provides a barrier at zero current conditions[17]. The penetration experiments (iii), illustrated that primary ions only react with the active components situated at the electrode surface but do not enter the membrane phase under zero current conditions, provided that the counter ion is lipophilic.

Chemisorption studies were used to form a model of the formation of electrode potential. An electrochemical equilibrium requires the presence of counter ions in the solution layer close to the solid surface in the same amount, and similarly high concentration as on the surface.

- Material transport cannot be regarded as the potential determining step

- Ions are selectively bound to the surface
- Owing to the chemisorption of the ion, the equilibrium of statistically distributed ions and counter ions is upset, the electrode surface becomes charged while the counter ions stay in solution in contact with the electrode, i.e. a charge separation occurs
- The bulk membrane only affects the impedance of the electrode

Results by Buhlmann are in agreement with Pungor that the potential is determined at the surface and not the bulk of the membrane[16]

- Permselectivity is due to the complete exclusion of counter ions from the membrane phase, the added ionic sites through an ion exchange mechanism allow primary cations to enter the bulk without violating electroneutrality.
- Non response of rigorously purified membranes is not due to a high impedance effect
- The presence of ionic sites, either added intentionally or introduced as impurities of membrane components, gives ISE membranes an ion exchange capability.

This work also demonstrated leaching of K^+ using atomic absorption spectroscopy (AAS) into a 10^{-2} Me_4NCl receiving aqueous solution. This is not transmembrane leaching, as it was K^+ that was extracted regardless of whether the inner fill solution was NaCl or KCl, also the relatively short exposure times made transmembrane transport improbable. Transport of these cations must obey electroneutrality suggesting that either anions are transported in parallel, or cations in antiparallel direction within the membrane.

Bakker and Pretsch have published a lot of work recently on the theory of ISE response, proposing a model entitled the "The Phase Boundary Potential Model" The model relies on the following four assumptions:[11,22]

1. Membrane potential is governed by the phase boundary potential at the sample/membrane interface, the diffusion potential is negligible
2. The organic phase boundary contacting the sample is in chemical equilibrium with the aqueous sample solution.
3. Concentration values are used, as activity coefficients are constant for all ionic species in the membrane phase

4. The formation of ion pairs between the lipophilic ion exchanger (or ionic sites) and their counter ions is either the same for all ions or negligible.

Assumption 1 is based on experimental evidence which has shown that the diffusion potential is negligible and that the permselectivity can be explained in terms of the ionic additives from deliberately added anions or anionic impurities. Assumption 2 is valid as the phase transfer reaction is generally much faster that the relevant diffusion processes in both the aqueous and organic layer, therefore equilibrium conditions can be assumed. Assumption 3 is reasonable as the ionic strength in the membrane is defined by a low constant concentration of ionic sites. This allows simple relationships for mass balance and electroneutrality to be used. Assumption 4 is used for simplicity purposes, and the assumption that all ion pairs have nearly equal association constants has been verified to a certain extent.

The validity of the model which predicts a permselective Nernstian response was tested experimentally by monitoring the concentration of species in the membrane directly. This was achieved using the H^+ selective chromionophore ETH 2418 and monitoring its absorption when the membrane was in contact with a solution where the pH was varied. Results showed that the absorbance, and hence the activity of H^+ in the membrane, did not change in the pH range 2.5 to 11.5. These results were used to predict potentials of a H^+ selective electrode over the same pH range and results compared to a parallel experiment where a membrane of identical composition was used in a H^+ selective electrode. A Nernstian response of the electrode was observed in the pH range where the absorbance did not change i.e. from 2.5 to 11.5, and the measured values of potential were in good agreement with those predicted in the optode experiment. It was also significant that the optode experiment allowed prediction of the electrode response in the regions of cationic and anionic interference at low and high pH values respectively.

The model was extended[23] to predict the response functions in mixed solutions as well as neutral and charged carrier systems. However, the model is not applicable unless the electrodes exhibit a Nernstian response towards all the ions of interest, nor is it valid for precipitate based electrodes. The model requires a constant composition in the membrane bulk, it must have ion exchange properties and be sufficiently hydrophobic to prevent co-

extraction of sample counter ions and be sufficiently hydrophobic to prevent co-extraction of sample counter ions. To maintain a Nernstian response to the sample ion, a selective ionophore has to be used to prevent a mixed ion response, however this is conditional on the ligand not binding the sample too tightly.

In conclusion, there still seems to be little agreement in the literature on the response mechanism of membrane electrodes. The importance of anionic sites in the membrane either as impurities or as additives seems universally accepted as does the presence of a selective ionophore. Most authors now agree that it is an equilibrium process at the electrode sample interface that governs the response and not bulk transport within in the membrane.

4.1.4 Membrane Components

A typical membrane used in an ISE has the following composition by weight[24]; 66 % plasticiser (a water immiscible high boiling point liquid) 32 % PVC, 1.2 % ionophore (ion carrier) and 0.8% additive (a bulky lipophilic anion). To understand the contribution that each of these components makes to the membrane they will be discussed individually

4.1.4.1 PVC

PVC was first added to give mechanical support to the membranes. It is now realised that the PVC was also a very important source of anions which were present as impurities. These were identified[25] by X-ray fluorescence, secondary ion mass spectroscopy and X-ray photoelectron spectroscopy. They included sulfonates and sulfates from polymer-bound initiating groups, carboxylates from oxidation reactions and remainders of surfactants such as alkyl sulfates and phosphates. They found the amount of anion sites appears to be uncontrolled and dependent on the purification methods. It is ironic that the original inclusion of PVC was to provide mechanical stability to the liquid membrane, yet its inherent impurities proved to be more important for the correct functioning of the electrode, providing an ion exchange mechanism.

4.1.4.2 Plasticiser

The plasticiser percentage in membranes varies from 33 wt.% in commercial electrodes to 66 wt.% in ISE electrodes, and electrode performance deteriorates with decreasing plasticiser content[26]. The temptation is to regard the PVC as an inert support and the plasticiser as a free liquid. However the work of Fiedler and Ruzicka has shown that the membrane is more homogenous than heterogeneous[27]. They showed that the electrodes are functional only above a glass transition temperature similar to the melting point of a solid, which clearly demonstrated that the plasticised PVC has to be in a liquid like state with the plasticiser molecules and the PVC chains forming a true solution in which the ionophore and added salt are dissolved. The dielectric constant of the plasticised membrane is very important, and is a function of both the proportion of PVC to plasticiser and the nature of the plasticiser.

4.1.4.3 Ionophore

The original ionophores incorporated were macrocyclic antibiotics[11]. As synthetic macrocycles were developed these too were incorporated, and it was soon realised that non-macrocyclic complexing agents could also be used. The required ionophore had to be lipophilic enough to stay in membrane, selective to be of use in a sensor, and have fast complexation times. The suitability of an ionophore is often measured in terms of the strength with which it binds the ion of interest. This is measured in terms of a stability constant and is often expressed as a logarithm, the range of adequate complex formation for an ionophore to work effectively in a membrane is log K = 4 to 9 for a 1:1 stoichiometry[28]. The minimum binding strength is governed by the requirement that the ion must be present predominantly in the complexed form. However, if the complexation is too strong co-extraction of anion occurs.

4.1.4.4 Ionic additives

It is now accepted that anionic sites originally present in small concentration as impurities, are required for the permselective behaviour of ISE membranes. Tetraphenylborate salts were originally added to reduce the anionic interference observed in the presence of lipophilic anions such as SCN^- and ClO_4^-. It was realised that this addition has other benefits including a lowering of the membrane resistance and an influence on the selectivity coefficient[29].

The amount of ionic additive has a striking effect on the selectivity of the membrane which can result in the same membrane acquiring completely different selectivity[30]. Theory and experiment confirm that sensors requiring monovalent selectivity should only contain small amounts of additive whilst divalent selectivity requires a molar ratio of cation to carrier of 0.7. This effect was illustrated by Simon et al using a neutral carrier ETH1692 and varying the amounts of potassium tetrakis(p-chlorophenyl)borate (KTpClPB). In this work the proportion of additive was varied from 0 to 200% of the ionophore, and the results obtained were in very good agreement with theory. This dependence of the selectivity on the additive makes the membrane very sensitive to loss of KTpClPB. They prepared membranes containing 95 and 110 mole percent additive which were soaked in 0.1mol dm^{-3} $MgCl_2$ for one month which resulted in 10 – 15% loss of additive. An excess of additive is self correcting, membranes which have KTpClPB in excess of valinomycin levels, spontaneously lose it until its concentration becomes exactly the same as that of the valinomycin itself.[31]

4.1.5 Silver ionophores

The selectivity of liquid membranes has been shown to depend on the complexation specificity of the ionophore as well as the composition of the membrane (vide infra). The selectivity of these carriers for cations has been shown to depend on such factors as the number and type of donor atoms and on the size match between the metal ion and the ionophore[32-34]. In this section a range of silver ionophores are reviewed with emphasis on those that have been incorporated into membrane electrodes. The ionophores are compared in terms of their selectivity for silver over interfering metal ions which is usually expressed as log $K_{Ag,M}$. Reported selectivity values vary from 1 (poor) to 6 (excellent). The method of determination is normally given as FIM for the fixed interference method or SSM for the separate solution method as discussed in section 4.1.2.

4.1.5.1 Thiacrown ethers.

Thiacrown ethers are among the first compounds to be incorporated into PVC membrane electrodes, such as those membrane electrodes prepared by Lai and Shih using a range of diether crown ethers[35]. Of those tested, they found that 1,4-dithia-15-crown-5 **22A** showed the best sensitivity (40mV dec^{-1}) and showed good selectivity coefficients towards

alkali, alkaline earth and transition metals with log $K_{Ag,M}$ (FIM) values higher than -3.5, although mercury was still a strong interferent (+0.8), as shown in Figure 4.3.

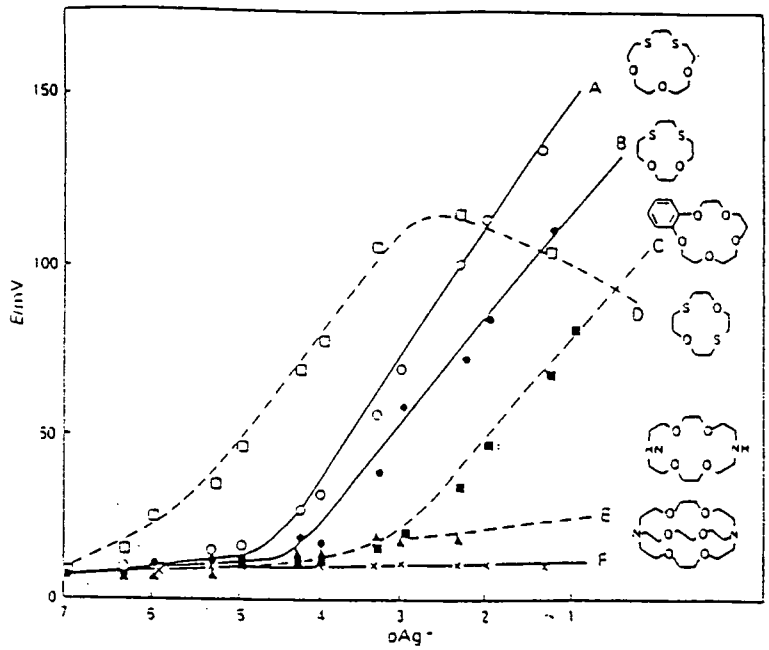

Figure 4.3 Compounds (**22** A-F) synthesised by Lai and Shih[35] and their responses towards Ag^+.

Interestingly, some cryptand ligands (molecules **22E** and **22F** in Figure 4.3) were also tested in this study and these showed very little response, which was a surprising result owing to their similar cavity dimensions to the polyethers tested. The authors rationalised this result by arguing that the cryptands formed very strong complexes which resulted in difficulty in exchanging the Ag^+ between the membrane and the test solution.[36] The 1,7-diether ether (molecule **22D**) showed a very good response at low levels of Ag^+ but tailed off at higher concentrations, which would appear to suggest that this ionophore has a very high affinity for silver at low concentrations, but rapidly becomes less responsive at higher concentrations as the available complexation sites become filled. Similar selectivity values towards alkali, alkaline earth and transition metals was achieved by Oue *et al* [37,38] also using thia- and dithia-crowns, but they achieved better selectivity towards Hg^{2+}.

A range of 14-crown-4 compounds was synthesised and the performance of the corresponding membrane ISE's analysed[39]. This study investigated variation of ring size, number and degree of oxidation of sulfur atoms, and size of bulky substituent in cyclic as

well as acyclic thioether molecules. The best silver ionophore was **23** with selectivities of the order $-\log K_{Ag,M}$ (SSM) = - 4 and - 5 for the alkali / alkaline earth metal ions and heavy metal ions respectively. This was attributed to the presence of the bulky pinan substituent, which prevented the formation of stable complexes with other interfering ions, rather than this structure having an optimum binding geometry for silver ion.

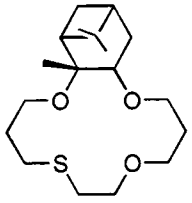

23

Macrocyclic polythia ethers (**24**, **25** and **26**) have been used by Casabó *et al.* incorporating aromatic rings as macrocyclic components[40]. These were tested as membrane electrodes and showed an excellent Nernstian response, (Figure 4.4) in the range 10^{-7}–10^{-2} mol dm^{-3}, as well as good selectivity towards a wide range of cations, including values for mercury which ranged between log $K_{Ag,M}$ (FIM) = -2.1 to -2.6. The authors could not explain this high selectivity but they reasoned that it could be attributed to "electronic factors or mobility problems inside the membrane".

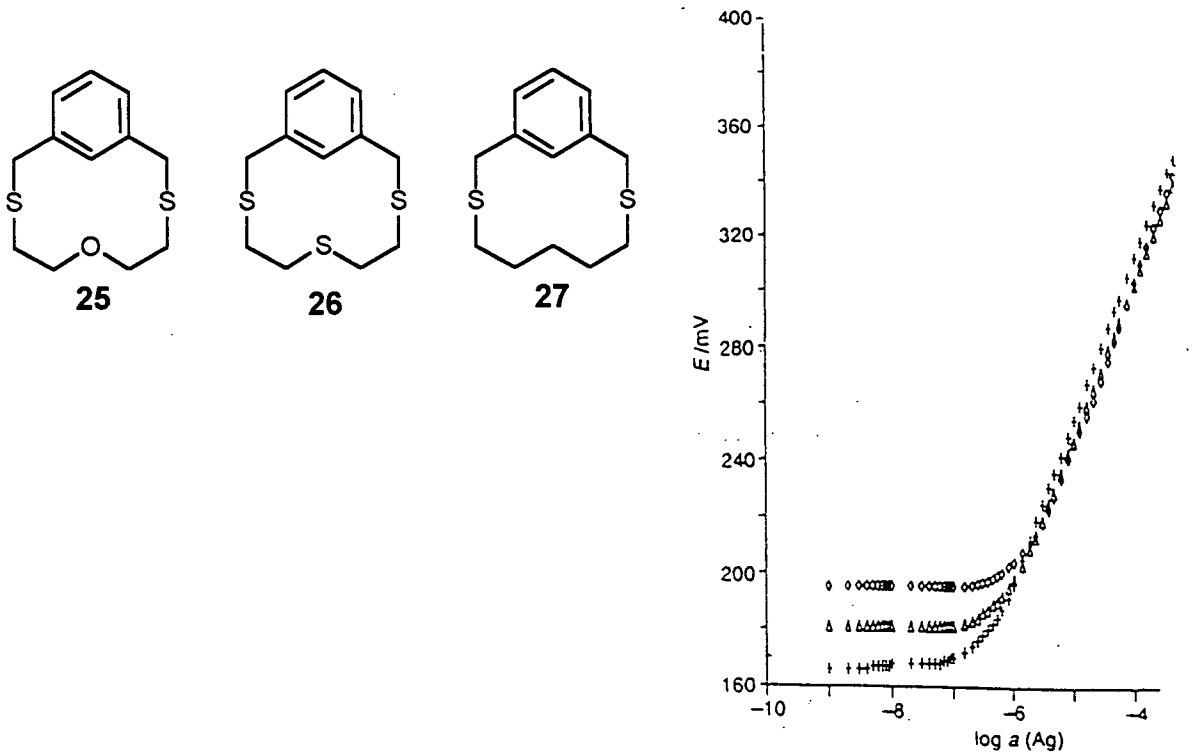

Figure 4.4. Polythia ethers prepared by Casabó[40] and their response to silver 2(+), 3(□) and 4(Δ)

4.1.5.2 Calixarenes

Calixarenes are a relatively new class of macrocycles and have been synthesised with a wide range of functional groups suitable for the selective complexation of alkali and alkaline earth metals. Recently, new calixarenes have been synthesised which incorporate nitrogen and sulfur atoms making them suitable for silver binding.[41] A range of calixarenes exhibited acceptable silver responses with one bearing $CH_2CO_2C_2H_4SCH_3$ groups displaying almost Nernstian response (50 mV dec^{-1}) with a detection limit in the order of 10^{-4} mol $dm.^{-3}$ Further work was carried out on incorporating this ionophore it into both membrane and membrane-coated glassy carbon electrodes. From selectivity coefficients determinations Na^+ and Hg^{2+} were the main interferents with log $K_{Ag,M\ (SSM)}$ values between 0 and +2.0. The best selectivities were over the heavy metal ions such as Pb^{2+} and Cd^{2+} which were of the order log $K_{Ag,M\ (SSM)}$ = -3.0; however, K^+ was still a major interferent at log $K_{Ag,M\ (SSM)}$ = -2.1. This high interference from the alkali metal ions is due to the presence of the hard oxygen atoms in the ester group. In a later publication by the same group, the effect of conformation of the calixarene on silver binding was

investigated.[42] A calixarene with practically the same chemical structure, but in a partial cone conformation, showed superior selectivity performance than that of the cone conformation. This was accounted for by the increase in the size of the cavity which disfavours binding by the smaller interfering cations.

Work on calixarenes was extended by Malinowska *et al.* with calix[4]arenes functionalised with $C_2H_4SCH_3$ groups incorporated into PVC membranes.[43] These electrodes showed good responses to silver over a wide range of concentrations in the presence of alkali, alkaline earth and transition metals and for mercury showed high selectivity (log $K_{Ag,M(FIM)}$ = -2.5). When comparing the values for the two calix[4]arenes one bearing two $C_2H_4SCH_3$ groups, the other bearing four it was found that the number of sulfur donor atoms in the receptor molecule does not influence significantly, the selective complexation of silver ions.

4.1.5.3 Acyclic Sulfides.

Recently there has been a move towards the use of acyclic sulfides in the design of silver ionophores. Brzózka *et al.* noticed the selectivities of thia-crown ethers were similar in spite of different numbers and positions of the sulfur atoms in the rings, which prompted them to investigate acyclic thioethers.[44] Two groups of lipophilic sulfides were synthesised and their structures are shown below.

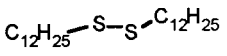

27

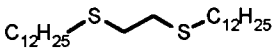

28

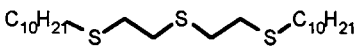

29

R =

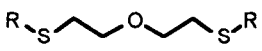

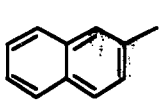

30

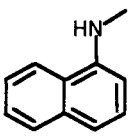

31

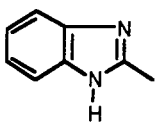

32

The first two sulfides compounds tested, **27** and **28** showed Nernstian response whilst the third **29** deviated at higher concentrations. This deviation was thought to be indicative of this molecule forming an extremely strong complex with silver, (this so-called S-curve behaviour has been described by Cobben using model calculations[45]). The second group of sulfides (**30** - **32**) contain one oxygen atom which has the effect of reducing the selectivity over other transition metal ions but enhancing that of silver over mercury. Interestingly, it is the ionophore **30**, functionalised with pendant naphthalene groups, which displays the best Ag^+ selectivity. This is consistent with the affinity of Ag^+ for aromatic ligands which was discussed in section 1.1.2.

Casabó *et al* investigated the acyclic analogues of the polythioether macrocycles described earlier and found no significant difference in silver selectivity between them and their cyclic analogues.[46] This led the authors to postulate that it is factors such as the geometrical arrangement of the thioether atoms in the receptor, the Ag^+ affinity for sulfur atoms, and the tendency for linear coordination which are important in silver complexation, not the cyclic or acyclic nature of the ligand.

The potential of simple thioethers to act as sensor molecules was also explored by Casabó *et al*, who after a systematic search of the literature, hypothesised that "the macrocyclic nature of the cavity size of thioether ligands was not the main basis for good selectivity for Ag^+, but rather simply the existence of the thioether group in the sensor molecule".[47] To confirm their hypothesis they took "common lab-shelf chemicals" containing the thioether moiety, *viz.*, EtSEt, PhSEt and PhSPh and incorporated these into PVC membrane electrodes. They obtained Nernstian responses for all three electrodes and found very little difference in their response parameters, thus showing the absence of an influence of the nature of the moieties attached to sulfur. Selectivity studies were also reported for a range of metal ions and these electrodes displayed log $K_{Ag,M(FIM)}$ values around -5, although a value for the selectivity towards mercury was not reported. This was reported in a later paper by the same group when they incorporated the diphenyl thioether into a CHEMFET device.[48] In this work the selectivity series was extended to include a value for mercury of log $K_{Ag,M(FIM)} = -1.8$. This is a relatively high interference which is attributed to the simplicity of the molecule.

4.1.5.4 Other Ionophores

Silver selective electrodes have also been reported with other classes of ionophores. Among these is a pyridinophane which is an interesting silver ionophore as it does not contain any sulfur atoms.[49]

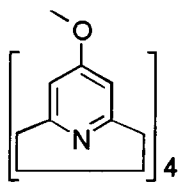

33

The selectivities reported were log $K_{Ag,M}$ (SSM) = -2 to –3 for the alkali / alkaline earth metal ions and –3 to –4 for the heavy metal ions. The high alkali / alkaline earth metal ion interference was due to the hard donor atoms; this ionophore also bound mercury irreversibly.

A series of podands containing nitrogen and sulfur atoms were recently reported.[50-52] Results from this work presented an exception to the "simple existence of a sulfur atom" hypothesis of Casabó as the nature of the podand had a significant effect on the response of the membrane electrodes.

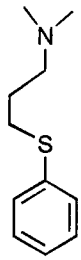

34

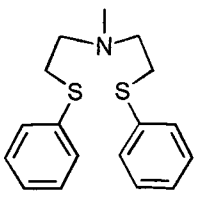

35

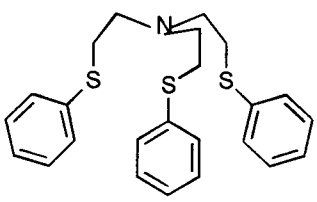

36

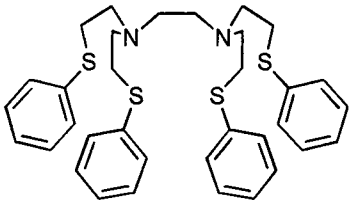

37

The podands **34** and **35** gave negligible slopes compared to **36** and **37** which displayed near Nernstian slopes. The reported selectivities were also an order of magnitude higher for the podands **36** and **37** than for **35**.

4.2 Experimental

4.2.1 Materials

Of the ionophores employed in this work, **8d** was synthesised as described in Section 2.2, ionophore **23** was supplied by Fluka and ionophore **24** was synthesised by Teasdale.[53] The membrane components, PVC (high molecular weight) potassium tetrakis(4-chlorophenyl) borate (KTpClPB), 2-nitrophenyl octyl ether and bis(2-ethylhexyl)sebecate DOS were obtained from Fluka. Silver nitrate was obtained from Aldrich.

4.2.2 Membrane preparation

Membranes were prepared according to the procedure widely used by Craggs *et al.*[24] Typically, the following compositions were used: 1.2 wt % ionophore, 0 to 70 mol % (of ionophore) KTpClPB, 64 – 67 wt % plasticiser (oNPOE or DOS) and 33 wt % PVC. The components were dissolved in 5 cm^{-3} of freshly distilled THF and were agitated overnight on a mechanical shaker. The resulting syrup was poured into a glass mould and the THF solvent allowed to evaporate slowly at room temperature over a period of 24-48 h. A semi-transparent flexible film resulted, from which a disk of 9 mm in diameter was cut using a cork borer and positioned in the electrode. The electrodes was assembled, including a 10^{-3} mol dm^{-3} $AgNO_3$ inner fill solution, and immersed in a conditioning solution of 10^{-3} mol dm^{-3} $AgNO_3$ for 24 h.

4.2.3 Techniques Employed

4.2.3.1 Separate Solution Method

Electrode Calibration

The electrodes were calibrated using solutions of $AgNO_3$ in the range 10^{-6} to 10^{-1} mol dm^{-3}. The potentiometric set-up allowed six electrodes to be measured simultaneously. The first calibration was run in ascending order starting with the 10^{-6} mol dm^{-3} solution. The electrodes were rinsed with distilled water between each reading. The second calibration was run in the reverse order *i.e.* starting with the most concentrated solution and working down. The final calibration was in ascending order. This technique was used to investigate the reversibility of the electrode response, and also provided three sets of values of potential for each value of concentration. The reference electrode was an Orion double junction electrode with a silver/silver chloride inner reference and a KNO_3 bridge solution.

Selectivity Coefficients Determination

Selectivity coefficients were determined using the separate solution method.[7] In this technique the response of the electrode in a pure solution of the ion to be determined, in this case Ag^+, is compared to the potential in a pure solution of an interferent ion of the same concentration. Metal nitrate solutions of 10^{-1} mol dm^{-3} were used for silver and the interferent ions. The potential of the silver ion was first determined and the electrodes were then rinsed with distilled water before the potential of the interfering ion was determined. This process was repeated for all the interferents, allowing a silver ion solution to be determined between each interferent ion. This technique allows the electrode to be monitored for drift, which could occur if interfering ions were to bind irreversibly.
Selectivities were calculated using the Nicolsky-Eisenman equation (4.8)

$$K_{ij}^{Pot} = 10^{\frac{(E_j - E_i)z_i F}{2.303\,RT}} \quad \frac{a_i}{(a_j)^{z_i/z_j}} \qquad (4.8)$$

where

K_{ij}^{Pot} Potentiometric stability constant for the primary ion i over the interfering ion j

E_i, E_j Potentials for the primary and interfering ions, respectively

z_i, z_j Charges for the primary and interfering ions, respectively

a_i, a_j Activities of the primary and interfering ions, respectively

R Gas constant

F Faraday constant

T Temperature in Kelvin

This equation can be simplified by combining the constants in the first term of equation (4.8) to give the theoretical slope S, which at 25 °C has a value of 59.16. The charge on the primary silver ion is +1, so the term z_i reduces to unity. In addition the concentration of the primary and interfering ions are equal, and we are using concentration instead of activity, $a_i = a_j = 0.1$. Therefore the second term of equation 4.8 simplifies greatly. This allows equation 4.8 to be written as follows:

$$K_{ij}^{Pot} = 10^{\frac{\Delta E}{S}} (0.1)^{1/z_j} \qquad (4.9)$$

where

S : Theoretical slope, 56.16 at 25°C.

ΔE : $E_i - E_j$

Selectivity coefficients are normally expressed as -log K

$$-\log K_{ij}^{Pot} = \frac{\Delta E}{S} + \log(0.1)^{1/z_i} \qquad (4.10)$$

Equation 4.10 was then used to calculate the selectivity coefficients.

4.2.3.2 Constant Volume Dilution Method

This method was introduced by Horvai and Pungor for calibration of ion-selective electrodes.[54] It is regarded as a superior technique to the SSM as it more closely represents the working environment of a sensor, i.e where the primary ion is determined in a background of interfering ion. However, the analysis time for an electrode calibration is longer (typically 25 minutes) and specialised constant volume and reference cells are required. The values for slope determined for a given electrode using this technique is generally higher than the corresponding value determined using the SSM. This is due to a hystersis or memory effect of the ion in contact with the membrane as the solution is diluted, and does not occur in the SSM as the electrode is rinsed with distilled water between determinations.

It involves immersion of an electrode into a solution diluted with respect to one of the components which influences the potential. If an electrode responds in a Nernstian fashion, then its measured potential is proportional to ln C (where C is concentration in mol dm^{-3}). Such an electrode responding to a continuously diluted solution would give a linear response to potential versus time.

The experiment involves the continuous dilution of a fixed volume of stirred, solution either by water for a calibration, or a background electrolyte for selectivity determinations. The relationship between the concentration and time can be derived as follows.

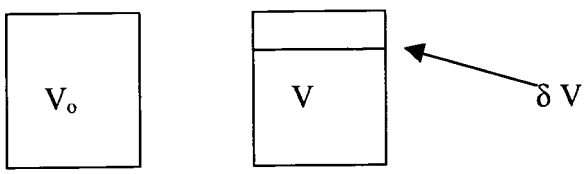

Dilution of the cell with a solution not containing the primary ion results in a volume δ V being replaced by the diluent. The new concentration of the primary ion (C') is given by equation 4.11.

$$C' = \frac{CV}{V_o} = \frac{C(V_o - \delta V)}{V_0} \quad (4.11)$$

Rearranging and substituting $\delta C = C' - C$ gives

$$\frac{\delta C}{C} = -\frac{\delta V}{V} \quad (4.12)$$

If the dilution is continuous then $\delta V \rightarrow dV$

$$\frac{dC}{C} = \frac{dV}{V} \quad (4.13)$$

For a flowrate of ω (m^3s^{-1}), $dV = \omega\, dt$, where t is the dilution time in seconds. Substitution into equation 4.13, and integration, gives:

$$\int_{C_0}^{C} \frac{dC}{C} = -\int_0^t \frac{\omega dt}{V_0} \quad (4.14)$$

$$\ln C = \ln C_0 - \frac{\omega t}{V_0} \quad (4.15)$$

where C_0 is the initial concentration of the primary ion in the fixed volume and C is its concentration at time t. As the initial results are plotted in the form of potential versus time and the final plots are presented in the form of potential versus –log C, the following conversion is used;

$$-\log C = -\log C_0 + \log\left(e^{-\omega t/V_0}\right) \quad (4.16)$$

The experimental setup is shown in Figure 4.5. The solution is drawn through the constant volume cell, past the reference cell and on to waste by a peristaltic pump. The flow rate was measured by timing the filling of a volumetric flask. This flow rate was used to calculate the volume of the constant volume cell by measuring the time required to fill it. The constant volume and the reference cells were made in house and the system was thermostated at 25°C.

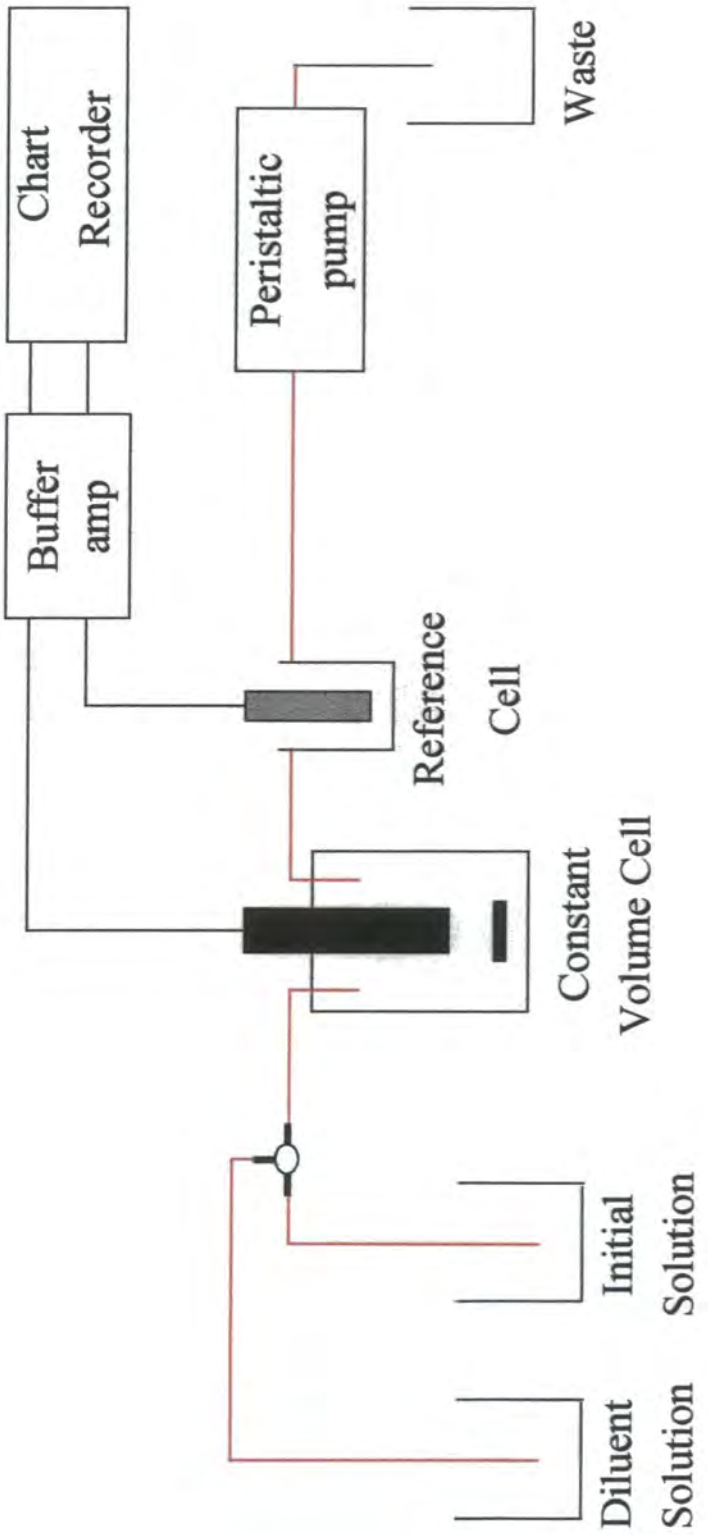

Figure 4.5 Schematic representation of experimental set-up for constant dilution

The determination of a limit of detection, or a selectivity coefficient of an electrode requires determining the range of activity where the electrode responds in a Nernstian fashion to the primary ion. The response of an electrode to the primary ion i and the interfering ion j is shown in Figure 4.6.

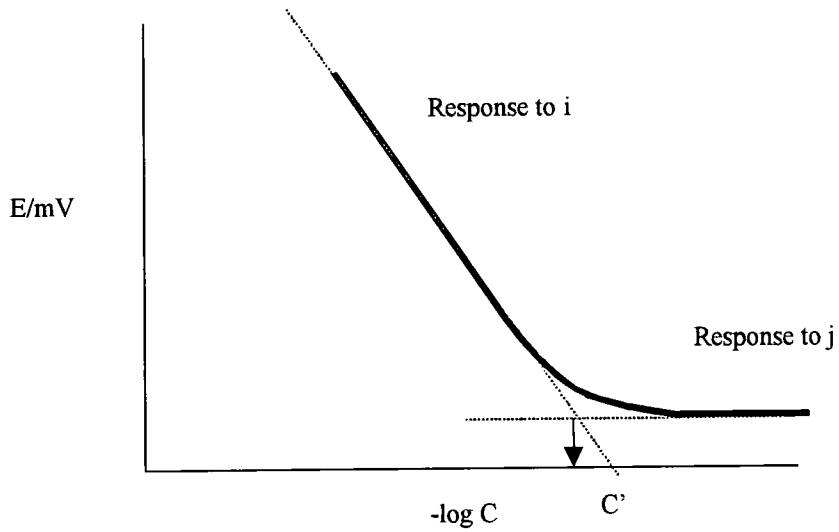

Figure 4.6 Ideal response curve for an electrode on dilution with an interfering ion.

If the electrode response levels out upon dilution then the point C' is where the electrode is responding equally to both ions. An expression relating this concentration to the selectivity coefficient can be derived as follows.

At high concentration of primary ion the potential is governed by i

$$E_i = E_0 + k \log C_i \qquad (4.17)$$

At low concentrations of i, the electrode response is governed by j

$$E_j = E_0 + k \log\left(K_{ij} C_j^{z_i/z_j} \right) \qquad (4.18)$$

Combining equations 4.17 and 4.18, at concentration C' where $E_i = E_j$ gives

$$C' = K_{ij} C_j^{z_i/z_j} \quad (4.19)$$

This can be rearranged to give an expression for the selectivity coefficient

$$K_{ij} = \frac{C'}{C_j^{z_i/z_j}} \quad (4.20)$$

The situaition represented in Figure 4.6 represents and ideal response behavior which is not always observed. It is more common for the response to decrease on dilution and not level out, this response is shown in Figure 4.7.

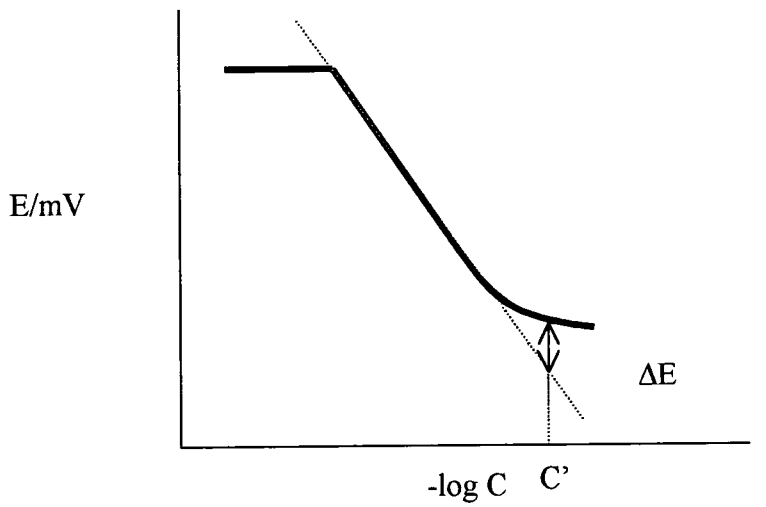

Figure 4.7 Response curve when the potential does not level out on dilution with an interferent

In this situation a different methodology is used which involves comparison of the electrode response for the pure primary ion and the mixed response.

The primary response is given by

$$E_i = E_0 + k \log C_i \quad (4.17)$$

The response in mixed solution is given by

$$E' = E_0 + k\log\left(c_i + K_{ij}c_i^{z_i/z_j}\right) \quad (4.21)$$

At the point C' on Figure 4.7, $C_i = C' = K_{ij}C_j$, the difference in potential ΔE between the pure solution and the mixed ion solution, each with primary ion concentration C' is

$$\Delta E = E' - E_i = k\log 2 \quad (4.22)$$

$$\Delta E = \frac{2.303RT}{z_i F}\log 2 \quad (4.23)$$

$$\Delta E \cong \frac{18}{z_i}mV \quad (4.24)$$

The concentration C' can be determined by extrapolation of the linear plot to the point where an 18 mV deviation occurs from the Nernstian response.

4.3 Results

4.3.1 Choice of Ionophore

In this section compounds **7a-d** (whose synthesis was described in Chapter 2) were used to prepare polymer membranes suitable for incorporation in ISEs. The use of ISEs for potentiometry does not require a molecule with transducer properties, but rather a molecule which binds reversibly the ion of interest[11]. The results from solution studies as described in section 3.3, indicate that these molecules do have an affinity for silver. A membrane composition without additive was selected to optimise the binding contribution of the molecule, as it was feared that the soft tetraphenylborate anion would bind silver.

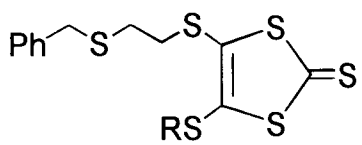

R
7a Me
7b Et
7c iPr
7d nBu

7a-d

In this experiment the effect of changing the lipophilicity of the thione in the range **7a-d** was investigated. A series of membrane compositions was prepared as shown in Table 4.1.

Electrode	Molecule	PVC Weight %	Plasticiser Weight %	Molecule Weight %
E1	7a	31.8	67	1.2
E2	7b	31.8	67	1.2
E3	7c	31.8	67	1.2
E4	7d	31.8	67	1.2

Table 4.1 Compositions of electrodes prepared from thiones **7a-d** .

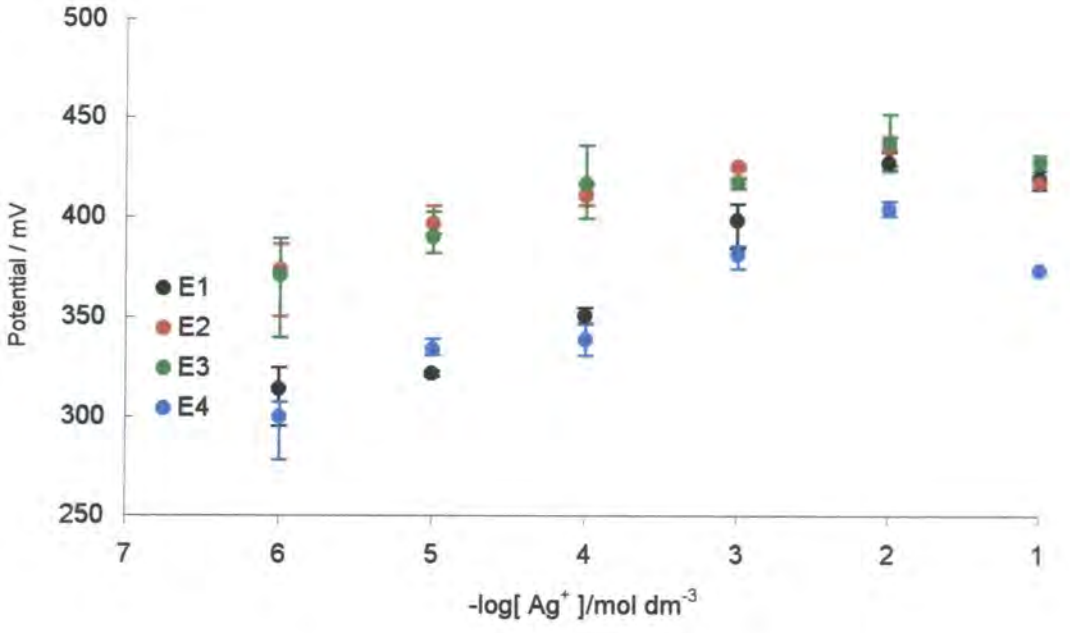

Figure 4.7 Calibration plots of electrodes 1 to 4 prepared using compounds **7a-d**.

The calibration plots of electrodes E1-E4 are shown in Figure 4.7. The potentials of these electrodes show considerable scatter (up to ±20mV), and it is also significant that all electrodes show a decrease in potential on increasing the silver concentration from 10^{-2} to 10^{-1} mol dm^{-3}. The degree of nonlinearity of these electrode slopes made the accurate determination of slopes difficult but approximate values show that they are all sub Nernstian with values from 15 to 30 mV dec^{-1}.

These electrode characteristics suggest that all of these electrodes are binding silver irreversibly. It is significant that this behaviour is not affected by the change in ionophore lipophilicity (i.e. on going from R=methyl to R=butyl group for electrodes E1 to E4). This suggests that binding is occurring at another site such as the thione group and not at the ligating chain which was the initially proposed binding site.

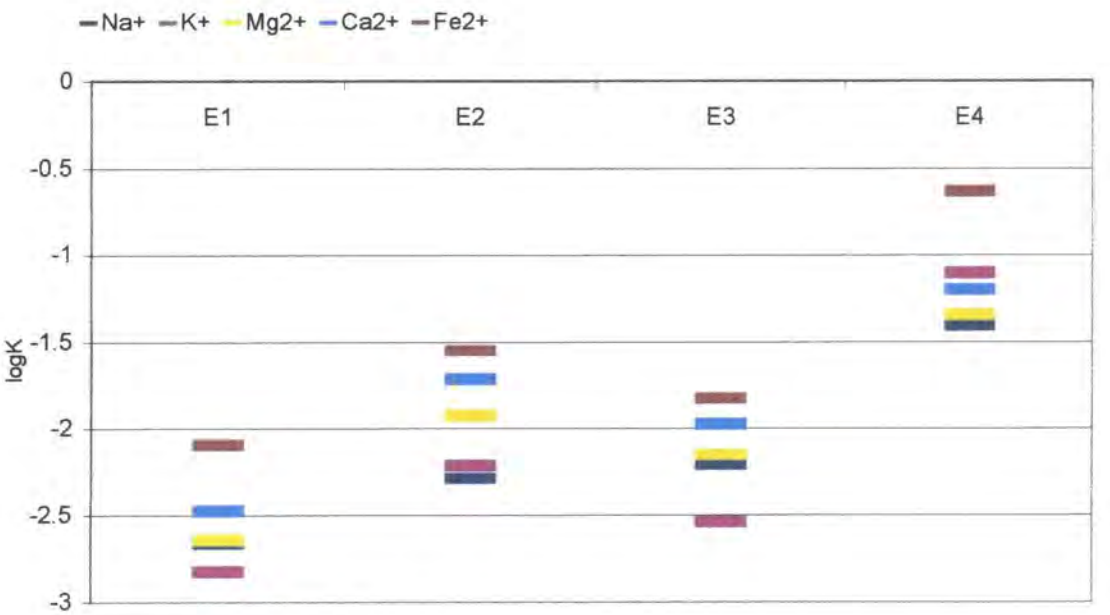

Figure 4.8 Selectivities of E1 to E4 prepared from compounds **7a-d** for silver over a range of cations

The selectivity of E1 to E4 for silver ion over a range of metal ions of interest to Kodak was determined by the separate solution method. The results are expressed as logarithms of the selectivity coefficient $K_{Ag/M}$ (defined in section 4.2.3.1) and are shown in Figure 4.8. The values for the E1 to E4 decrease with increasing lipophilicity except for E3 which breaks this trend. This indicates that the increasing lipophilicity results in an increase in binding of the interfering cations, this trend is not readily explicable.

The results of the calibration plots of thiones **7a-d** indicate that the backbone of the molecule is binding silver strongly, with the most likely binding site being the thione group. This thione can easily be converted to a ketone using mercuric acetate and this reaction was described in chapter 2 to form the analogous compounds **8a-d**. This series of ketones was used to make a new set of membranes, using the same composition as that used for compounds **8 a-d** and the new electrodes were numbered as shown in Table 4.2

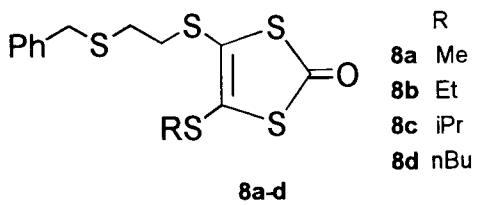

8a-d

R	
8a	Me
8b	Et
8c	iPr
8d	nBu

Electrode	E5	E6	E7	E8
Compound	**8a**	**8b**	**8c**	**8d**

Table 4.2 Numbering of electrodes prepared using compounds **8a-d**.

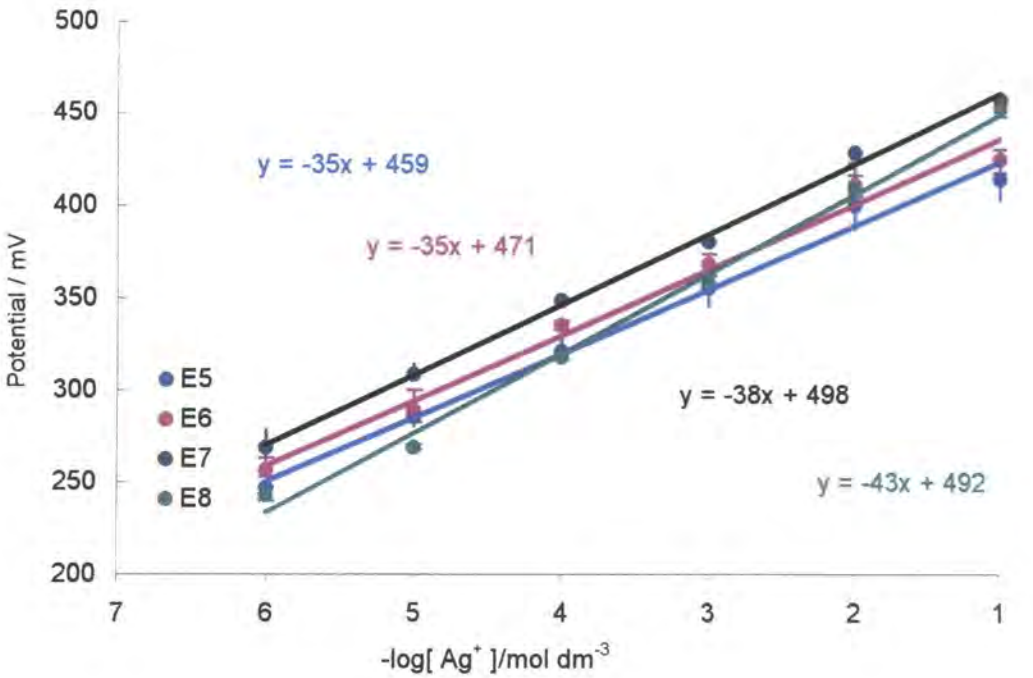

Figure 4.9 Calibration of E5 to E8 prepared using compounds **8a-d**.

The calibration plots of E5 to E8 are shown in Figure 4.9. In this series, there is a clear change in electrode response upon increasing the lipophilicity of the molecule, as the slope of the response increases from 35 mV dec^{-1} for the methyl group to 43 mV dec^{-1} for the butyl group. These results contrast with those in Figure 4.7, where no difference in response was observed upon changing the lipophilicity. This result is significant for two reasons as it suggests : (i) that the main mode of silver binding is at the intended side-chain binding site and (ii) the extent of this binding can be controlled by varying the functionality in the side-chain.

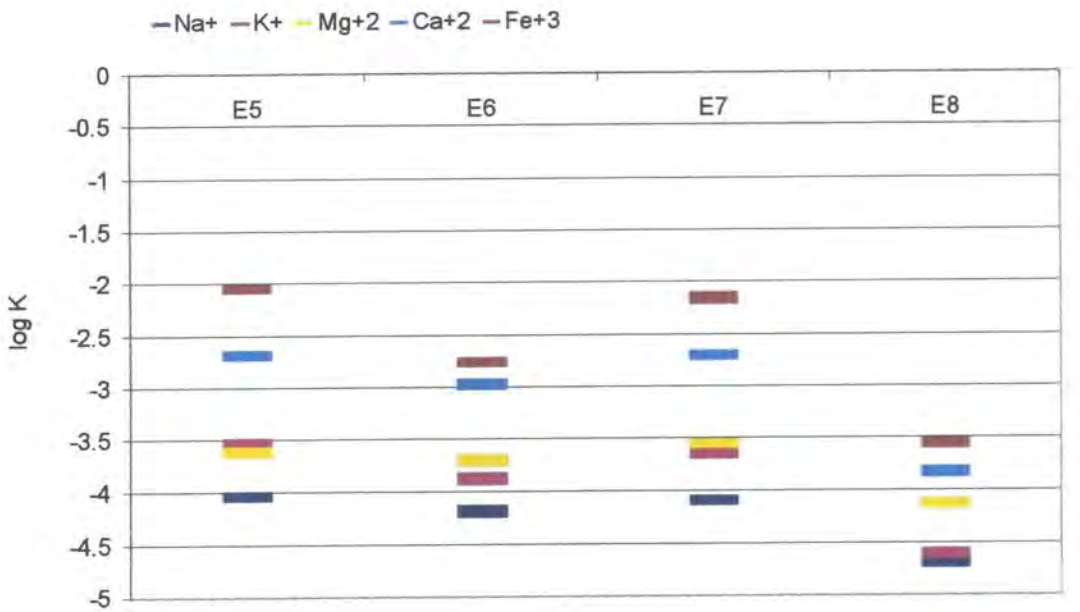

Figure 4.10 Selectivities of E5 to E8 prepared using compounds **8a-d**.

The selectivities of E5 to E8 are shown in Figure 4.10. These results, like the calibration results, demonstrate an improved electrode performance in the series E5 to E8 compared to E1 to E4, i.e. changing from the thione to the ketone is beneficial. The values for the selectivities of the electrodes improve with increasing lipophilicity, in particular the value for $K_{Ag+/Fe+3}$ improves from –2.0 for electrode E4 to –3.5 for E8. The range of silver selectivities (which reflects the overall silver selectivity) for each electrode also decreases with increasing lipophilicity, i.e. the difference between the values of $K_{Ag+/Fe+3}$ and $K_{Ag+/Na+}$ for E5 is 2.0 and for electrode E8 is 1.2. It is interesting that the values for E7, which contains the isopropyl group, do not fall into the lipophilicity trend with the other electrodes. In fact the overall trend towards improved silver selectivity with increasing lipophilicity in the range E5-E8, is the opposite to that observed in Fig 4.8 for E1 to E4. This difference is indicative of a different mode of binding in the ionophore series **7a-d** compared to **8a-d** which is further evidence that it is the thione group in the series **7a-d** which binds silver and not the side chain.

4.3.2 Optimum Membrane Composition.

In the previous section, compound **8d** was selected for its suitability in membrane electrodes based on calibration and selectivity experiments using membrane compositions based on the widely used Moody and Thomas composition.[24] In this section, the plasticiser and percentage additive were varied to optimise the membrane composition for use in silver ion measurements. The response of **8d** was compared to a commercially-available silver ionophore **25** using calibration and silver selectivity experiments.

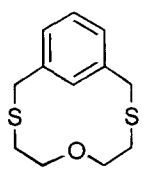

25

4.3.2.1 Calibration Plots of oNPOE Plasticised Membranes .

A series of membranes was prepared by varying the plasticiser and the percentage additive content. The first series of membranes were formulated using oNPOE as the plasticiser with concentrations of 0, 30 and 70 mol % of additive relative to the ionophore, as shown in Table 4.3.

Electrode	Compound	PVC Weight %	oNPOE Weight %	Ionophore Weight %	KTpClPB Mole %
E9	-	33	67.00	0	0
E10	-	33	66.43	0	30
E11	-	33	65.93	0	70
E12	**8d**	33	65.80	1.23	0
E13	**8d**	33	66.34	1.23	30
E14	**8d**	33	64.73	1.23	70
E15	**25**	33	65.80	1.23	0
E16	**25**	33	65.06	1.23	30
E27	**25**	33	64.07	1.23	70

Table 4.3. Formulation of electrodes used to optimise membrane composition.

In this section the electrodes are compared in groups of three, each graph containing an electrode without ionophore (dummy), an electrode with ionophore **8d** and an electrode with ionophore **25**. The plots of the electrodes are the average of three measurements, the error bars representing the degree of scatter. The responses are compared for reproducibility, linearity and slope in the linear portion of the response curve.

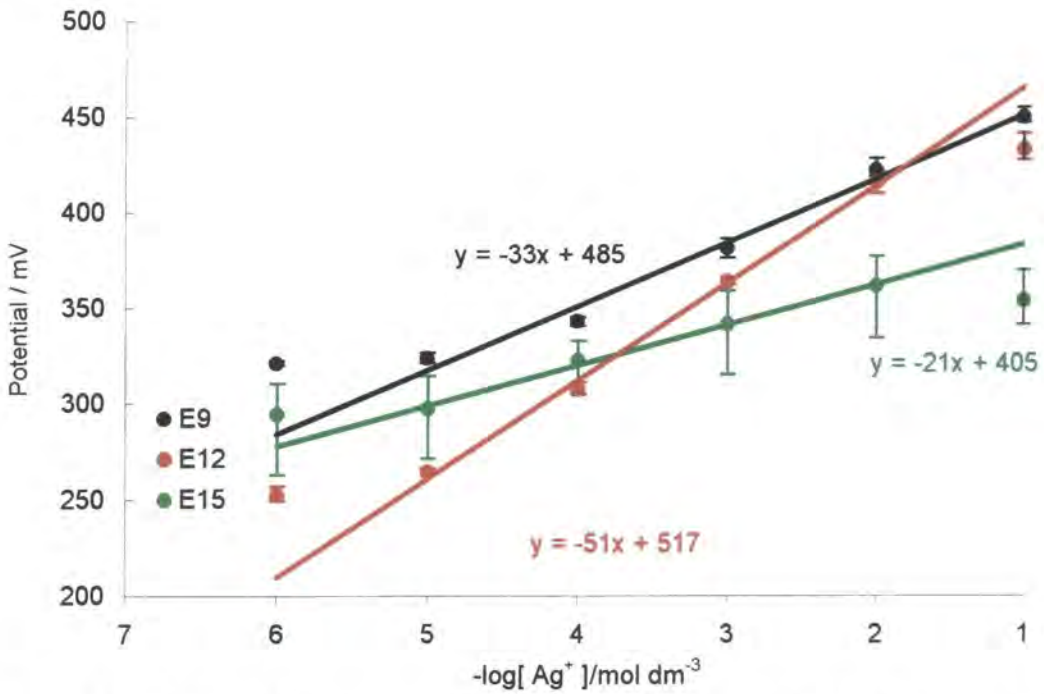

Figure 4.11 Calibration of electrodes E9 (dummy), E12 (**8d**) and E15 (**25**) prepared using oNPOE as plasticiser with no additive.

The response of the electrodes without additive is shown in Figure 4.11. It can be seen that there is very little scatter in potential values of 2 to 5 mV for the E9 (dummy) and E12 (**8d**) electrodes, but a lot of scatter (up to 50 mV) for the electrode E15 (**25**), this suggests that this ionophore is binding Ag^+ irreversibly. The tailing off of the potential at higher concentrations for E15 is also indicative that the electrode is binding silver irreversibly. Of the electrodes it is only E12 which shows a near Nernstian slope of 52 mV dec^{-1} which suggests that silver is being bound reversibly by this ionophore. Electrode E9 shows a small response to change in silver concentration which is surprising, as this

electrode does not contain any ionophore. This response is probably due to anionic sites in the membrane caused by impurities in the PVC.

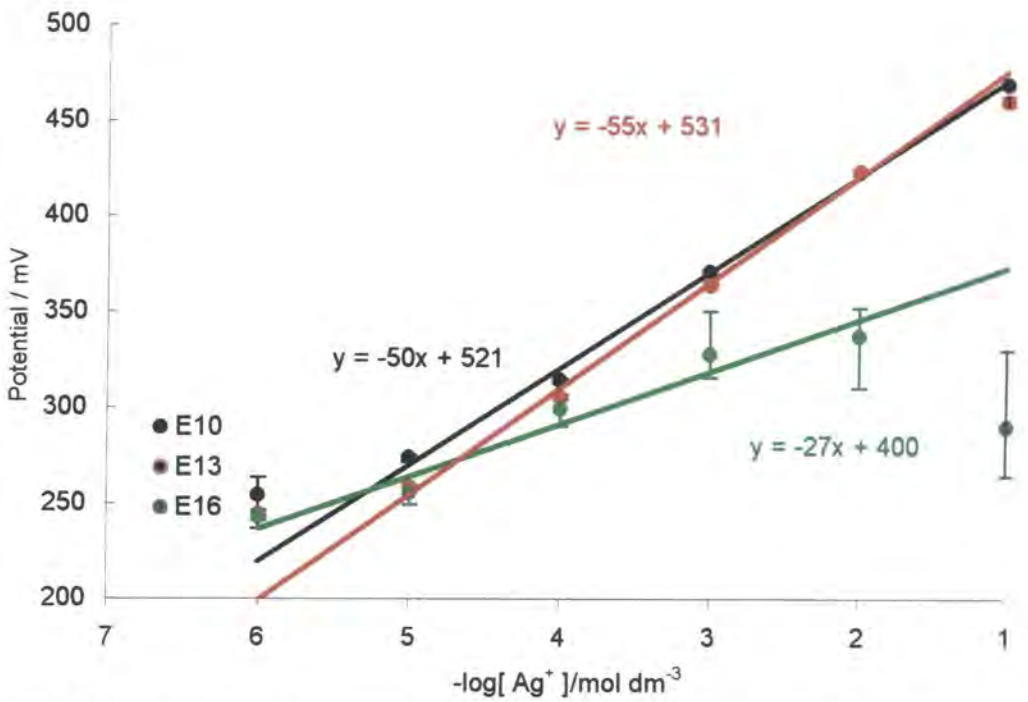

Figure 4.12 Calibration of electrodes E10 (dummy), E13 (**8d**) and E16 (**25**) prepared using oNPOE as plasticiser with 30% additive.

The effect of the additive on the response of these electrodes to silver ion can be seen from the calibration of electrodes E10, E13 and E16 as shown in Figure 4.12. The values for the electrode E16 (**25**) are even more scattered and show a more pronounced tailing off at lower [Ag^+] than those observed for the corresponding electrode E15, as shown in Figure 4.11. This indicates an increase in the irreversible binding of silver ion by this electrode on addition of the additive. It is also interesting to note that the response of the electrode E10 has significantly improved compared to the corresponding dummy electrode E9, the slope has improved from 33 to 50 mV dec^{-1}. The response for the electrode E13 (**8d**) has also improved from 51 to 55 mV dec^{-1} which is a smaller increase than that observed for the dummy electrode E10. These combined observations indicate that the additive binds the Ag^+ ion, the effect is most pronounced in the dummy electrode E10. The extra binding contribution of the additive is not as pronounced in the electrode E13 as compound **8d** is already binding silver ion.

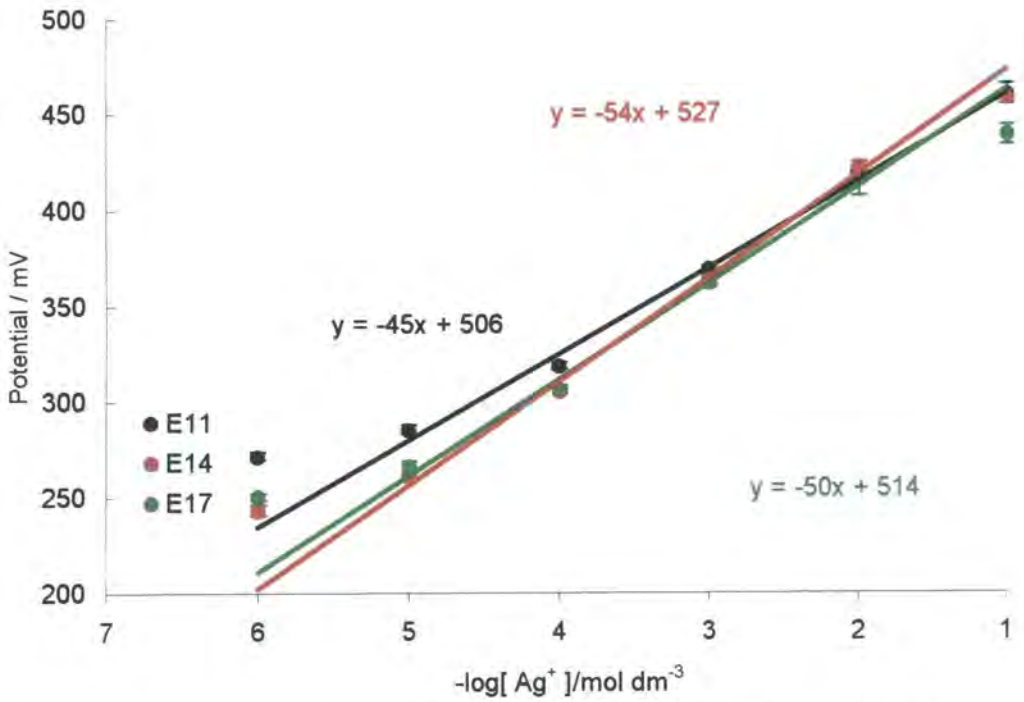

Figure 4.13 Calibration of electrodes E11 (dummy), E14 (**8d**) and E17 (**25**) prepared using oNPOE as plasticiser with 70 mole % additive.

Increasing the concentration of the additive to 70 mole % has a pronounced effect on the electrodes and in particular the electrode E17 which contains the Fluka ionophore (**25**). The small degree of scatter (±2 to 7 mV) between different potential readings, as reflected by the small error bars indicates an increase in reproducibility of electrode E17. In fact, the values are of similar magnitude to those of the dummy (E11) and **8d** (E14) electrodes. It is also significant that the value of the slope for electrode E17 of 51 mV dec^{-1} is now within a 10 mV dec^{-1} range of the other two electrodes E11 and E14, unlike the results shown in Figure 4.12, where the value for the slope for compound **25** was approximately half the value of either of the other two electrodes. This suggests that it is the additive which is binding the silver and not the ionophore **25.** The increased additive has the opposite effect on the responses of electrodes E11 and E14 causing a decrease in response in both electrodes. These results suggest that the extra binding contribution by additive now results in these electrodes binding silver too strongly.

4.3.2.2 Silver Selectivities of oNPOE Plasticised Membranes.

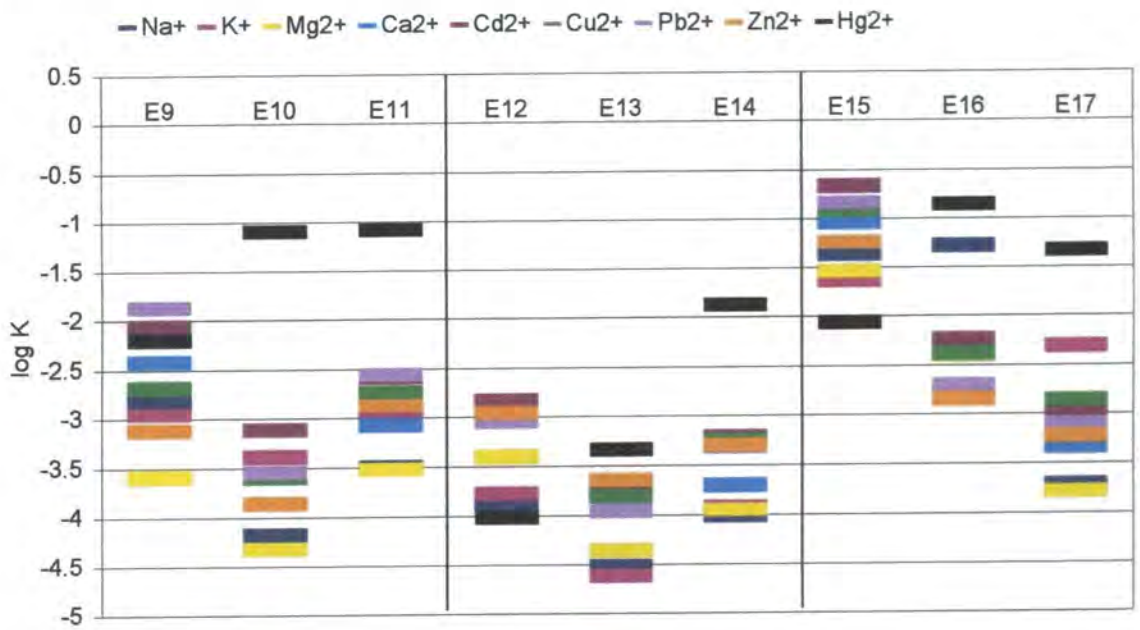

Figure 4.14 Silver selectivities of electrodes E9 to E17 over a range of cations.

The results for electrodes E9 to E17, which are shown in Figure 4.14, illustrate the pronounced effect the additive has on the selectivity of the membrane electrode. Looking first at the dummy electrodes E9, E10 and E11, it can be seen that the 30 mol % additive in electrode E10 results in an increase of almost two orders of magnitude in the selectivities compared to electrode E9. When the additive is further increased to 70 mol % in electrode E11 the selectivities are decreased across the range of cations. It is also interesting to note that the highest selectivities observed are those over the smaller cations Na^+ and Mg^{2+} and the worst selectivity is over Hg^{2+}. This is in agreement with the convention that the soft polarisable tetraphenylborate anion of the additive prefers soft cations such as silver and mercury over the hard cations such as sodium and magnesium.

A similar trend is observed for the electrodes E12, E13 and E14 where the optimum percentage additive appears to be 30 mol %. The order of selectivity in the cation range is similar, with highest selectivity observed over the smaller cations Na^+, Mg^{2+} and K^+. However, it is the electrode E12 with no additive which gives the best selectivity over Hg^{2+}

with a value of $\log K^{Pot}_{Ag/Hg}$ = – 4.0 which is among the best values reported in the literature.[39,51] This suggests that **8d** is significantly more selective than the additive for Ag^+ over Hg^{2+}.

The Fluka silver ionophore **25**, E15-17 displays completely different behaviour upon addition of additive when compared to the dummy and **8d** electrodes. The first point worthy of note is the optimal selectivity observed for electrode E17 which has 70 mol% additive; in fact it appears that the additive is playing a more active role in the selectivity than the ionophore. What is also interesting to note is the poor selectivities observed for the smaller cations such as Na^+ and K^+ for electrode E16 and E17, which is the opposite behaviour to that observed for electrodes E9 to E15. This could be due to binding by the hard oxygen atom of ionophore **25** which prefers the small hard cations.

4.3.2.3 Calibration Plots of DOS Plasticised Membranes

A second set of membrane compositions were prepared using DOS as plasticiser. From the work on the oNPOE membranes the optimum percentage additive was found to be 30 mole %, so this amount of additive was used to prepare the DOS plasticised membranes. The membranes were formulated and numbered as shown in Table 4.4.

Electrode	Compound	PVC Weight %	DOS Weight %	Ionophore Weight %	KTpClPB Mole %
E18	-	33	67.00	0	0
E19	-	33	66.54	0	30
E23	**8d**	33	65.80	1.23	0
E21	**8d**	33	65.34	1.23	30
E22	**25**	33	65.80	1.23	0
E23	**25**	33	65.06	1.23	30

Table 4.4 Compositions of DOS plasticised membranes E18 to E23.

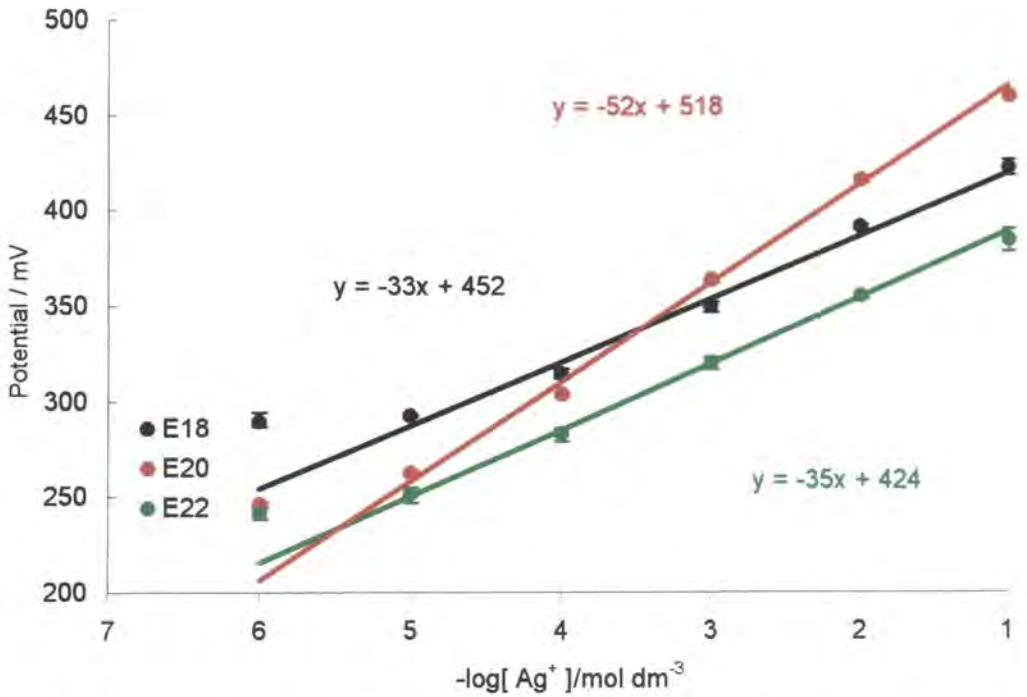

Figure 4.15 Calibration of electrodes E18 (dummy), E20 (**8d**) and E22 (**25**) prepared using DOS as plasticiser with no additive.

Changing the plasticiser reduces the dielectric constant of the membrane from ε = 23.06 for oNPOE to ε = 3.88 for DOS[55]. This appears to have a pronounced effect on the responses of all the electrodes as can be seen in Figure 4.15. The most striking difference is in the decrease in scatter of the electrode E22 (**25**), which now appears to have a response of comparative reproducibility to the electrodes E18 and E23. This suggests that the lower dielectric constant has acted to reduce the strength of the binding of the ionophore **25** for Ag^+. It is also significant that the linear range of all the electrodes has been extended to higher concentrations. All electrodes display good linear fits in the concentration range of -log [Ag] =1 to 5, compared to the linear regions of the oNPOE plasticised electrodes which was –log [Ag] = 2 to 5, this could also be explained by a lowering of the silver ion binding which allows Nernstian response at higher concentrations. The slopes of electrodes E18 and E23 are almost identical to those of the corresponding oNPOE plasticised electrodes, however the slope of E22 (-34 mV dec^{-1}) has improved considerably from the equivalent oNPOE plasticised electrode E9 (-21 mV dec^{-1}).

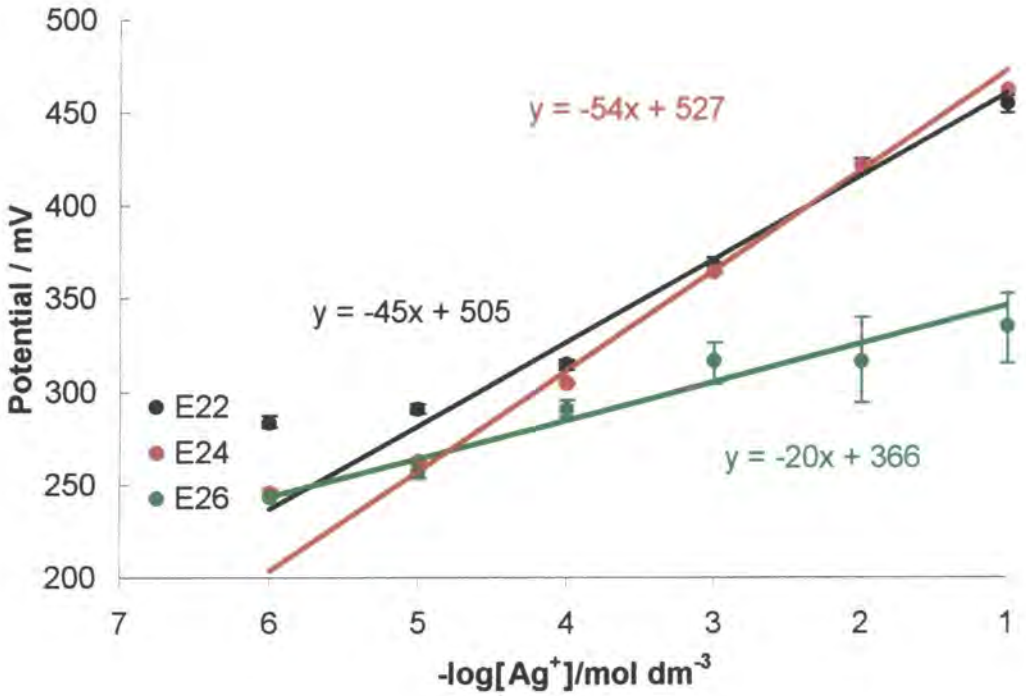

Figure 4.16 Calibration of electrodes E19 (dummy), E21 (**8d**) and E23 (**25**) prepared using DOS as plasticiser with 30 mol % additive.

The effect of the additive on the DOS plasticised membrane is quite pronounced. The most significant change is with electrode E23, which shows considerable scatter presumably due to binding by the additive. This is a surprising result, as the corresponding DOS plasticised membrane without additive (E22) showed very little scatter. It appears that whatever stability effect the DOS had on this membrane containing **25** in E22 has been reversed by the presence of additive in E23. This suggests that the ionophore **25** only binds reversibly in a membrane of low dielectric constant such as a DOS plasticised membrane with no additive, and that the presence of the additive increases this dielectric constant out of the working range of the membrane.

The effect of the change in plasticiser has a less pronounced effect on the electrodes E19 (dummy) and E21 (**8d**). However, the slope of the dummy electrode increases slightly less upon addition of additive in the DOS plasticised membrane (i.e. E18 to E19) compared to the corresponding oNPOE plasticised membrane (i.e. E9 to E10)

4.3.2.4 Silver Selectivities of DOS Plasticised Membranes.

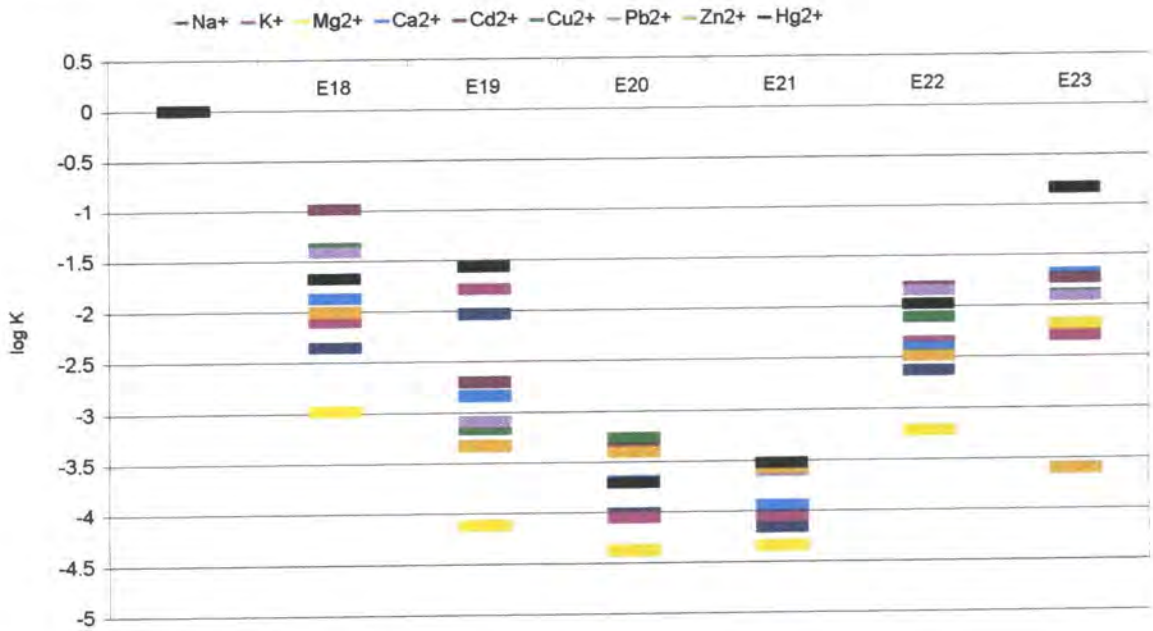

Figure 4.17 Silver selectivities for DOS plasticised membranes.

The selectivities across the range of electrodes are very similar, with the same trends evident for the DOS plasticised membranes as those observed for the oNPOE plasticised membranes in Figure 4.14. The selectivity series for electrode E21 (**8d**) with additive is very similar to that of the corresponding oNPOE plasticised membrane E13 apart from a slightly better value for the Hg^{2+}. However, the effect of the additive addition is not as pronounced in the DOS as it is in the oNPOE plasticised membranes, resulting in a shift of approximately half an order of magnitude in silver selectivities compared to an order of magnitude.

4.3.3 Calibration and selectivity results using constant dilution.

The fixed interference method (FIM) was used in this section to determine the limit of detection and silver selectivity of a membrane electrode prepared using **8d**. This technique has several advantages over the separate solution method as described in section 4.2.3.2. The results obtained with a membrane electrode of **8d** were compared to those obtained with compound **38** which is a 14 crown 4 used by Singh in previous work towards a silver ion sensor for Kodak[56].

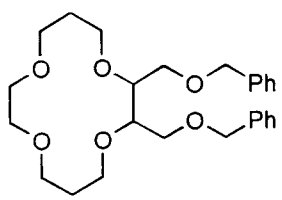

38

The electrode compositions used are based on those widely used by Moody *et al* i.e oNPOE as plasticiser with 30 mol% additive and correspond to those prepared as described in Table 4.3[24]. In this section E13 (**8d**) and a new electrode E24 (**38**) were compared by constant dilution experiments. The results for the electrode calibrations are shown in Table 4.5 and those for the electrode selectivities are shown in Table 4.6.

Compound	Slope mV/dec^{-1}	Limit of Detection -log C
E13(**8d**)	62 ±4	4.6±0.4
E24(**38**)	62±5	5.0±0.4

Table 4.5 Calibration results for compounds.

The values obtained for the electrode calibrations for the two electrodes are comparable as shown in Table 4.5, both values are super Nernstian which is typical of this technique owing to a hysteresis effect as discussed in section 4.2. The limit of detection for E24 (4.96) is slightly higher than that for E13 (4.61) but both values are typical of those obtained for membrane electrodes using this technique.

	Na^+	K^+	Mg^{2+}	Ca^{2+}	Fe^{3+}
E13 (**8d**)					
Slope mV dec^{-1}	66 ± 7	61 ± 3	60 ± 2	57 ± 2	65 ± 3
LD (-log C)	4.5 ± 0.3	4.6 ± 0.2	3.7 ± 0.2	3.6 ± 0.1	4.2 ± 0.1
$-\log K_{ij}^{pot}$	3.5 ± 0.3	3.6 ± 0.2	3.2 ± 0.2	3.2 ± 0.1	3.8 ± 0.1
E24 (38)					
Slope mV dec^{-1}	46 ± 5	61 ± 4	60 ± 1	60 ± 7	-
LD (-log C)	2.3 ± 0.2	2.7 ± 0.0	2.7 ± 0.1	1.3 ± 0.1	-
$-\log K_{ij}^{pot}$	1.2 ± 0.2	1.7 ± 0.0	3.2 ± 0.1	1.8 ± 0.1	-

Table 4.6 Selectivities of electrodes E16(**8d**) and E24(**38**) over a range of cations.

The electrode selectivities for the two electrodes E13 and E24 are compared in Table 4.6. It can be seen that the selectivities over the monovalent cations Na^+ and K^+ for electrode E13 are significantly better (ca. 2 orders of magnitude) that those of the electrode E24. The selectivities of the electrodes over Mg^{2+} are in good agreement, which is surprising as a better selectivity would have been expected for electrode E13. The value for

Ca^{2+} for E13 is half an order of magnitude better than that for E24. Over all E13 shows very good selectivity for silver and is significantly better than E24.

4.4 Conclusions

The potentiometric results in this chapter report the successful incorporation of newly synthesised ionophores into silver selective ISE's. The binding of silver was shown to depend of the lipophilicity of the molecule; compound **8d** functionalised with a butyl group displaying the best results. This compound (**8d**) was then compared to a literature ionophore (**25**) and a compound used in previous work for Kodak (**38**) and was shown to display superior response. Changing of the plasticiser had only a slight effect on the electrode selectivity and the optimum additive concentration was 30 mol % of the ionophore. The silver selectivity coefficients were in the order of $-\log K = 4.5$ for the SSM and $-\log K = 3.5$ for the constant dilution method.

4.5 Bibliography for Chapter 4

1. R. G. Bates, "Determination of pH", John Wiley & Sons, New York, 1964.
2. P. Debye and E. Huckel, *Physikalische Zeitschrift*, 1923, **24**, 185.
3. G. Eisenman, D. O. Rudin and J. U. Casby, *Science*, 1957, **126**, 831.
4. W. E. Morf, "The Principles of Ion-Selective Electrodes and of Membrane Transport", Elsevier, Budapest, 1981.
5. Z. Haber and Z. Klemensiewitz, *Z. Phys. Chem*, 1909, **67**, 385.
6. G. J. Moody and J. D. R. Thomas, "Selective Ion Sensitive Electrodes", Merrow, London, 1971.
7. G. G. Guilbault, R. A. Durst, M. S. Frant, H. Freiser, E. H. Hansen, T. S. Light, E. Pungor, G. Rechnitz, N. M. Rice, T. J. Rome, W. Simon and J. D. R. Thomas, *Pure Appl. Chem.*, 1976, **48**, 127.
8. Y. Umezawa, K. Umezawa and H. Sats, *Pure Appl. Chem.*, 1995, **67**, 507.
9. E. Bakker, *Anal. Chem.*, 1997, **69**, 1061.
10. V. P. Gadzekpo and G. D. Christian, *Anal. Chim. Acta*, 1984, **164**, 279.
11. E. Bakker, P. Bühlmann and E. Pretsch, *Chem. Rev.*, 1997, **97**, 3083.
12. R. Buck and E. Lindler, *Pure Appl. Chem.*, 1995, **66**, 2527.
13. T. Sokalski, A. Ceresa, T. Zwickl and E. Pretsch, *J. Am. Chem. Soc.*, 1997, **119**, 11347.
14. S. Mathison and E. Bakker, *Anal. Chem.*, 1998, **70**, 303.
15. E. Bakker, *Sens . Actuators, B*, 1996, **35**, 20.
16. P. Bühlmann, S. Yajima, K. Tohda, K. Umezawa, S. Nishizawa and Y. Umezawa, *Electroanalysis*, 1995, **7**, 811.
17. E. Pungor, *Electroanalysis*, 1996, **8**, 348.
18. J. Bricker, S. Daunert, L. G. Bachas and M. Valiente, *Anal. Chem.*, 1991, **63**, 1585.
19. M. L. Iglehart, R. P. Buck and E. Pungor, *Anal. Chem.*, 1998, **60**, 290.
20. G. Horvai, E. Graf, K. Toth, E. Pungor and R. P. Buck, *Anal. Chem.*, 1986, **58**, 2735.
21. E. Pungor, *Pure Appl. Chem.*, 1992, **64**, 503.
22. E. Bakker, M. Nagele, U. Schaller and E. Pretsch, *Electroanalysis*, 1995, **7**, 817.

23. E. Bakker, R. K. Meruva, E. Pretsch and M. E. Meyerhoff, *Anal. Chem.*, 1994, **66**, 3021.
24. A. Craggs, G. J. Moody and J. D. R. Thomas, *J. Chem. Ed.*, 1974, **51**, 542.
25. A. van den Berg, P. D. van der Wal, M. Skowronska-Ptasinska, E. J. R. |Sudholter and D. N. Reinhoudt, *Anal. Chem.*, 1987, **59**, 2827.
26. U. Oesch and W. Simon, *Anal. Chem.*, 1980, **52**, 602.
27. U. Fielder and J. Ruzicka, *Anal. Chim. Acta*, 1973, **67**, 179.
28. E. Bakker, M. Willer, M. Lerchi, K. Seiler and E. Pretsch, *Anal. Chem.*, 1994, **66**, 516.
29. D. Ammann, W. E. Morf, P. Anker, P. C. Meier, E. Pretsch and W. Simon, *Ion-Sel. Electr. Rev.*, 1983, **5**, 3.
30. P. C. Meier, W. E. Morf , M. Laubli and W. Simon, *Anal. Chim. Acta*, 1984, **156**, 1.
31. E. Linlder, E. Graf, Z. Niegreisz, K. Toth, E. Pungor and R. P. Buck, *Anal. Chem.*, 1988, **60**, 295.
32. H. An, J. S. Bradshaw and R. M. Izatt, , 1992, 1875.
33. R. D. Hancock and A. E. Martell, , 1989, 89.
34. L. F. Lindoy, *Pure Appl. Chem.*, 1997, **69**, 2179.
35. M. Lai and J. Shih, *Analyst*, 1986, **111**, 165.
36. J. Christensen, D. Eatough and R. Izatt, *Chem. Rev.*, 1971, **74**, 351.
37. M. Oue, K. Akama, K. Kimura, M. Taneka and T. Shono, *Anal. Sci.*, 1989, **5**, 165.
38. M. Oue, K. Akama, K. Kimura, M. Taneka and T. Shono, *J. Chem. Soc., Dalton Trans.*, 1989, 891.
39. D. Siswanta, K. Nagatsuka, H. Yamada, K. Kumakura, H. Hisamoto, Y. Shichi, K. Toshima and K. Suzuki, *Anal. Chem.*, 1996, **68**, 4166.
40. J. Casabó, L. Mestres, L. Escriche, F. Texidor and C. Pérez-Jiménez, *J. Chem. Soc., Dalton Trans.*, 1991, 1969.
41. K. O'Connor, G. Svehla, S. Harris and M. McKervey, *Talanta*, 1992, **39**, 1549.
42. K. O'Connor, W. Henderson, E. O'Neil, D. W. M. Arrigan, S. Harris, M. McKervey and G. Svehla, *Euroanalysis*, 1997, **9**, 311.
43. Z. Malinowska, Z. Brzózka, K. Kasiura, R. J. M. Egberinek and D. Reindoudt, *Anal. Chim. Acta*, 1994, **298**, 245.
44. W. Wróblewski and Z. Brzózka, *Sens . Actuators, B*, 1995, **24**, 183.

45. P. L. H. M. Cobben, "Sensors for Heavy Metal ions based on ISFets", University of Twente, 1992.

46. J. Casabó, T. Flor, M. I. Romero, F. Teixidor and C. Pérez-Jiménez, *Anal. Chim. Acta*, 1994, **294**, 207.

47. F. Teixidor, M. A. Flores, L. Esriche, C. Viñas and J. Casabó, *J. Chem. Soc., Chem. Comm.*, 1994, 963.

48. A. Errachid, J. Baussells, A. Merlos, J. Esteve, F. Teixidor, J. Pérez-Jiménez, J. Casabó and J. Bartolí, *Sens . Actuators, B*, 1995, **26**, 321.

49. W. Hasse, B. Ahlers, J. Reinbold, K. Cammann, G. Brodesser and F. Vögtle, *Sens . Actuators, B*, 1994, **18**, 380.

50. S. S. Lee, M. K. Ahn and S. B. Park, *Analyst*, 1998, **123**, 383.

51. S. Chung, W. Kim, S. B. Park, I. Yoon, S. S. Lee and D. D. Sung, *J. Chem. Soc., Chem. Comm.*, 1997, 965.

52. S. Chung, W. Kim, S. B. Park, D. Y. Kim and S. S. Lee, *Talanta*, 1997, **44**, 1291.

53. A. Teasdale, "Synthetic Ionophores for Cations", Ph.D., University of Durham, 1993.

54. G. Horvai and E. Pungor, *Anal. Chim. Acta*, 1976, **82**, 45.

55. R. D. Armstrong and G. Horvai, *Electrochim. Acta*, 1990, **35**, 1.

56. D. M. Singh, "Electroanalysis of Chloride, Bromide and Silver Ions", Ph.D., University of Newcastle upon Tyne, 1994.

CHAPTER FIVE

Determination of Silver in Photographic Emulsion

5.1 Introduction

This chapter focuses on the analysis of silver ion in photographic emulsions. The new membrane electrodes (whose composition was optimised as described in chapter 4) were compared to silver halide electrodes in terms of their sensitivity and response times. The challenges of working at high halide concentrations and working in a gelatin environment are first introduced.

5.1.1 The Halide Buffering Effect.

Of the problems expected when measuring silver ion concentration in photographic emulsions, the high halide concentration and consequent low silver ion activity posed the greatest challenge. The normal lower detection limit of potentiometric ISE's is in the micromolar range; however, the silver ion activity in photographic emulsions lies in the micro to nanomolar range. To simulate the silver ion concentrations in photographic emulsion, aqueous solutions of silver halides can be prepared. When a sample of a silver halide is dissolved in water, the silver and halide concentration are equal, and the product of their concentrations is termed the solubility product, (equation 5.1)

$$AgX \longrightarrow Ag^{+} + X^{-}$$

$$Ksp = [Ag^{+}]\,[X^{-}] \qquad (5.1)$$

The silver ion activity can be decreased by increasing the concentration of halide. The addition of halide will cause the above equilibrium to re-adjust until the product of the silver and halide ions equals the solubility product. In practice, the extent of this adjustment has to be calculated. This buffering effect can be seen by taking the example of silver chloride. At 40 °C it has a solubility product of 6.31×10^{-10} mol^2 dm^{-6}. At this concentration the silver and halide ion concentrations are equal at 2.51×10^{-5} mol dm^{-3}. The addition of C mol dm^{-3} of chloride ion to this solution results in a shift in the equilibrium, as shown in Table 5.1. The product of the equilibrium concentrations equals the solubility product, so solving the resulting quadratic equation for X yields the extent of the adjustment and hence the final equilibrium concentrations.

Concentration	Ag^+	Cl^-
	mol dm^{-3}	mol dm^{-3}
Initial	2.51×10^{-5}	2.51×10^{-5}
Added Chloride	2.51×10^{-5}	2.51×10^{-5} + C
Equilibrium	2.51×10^{-5} - X	2.51×10^{-5} + C-X

Table 5.1 Buffering effect of silver chloride upon addition of chloride ion

The buffering effect of the chloride ion can be seen by comparing its effect at low and high concentrations by simulated calculations. When a sample of AgCl is dissolved in deionised water, the equilibrium concentrations of the silver and chloride ions are equal at 2.51×10^{-5} mol dm^{-3}. To illustrate the buffering effect of the silver chloride system, the expected equilibrium concentrations and the unbuffered concentrations (i.e. adding Cl^- to water) of silver ion were calculated for a series of additions of chloride. These were plotted versus added chloride ion as shown in Figure 5.1. It can be seen that the buffering effect is very slight at low chloride concentrations as the buffered and unbuffered plots are almost identical.

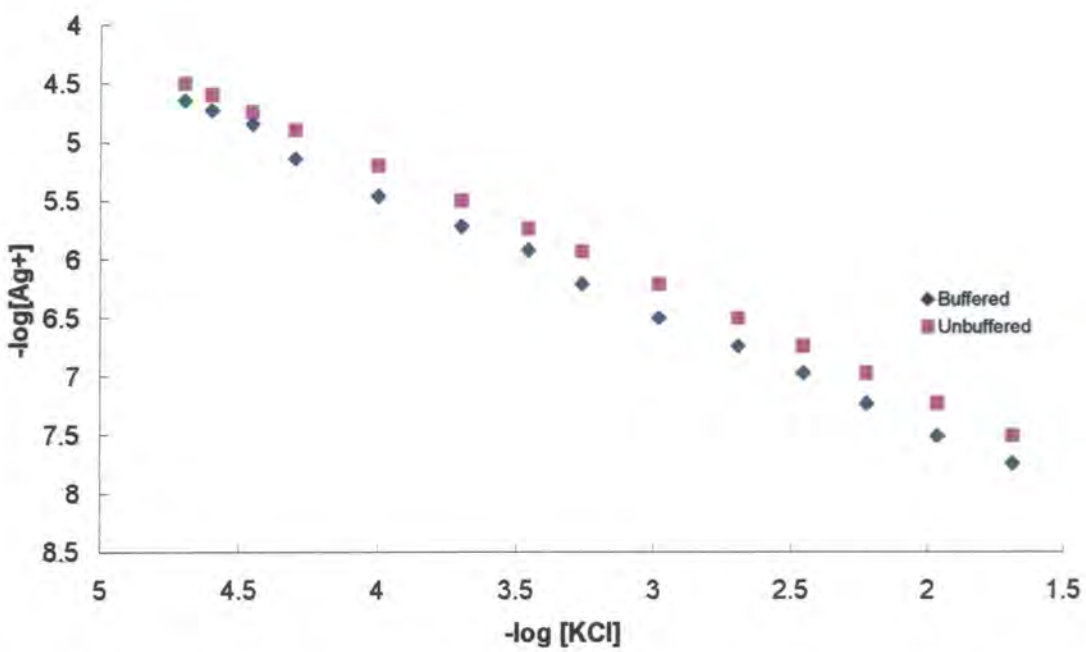

Figure 5.1 Predicted plots of buffered versus non buffered concentrations of silver ion upon addition of chloride ion starting from $[Ag^+] = [Cl^-] = 2.51 \times 10^{-5}$ mol dm^{-3}

The situation is very different when one of the species is at a higher concentration, which is more typical. In the preparation of photographic emulsion the halide concentration is often of the order of 10^{-3} mol dm^{-3} before any silver is added. This high starting halide concentration strongly buffers the solution against addition of silver ion up to the point where the silver and halide ions have equal concentrations. A simulated titration is shown in Figure 5.2

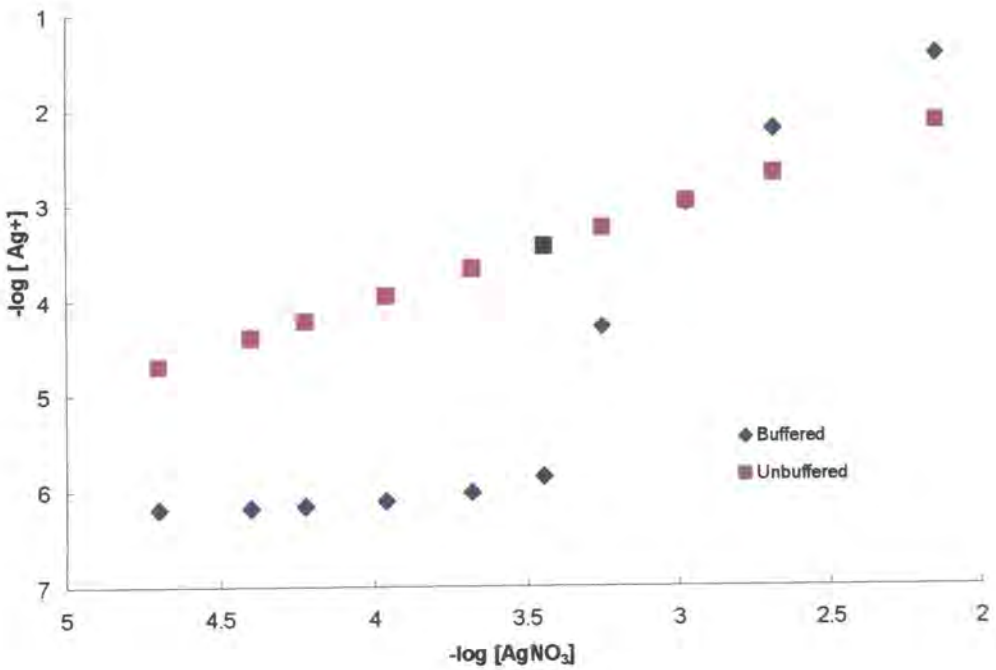

Figure 5.2 Predicted plots of buffered versus non buffered concentrations of silver ion upon addition of chloride ion starting from $[Cl^-] = 1 \times 10^{-3}$mol dm^{-3}

5.1.2 Gelatin

The original role of gelatin was completely mechanical, in that it provided a transparent flexible medium which permitted coating and subsequent drying to form a layer[1]. However, it was soon realised that gelatin had many properties suitable for photography and attempts to replace it with synthetic polymers have been met with limited success. Silver halide grains require a medium for crystallisation, this is the property of colloid protection and is the ability to control crystal growth and maintain suspension. This property, as well as other requirements such as cross-linkability and swelling, are fulfilled by gelatin with such success that it is still in use in photography more than a century after its first use.

The principal component is an animal protein called collagen, this is the most abundant protein in higher animals and is found in stress bearing structures such as skin, bone, cartilage and tendons[2]. Collagen is associated with many other substances such as non-collagen protein, mucopolysaccharides, polynucleic acids and lipids, which are removed in the preparation of gelatin. The structure of collagen is well known, approximately every third amino acid is glycine and about ten percent is hydroxyproline, which is an amino acid unique to collagen. Cystine is rarely found, and thus the di-sulfide bridge is not a factor in collagen conformation. The remaining two thirds of the amino acids are non-polar or hydrophobic.

The interaction between gelatin and silver ion has been examined in some detail using a range of techniques, and it has been found that methionine is the principle complexation agent in basic and neutral environments[3,4]. Further work has shown that a good correlation exists between the total specific silver binding sites and the methionine content of gelatin[5]. Binding stoichiometries of 1:1 and 2:1 methionine to silver ion have been found, depending on the ratios present.

Radiolytic reduction of silver ions and the subsequent formation of silver clusters was studied in aqueous gelatin, and compared with parallel processes in aqueous solutions[6]. The reduction of Ag^+ ions in aqueous solution leads to the formation of Ag^0, which forms various complexes with Ag^+ resulting in formation of oligomeric clusters. These clusters

eventually lead to the formation of colloidal Ag particles, which can be characterised by a sharp surface plasmon absorption band in the 380-400 nm range. This work showed that the gelatin affects both reduction and agglomeration relative to absence of gelatin, the former being slower in gelatin containing solutions. Interestingly this work showed that the small clusters bind to gelatin more strongly than the Ag^+ itself. This may be interpreted as an indication that hydrophobic interactions contribute to the Ag^+ binding. It appears that the gelatin can stabilise more than one type of Ag^+ particle, leading the authors to postulate the coexistence of several microdomains in the gelatinous regions.

The photographic activity of the gelatin depends more on the substances associated with it than the protein itself[7]. These substances are numerous, and of particular interest are the sulfur containing compounds. These are categorised according to their photographical activity and include thiosulfates and thioureas which are active, and sulfates which are deemed inactive. Of the active sulfur containing components the most important is cysteine which is derived from the protein collagen. Despite the gelatin preparation process in which the cysteine is significantly removed, part of this amino acid remains in the final product. The decomposition of cysteine involves several decomposition and redox reactions, which occur either simultaneously or successively. In strong basic conditions cysteine forms sulfide and polysulfides, which on contact with air form sulfites and sulfur. These then react to form thiosulfate, which in turn can be oxidised to polythionates. The presence of the former has been proven experimentally, whilst the presence of polythionates such as tetrathionate has never satisfactorily been demonstrated. This discussion illustrates the plethora of sulfur containing components in gelatin, any or all of which have the potential to bind silver.

Originally, the gelatin was used as manufactured, this gelatin was termed active gelatin as it contained active micro-components whose concentrations were adjusted empirically[7]. More recently, rigorous purification has produced inert gelatin which serves a more mechanical role. This has allowed a more precise addition of the active components. However, despite improvements in manufacturing techniques, even the purest gelatin still contains photographically active substances such as restrainers and reducers.

5.1.3 Determination of Silver Ion in Gelatin

Early determination of silver ion in photographic emulsions was by potentiometric titration. This method involved addition of thioacetamide to an alkaline solution containing Ag^+ ions which leads instantaneously to precipitation of silver sulfide at room temperature. This reaction proceeds in three steps, firstly the thioacetamide intermediate is produced (ammonia is evolved) then hydrogen sulfide along with the second by-product, acetate, and finally sulfide[8].This precipitation method was preferred to an earlier method which required a hot ammonia solution (objectionable odours) and thiourea. The potentiometric titration of silver sulfide proceeded with a sharp endpoint if the original solution does not contain a high concentration of slightly dissociated ammonia or thiosulfate complex. This titration was carried out in the batch mode but the hydrolysis of the by-products made this a time consuming procedure.

Recently work has been published on automation of this procedure using discontinuous flow analysis (DFA). This is a relatively new technique which has attracted interest owing to its rapid solution handling and ease of incorporation on-line in to a process stream[9]. A series of Ag^+ titrations were carried out in photographic emulsion but difficulties were encountered in the end point determination. This was attributed to the slowing of the response of the silver sensor. The sensor used was a silver wire electrode which was prone a build up of silver sulfide on the electrode surface, this was confirmed by cyclic voltammetry. This work published in 1998 illustrates that the biggest problem of silver ion analysis in gelatin remains the choice of silver electrode. The other problems such as sample pre-treatment and automation have been solved through experience with other analysis systems.

The silver wire electrode cannot be used in photographic emulsion owing to the problem of sulfide build up on the electrode. The silver sulfide electrode is also unsuitable owing to the nucleophilic sulfide groups on the electrode surface which attack the sensitiser compounds. Present technology at Kodak U.K, Harrow involves use of the silver/ silver chloride electrode to measure the free Cl^- from which the concentration of silver is then calculated. This is an indirect measurement and is both labour intensive and costly owing to the constant preparation of fresh electrodes. In this work a membrane ISE will be used to analyse the silver ion concentration directly.

5.2 Experimental

5.2.1 Apparatus

The potentials were recorded using a computer controlled high impedance voltage measuring equipment supplied by Molspin Ltd. This device was operated in the data logger mode which was set to take potential readings at one second intervals. Up to four input voltages could be determined simultaneously. The reference electrode was a silver/silver chloride gel electrode supplied by Kodak which was connected via a salt bridge containing 10^{-1} mol dm^{-3} KNO_3

5.2.2 Potentiometric Determinations in Silver Halide Solutions.

A saturated solution of a silver halide was prepared by adding an excess (100 mg) of silver halide to 25 ml of distilled water. The potentiometric cell was thermostated at 40° C and accommodated two ISEs and a reference electrode. The reference electrode was an Orion double junction electrode with an 0.1 mol dm^{-3} KNO_3 bridge solution. The potentials were recorded using a Molspin computer controlled data logger which was set to take potentiometric readings at 60 second intervals. The data were saved as text files which were then imported into Microsoft Excel v 7.0.

5.2.3 Potentiometric Determinations in Gelatin.

The samples of gelatin supplied by Kodak were solid at room temperature. A weighed sample of gelatin (30.7 g to provide 25 ml) was melted in the thermostated potentiometric cell and the data logger was initiated when the potentials of the electrodes had stabilised. The reference electrode was connected to the cell via the salt bridge assembly as shown in Figure 5.3. This consisted of a reservoir of an equitransferance solution such as 0.1 M KNO_3 connected to an electrode body via a flexible length of tubing. The electrical contact was made with a wick which ran through from the reservoir onto the electrode body. This wick became fouled in gelatin solution and could be pulled through the body to expose a fresh surface.

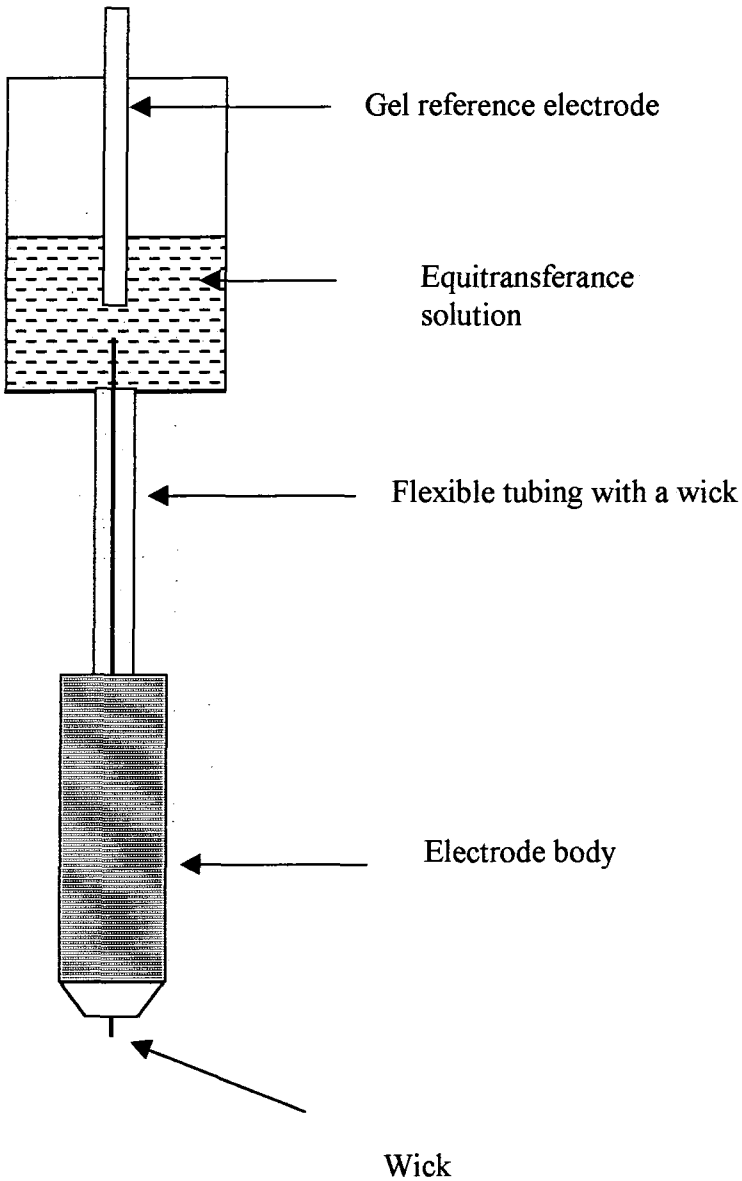

Figure 5.3 Reference electrode set up for analysis in gelatin.

5.3 Results

In this section, the membrane electrode E13 (**8d**) whose composition was optimised as described in Chapter 4, was applied to analysis of silver ion in photographic emulsion. The challenges for a sensor working in this environment were described in section 5.1 and work in this section focused on lowering the detection limit of the electrode. This work was stimulated by recent literature reports of large improvements in lower detection limits in ISEs by buffering of the inner reference electrode.

In recent work by Pretsch *et al* the lower detection limit of a lead ISE was improved by six orders of magnitude by buffering of the inner reference electrode filling solution using an organic ligand (effectively giving a 10^{-12} mol dm^{-3} Pb^{2+})[10]. An interferent cation which had a selectivity coefficient of 10^{5} was include to act as the charge carrier on the inner side of the membrane. In this work a buffered inner solution was prepared to provide an analgous system for a silver ISE. It was decided to use the chloride anion as a buffer and potassium as the interferent.

5.3.1 Analysis in Aqueous Halide Solutions

A solution of 10^{-2} mol dm^{-3} KCl saturated with AgCl has a silver ion activity of -log a = 7.2, this solution was used as an inner filling solution for a silver ion ISE, and its performance compared to a standard inner filling solution of 10^{-3} mol dm^{-3} $AgNO_3$. The responses of both electrodes were tested in the micro- to nanomolar range of silver ion activity by addition of KCl solution to a saturated aqueous solution of AgCl as shown in Figure 5.3. The silver ion activities were calculated using the Debye Huckel equation as described in section 4.1.1.2.

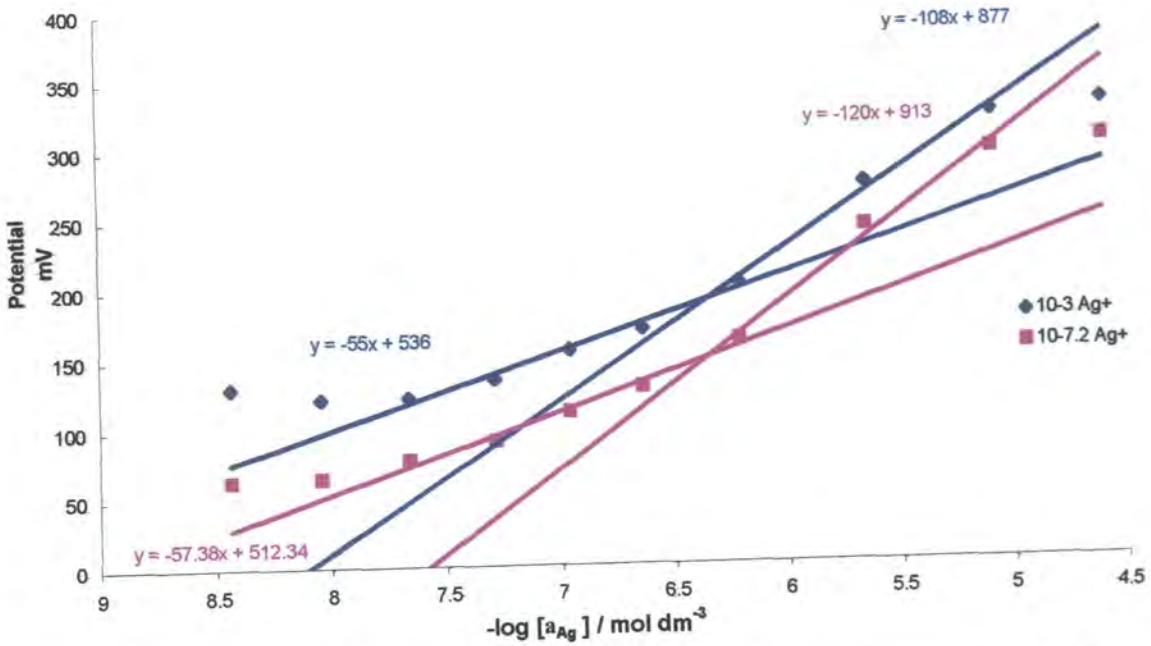

Figure 5.3 Comparison of the response of silver ion ISE with different inner fill solutions upon addition of KCl to a saturated AgCl solution.

The response curves for both electrodes display two linear regions. The first linear region is between –log a = 5 to 6.5 where both electrodes display super Nernstian slopes and is due to formation of halide complexes[7] of the form AgX_n where n = 1 to 4. In the second linear region, both electrodes display near Nernstian responses of 55 and 57 mV dec^{-1} for the 10^{-3} and $10^{-7.2}$ mol dm^{-3} inner solutions. The effect of changing the inner filling solution results in an increased value of the slope but does not result in an improvement in the lower detection limit.

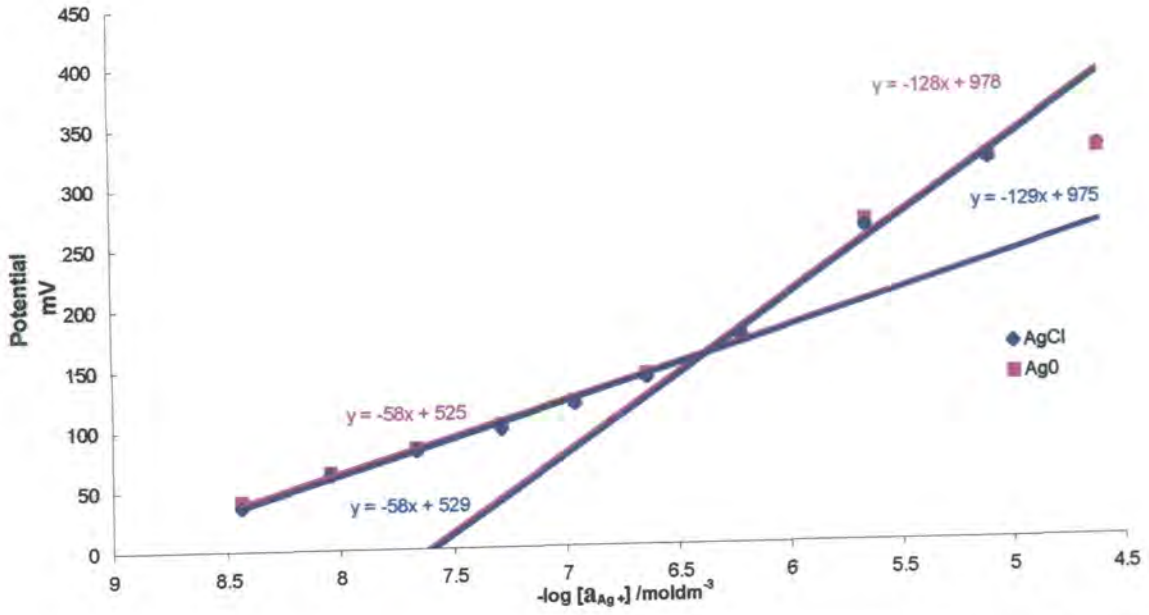

Figure 5.4 Response of silver bar and silver/silver chloride electrodes to additions of KCl to a saturated AgCl solution.

The same experiment was repeated for a silver bar and a silver/silver chloride electrode as shown in Figure 5.4. The responses of the solid electrodes are very similar to those of the membrane electrodes except that the solid electrodes respond better at concentrations down to –log a = -8.5. It is the silver chloride electrode which is presently employed at Kodak, so the response of the membrane electrode was compared directly to the silver chloride in further calibrations. The response of the membrane electrode with the $10^{-7.2}$ inner solution decreased over a period of three weeks and the values for slopes are shown in Table5.2

Day	Slope mV dec^{-1}
1	58
14	42
20	38

Table 5.2 Deterioration of the response of the membrane electrode containing the $10^{-7.2}$ Ag^+ inner solution with time.

Over this time the membrane became opaque and appeared as if the inner surface of the electrode was coated with silver chloride. Three other electrodes prepared with chloride buffered inner fill solutions also had silver chloride coated membranes. A standard electrode membrane which had a clear membrane was photographed along with a chloride coated and these are shown in Figure 5.5 (a) and (b) respectively. Therefore, the buffering of the inner reference solution with chloride ion was not effective in lowering the lower limit of detection but instead results in fouling of the membrane. Better results could probably be achieved by buffering with an organic ligand which would not precipitate on silver complexation

(a) (b)

Figure 5.5 The effect of silver chloride precipitation on the inner surface of electrode membrane (a) standard inner fill solution and (b) silver chloride precipitate

5.3.2 Analysis in Photographic Emulsion

The standard membrane inner filling (10^{-3} mol dm^{-3} $AgNO_3$) solution was used in a membrane electrode for analysis in photographic emulsion and its response was compared to a solid silver /silver chloride electrode. The sample of photographic emulsion supplied by Kodak was labelled 10^{-3} mol dm^{-3} Cl^-. A series of additions of $AgNO_3$ were calculated to produce a simulated titration curve as shown in Figure 5.6, which included five points up to 10^{-3} mol dm^{-3} and five further points resulting in a final concentration of 10^{-1} mol dm^{-3}.

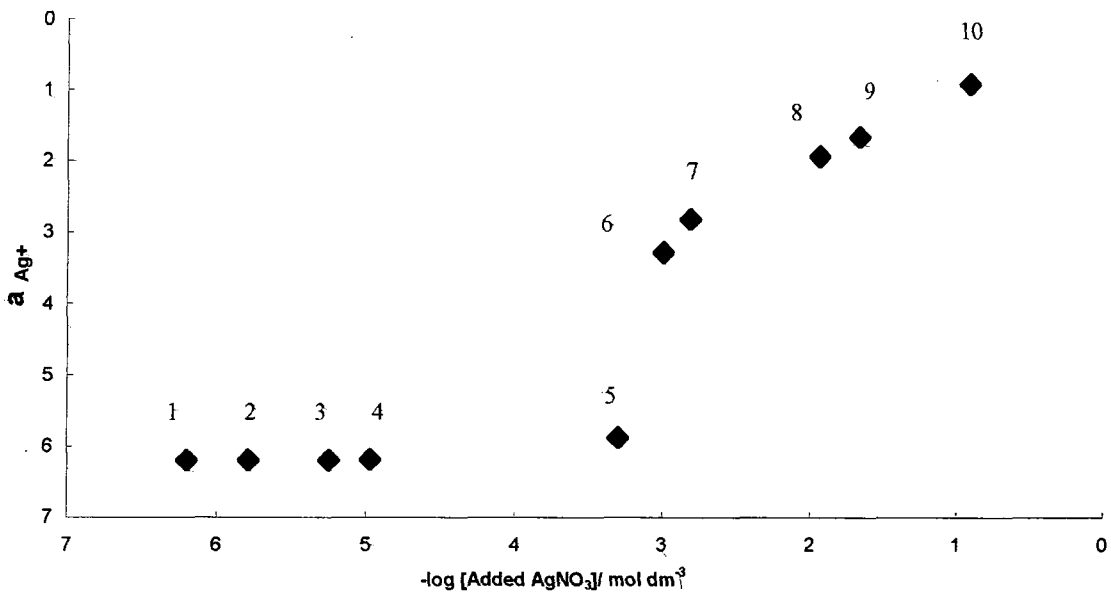

Figure 5.6 Predicted activities of silver ion upon addition of $AgNO_3$ to a 10^{-3} mol dm^{-3} KCl solution

However, when these additions of $AgNO_3$ were made to a sample of gelatin labelled 10^{-3} mol dm^{-3} Cl^- the plot in Figure 5.7 resulted. These additions (indicated by the arrows in Figure 5.7) correspond to the concentrations calculated in Figure 5.6.

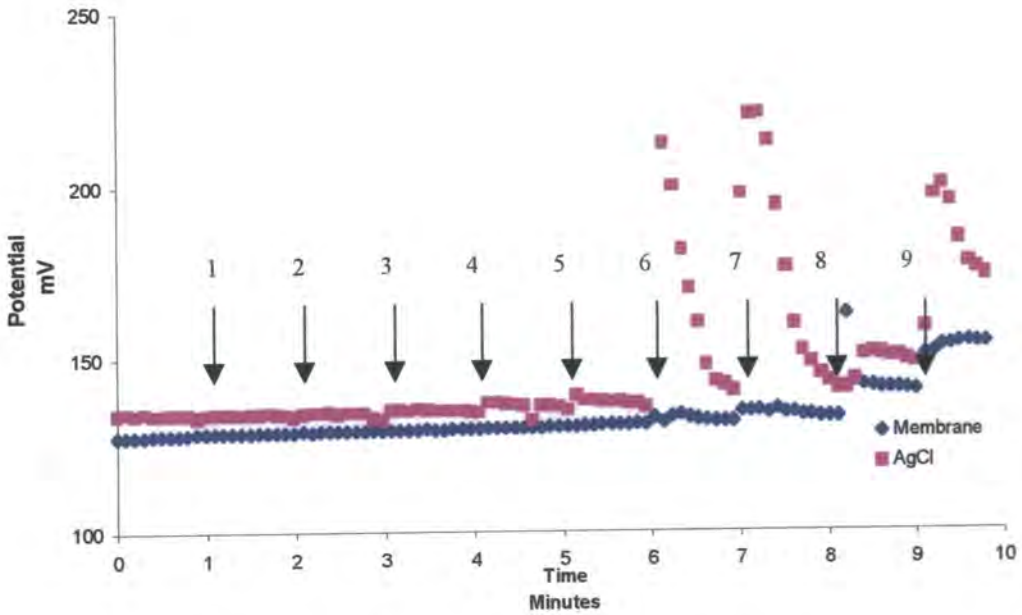

Figure 5.7. Addition of $AgNO_3$ (indicated by arrows) to photographic emulsion labelled "10^{-3} mol dm^{-3} Cl^-".

It is not until the concentration of added silver ion reaches 10^{-2} mol dm^{-3} (i.e. after eighth addition in Figure 5.6) that a change in potential is observed. This could be due to the fact that the concentration of chloride ion is higher than 10^{-3} mol dm^{-3} or that this emulsion contains bromide anion. It is interesting to note that the silver chloride electrode response to chloride is slower than the membrane electrode response to silver ion as is evident form the potential trace for additions seven to nine. At these additions, the added silver ion is being precipitated by the chloride ion in solution, so that the concentration of silver does not change while the change in chloride ion is observable.

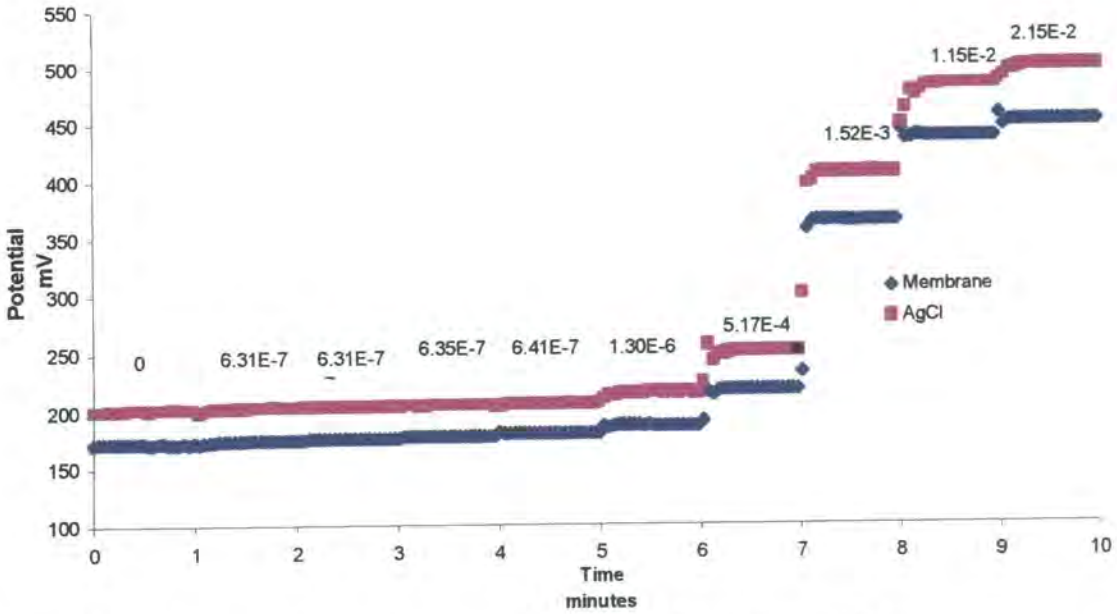

Figure 5.8 Addition of silver nitrate to a 10^{-3} mol dm^{-3} solution of KCl.

To ensure that there was no error in the calculated additions, the identical quantities of $AgNO_3$ were added to a 10^{-3} mol dm^{-3} solution of KCl and the resultant plots shown in Figure 5.8. It can be clearly seen that the precipitation of silver chloride starts after the added silver ion reaches a concentration of 10^{-3} mol dm^{-3} as predicted. The membrane electrode undergoes a 310 mV dec^{-1} shift in potential on going from the chloride to the silver side of the equilibrium whilst the AgCl electrode undergoes a 325 mV dec^{-1} shift in the same concentration range. These potentials were measured using a data logger (see section 5.2) which was set to take potential readings at one second intervals. It is significant that the membrane electrode shows faster response times than the AgCl electrode. This is evident when the responses of both electrodes are compared in the concentration ranges 5.17×10^{-4} to 1.52×10^{-3} mol dm^{-3} and 1.52×10^{-3} to 1.15×10^{-2} mol dm^{-3} corresponding to the seventh and eighth additions respectively. In these ranges, the membrane electrode stabilises in 1 to 2 seconds whilst the AgCl electrode requires 3 to 5 seconds

One of the design specifications of the silver sensor for Kodak, was that it operated at silver concentrations on both the halide and silver side of the equilibrium and through the precipitation, as this simulates the environment in which the halide emulsions are prepared, as described in section 5.1.3.

As the provided sample of emulsion seemed to contain more chloride than expected, the point of precipitation was determined experimentally by stepwise addition of $AgNO_3$ until a large jump in potential was observed. A series of additions were then formulated which allowed a titration curve to be drawn for the precipitation process from the halide to the silver side, labelled "Add Ag^+" in Figure 5.9. Equimolar additions of KCl were then made to the same solution to effect a precipitation from the halide to the silver side, labelled "Add Cl^-" in Figure 5.9. As the exact composition of the sample of emulsion is not known, the ionic strength can not be determined therefore the potential of the electrodes was plotted versus added $AgNO_3$.

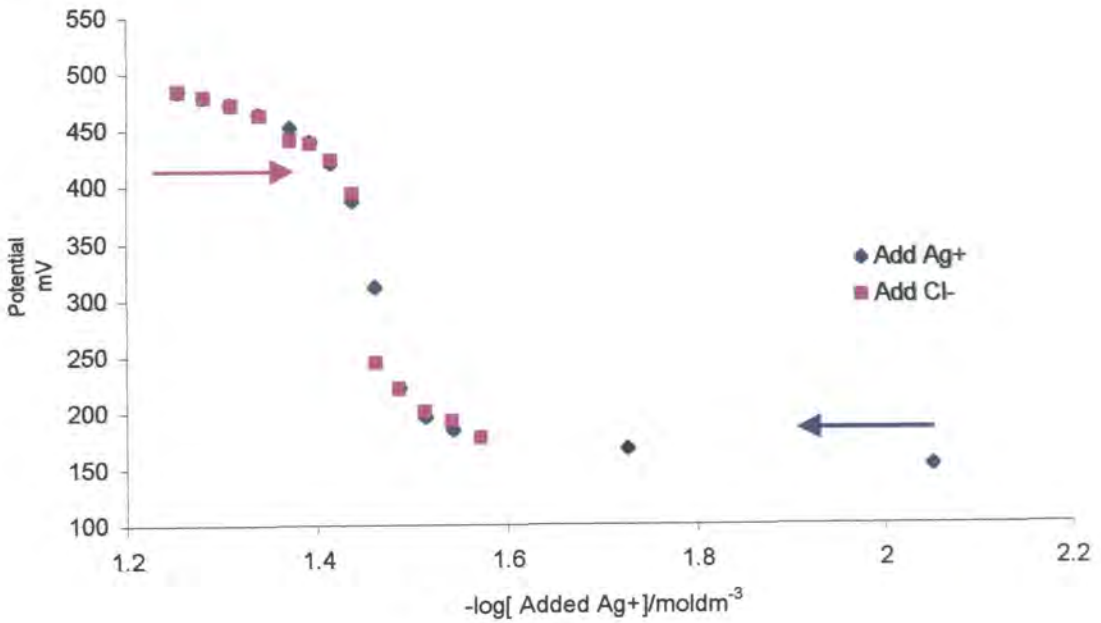

Figure 5.9 Response of membrane electrode to experimentally determined additions of $AgNO_3$ and KCl to investigate response near precipitation of AgCl.

The same experiment was repeated for the silver/silver chloride electrode and the results are shown in Figure 5.10.

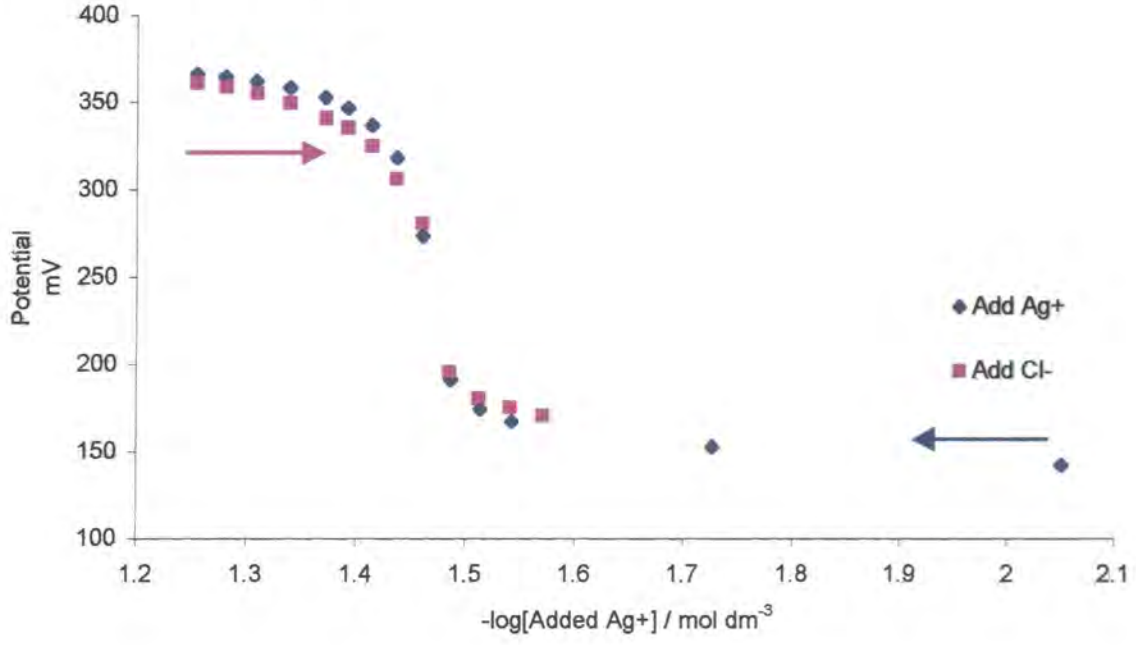

Figure 5.10 Response of silver chloride electrode to experimentally determined additions of $AgNO_3$ and KCl to investigate response near precipitation of AgCl.

The purpose of these experiments was to examine the response of the membrane electrode near precipitation of AgCl, the reproducibility of the electrodes is given by how closely the "Add Ag^+" and "Add Cl^-" potential traces overlap. It can be seen from the comparison of the membrane electrode response in Fig 5.9 and the AgCl electrode response in Fig. 5.10 that both electrodes show reproducible behaviour near precipitation. This result is significant as it demonstrates that the membrane electrode response is not affected by interference by any components of the photographic emulsion and its response in this environment matches the AgCl electrode which is currently in use at Kodak.

A sample of bromide emulsion was supplied by Kodak which was labelled 5 x 10^{-4} mol dm^{-3} bromide ion, the point of precipitation of AgBr was again determined experimentally for the membrane electrode in Figure 5.11 and for the silver/silver bromide electrode in Figure 5.12.

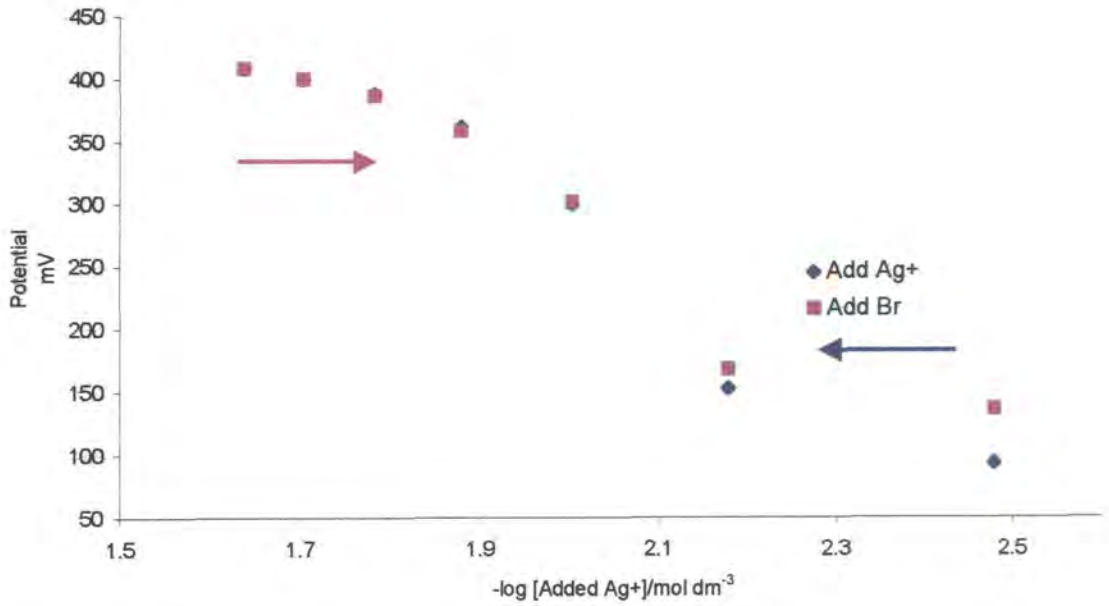

Figure 5.11 Response of a membrane electrode to addition of $AgNO_3$ to a bromide emulsion

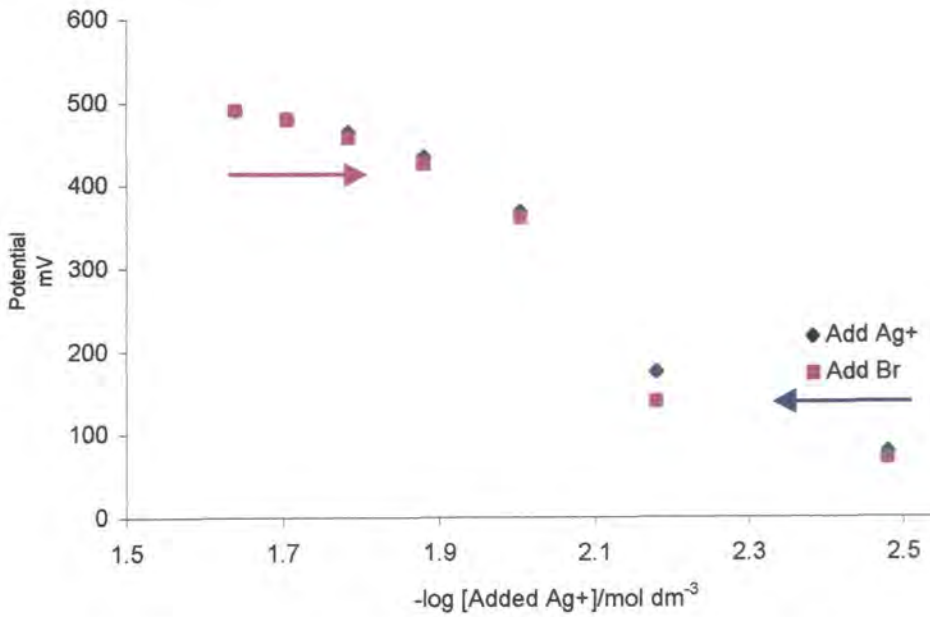

Figure 5.12 Response of a silver/silver bromide electrode to addition of $AgNO_3$ to a bromide emulsion

The membrane electrode again displays comparable reversibility to the silver/silver halide electrode through the precipitation of AgBr. The lower concentration of halide in the bromide emulsion is evident as the point of precipitation occurs at –log [Added Ag^+] = 2 for the bromide and 1.5 for the chloride. The reversible response of the membrane electrode in both chloride and bromide emulsions is impressive as it demonstrates that it can cope in either environment.

5.4 Conclusions on Chapter 5

In this chapter the newly developed silver ion electrode was tested in photographic emulsion. An attempt was made to follow a recent literature improvement on the lower detection limit but this was unsuccessful. This could be due to fact that buffering with the chloride ion is unsuitable or that this technique is not suitable for this electrode system, in fact this technique is still very recent, and is not fully understood. The electrode was applied to the successful and reproducible determination of silver ion in both chloride and bromide photographic emulsions.

5.5 Bibliography of Chapter Five

1. P. I. Rose, in "The Theory of the Photographic Process" (T. H. James Ed.), Macmillan Publishing Co., London, 1977, 51.
2. A. Veis, "The Macromolecular Chemistry of Gelatin", Academic Press, New York, 1964.
3. S. Tani and T. Takehior, *J. Photogr. Sci.*, 1993, **41**, 172.
4. H. Borginon, *J. Photogr. Sci.*, 1980, **28**, 111.
5. M. De Clercq and D. Rolin, *J. Photogr. Sci.*, 1994, **42**, 117.
6. S. Kapoor, D. Lawless, P. Kennepohl, D. Meisel and N. Serpone, *Langmuir*, 1994, **10**, 3018.
7. J. Pouradier, in "The Theory of the Photographic Process" (T. H. James Ed.), Macmillan Publishing Co., London, 1977, 67.
8. E. A. Butler, D. G. Peters and E. H. Swift, *Anal. Chem.*, 1958, **30**, 1379.
9. T. J. Cardwell, R. W. Cattrall, G. R. O'Connell, J. D. Petty and G. R. Schollary, *Electroanalysis*, 1992, **4**, 805.
10. T. Sokalski, A. Ceresa, T. Zwickl and E. Pretsch, *J. Am. Chem. Soc.*, 1997, **119**, 11347.

Research Colloquia and Conferences

The author attended the following colloquia

1995

October 13 Prof. R. Schmutzler, Univ Braunschweig, FRG.
Calixarene-Phosphorus Chemistry: A New Dimension in Phosphorus Chemistry

October 25 Dr.D.Martin Davies, University of Northumbria
Chemical reactions in organised systems.

November 1 Prof. W. Motherwell, UCL London
New Reactions for Organic Synthesis

November 8 Dr. D. Craig, Imperial College, London
New Stategies for the Assembly of Heterocyclic Systems

November 17 Prof. David Bergbreiter, Texas A&M, USA
Design of Smart Catalysts, Substrates and Surfaces from Simple Polymers

November 22 Prof. I Soutar, Lancaster University
A Water of Glass? Luminescence Studies of Water-Soluble Polymers.

December 8 Professor M.T. Reetz, Max Planck Institut, Mulheim
Perkin Regional Meeting

1996

January 24 Dr Alan Armstrong, Nottingham Univesity
Alkene Oxidation and Natural Product Synthesis

January 31 Dr J. Penfold, Rutherford Appleton Laboratory,
Soft Soap and Surfaces

February 14 Dr J. Rohr, Univ Gottingen, FRG
Goals and Aspects of Biosynthetic Studies on Low Molecular Weight Natural Products

February 21 Dr C R Pulham , Univ. Edinburgh
Heavy Metal Hydrides - an exploration of the chemistry of stannanes and plumbanes

March 6 Dr Richard Whitby, Univ of Southampton
New approaches to chiral catalysts: Induction of planar and metal centred asymmetry

March 7 Dr D.S. Wright, University of Cambridge
Synthetic Applications of Me_2N-p-Block Metal Reagents

March 12 RSC Endowed Lecture - Prof. V. Balzani, Univ of Bologna
Supramolecular Photochemistry

March 13 Prof. Dave Garner, Manchester University
Mushrooming in Chemistry

April 30 Dr L.D.Pettit, Chairman, IUPAC Commission of Equilibrium Data
pH-metric studies using very small quantities of uncertain purity

October 16 Professor Ojima, Guggenheim Fellow, State University of New York at Stony Brook
Silylformylation and Silylcarbocyclisations in Organic Synthesis

October 22 Professor Lutz Gade, Univ. Wurzburg, Germany
Organic transformations with Early-Late Heterobimetallics: Synergism and Selectivity

October 22 Professor B. J. Tighe, Department of Molecular Sciences and Chemistry, University of Aston
Making Polymers for Biomedical Application - can we meet Nature's Challenge?
Joint lecture with the Institute of Materials

October 23 Professor H. Ringsdorf (Perkin Centenary Lecture), Johannes Gutenberg-Universitat, Mainz, Germany
Function Based on Organisation

October 29 Professor D. M. Knight, Department of Philosophy, University of Durham.
The Purpose of Experiment - A Look at Davy and Faraday

October 30 Dr Phillip Mountford, Nottingham University
Recent Developments in Group IV Imido Chemistry

November 12 Professor R. J. Young, Manchester Materials Centre, UMIST
New Materials - Fact or Fantasy?
Joint Lecture with Zeneca & RSC

November 13 Dr G. Resnati, Milan
Perfluorinated Oxaziridines: Mild Yet Powerful Oxidising Agents

November 18 Professor G. A. Olah, University of Southern California, USA
Crossing Conventional Lines in my Chemistry of the Elements

November 27 Dr Richard Templer, Imperial College, London
Molecular Tubes and Sponges

December 3 Professor D. Phillips, Imperial College, London
"A Little Light Relief" -

December 11 Dr Chris Richards, Cardiff University
Sterochemical Games with Metallocenes

1997

January 15 Dr V. K. Aggarwal, University of Sheffield
Sulfur Mediated Asymmetric Synthesis

January 16 Dr Sally Brooker, University of Otago, NZ
Macrocycles: Exciting yet Controlled Thiolate Coordination Chemistry

January 21 Mr D. Rudge, Zeneca Pharmaceuticals
High Speed Automation of Chemical Reactions

February 4 Dr A. J. Banister, University of Durham
From Runways to Non-metallic Metals - A New Chemistry Based on Sulphur

February 12 Dr Geert-Jan Boons, University of Birmingham
New Developments in Carbohydrate Chemistry

February 18 Professor Sir James Black, Foundation/King's College London
My Dialogues with Medicinal Chemists

February 26 Dr Tony Ryan, UMIST
Making Hairpins from Rings and Chains

March 4 Professor C. W. Rees, Imperial College
Some Very Heterocyclic Chemistry

1997

October 15 Dr. R. Mark Ormerod, Department of Chemistry, Keele University
Studying catalysts in action

October 23 Prof. M.R. Bryce, University of Durham, Inaugural Lecture
New Tetrathiafulvalene Derivatives in Molecular, Supramolecular and Macromolecular
Chemistry: controlling the electronic properties of organic solids

October 29 Prof. Bob Peacock, University of Glasgow
Probing chirality with circular dichroism

October 28 Prof. A P de Silva, The Queen's University, Belfast
Luminescent signalling systems"

December 2 Dr C.J. Ludman, University of Durham
Explosions

December 3 Prof. A.P. Davis, Department. of Chemistry, Trinity College Dublin.
Steroid-based frameworks for supramolecular chemistry

1998

January 14 Prof. David Andrews, University of East Anglia
Energy transfer and optical harmonics in molecular systems

January 20 Prof. J. Brooke, University of Lancaster
What's in a formula? Some chemical controversies of the 19th century

January 28 Dr Steve Rannard, Courtaulds Coatings (Coventry)
The synthesis of dendrimers using highly selective chemical reactions

February 3 Dr J. Beacham, ICI Technology
The chemical industry in the 21st century

February 18 Prof. Gus Hancock, Oxford University
Surprises in the photochemistry of tropospheric ozone

February 24 Prof. R. Ramage, University of Edinburgh
The synthesis and folding of proteins

March 11 Prof. M.J. Cook, Dept of Chemistry, UEA
How to make phthalocyanine films and what to do with them.

March 17 Prof. V. Rotello, University of Massachusetts, Amherst
The interplay of recognition & redox processes - from flavoenzymes to devices

Conferences attended

1. ESEAC' 96 Durham, 25-29th March 1996.
2. SCI, Electrochem, '97, UCL 27-29th August 1997
3. RSC Young Researchers Meeting , April 6 th 1998
4. Butler Meeting XII, University of Newcastle Upon Tyne, July 8th 1998